Université de Montréal

Carotid Artery Biomechanical Parameters as Measured with Ultrasound Elastography in HIV Individuals – An Assessment of the Association to Coronary Atherosclerosis and Comparison to Traditional Cardiovascular Risk Factors

By Nura Shnqir

Programme de sciences biomédicales (option médecine expérimentale)

Faculty of Medicine

Master's Thesis / Mémoire de maîtrise

Thesis submitted for the Master's degree

Université de Montréal

Faculté des études supérieures

Ce mémoire intitulé:

Carotid Artery Biomechanical Parameters as Measured with Ultrasound Elastography in HIV Individuals – An Assessment of the Association to Coronary Atherosclerosis and Comparison to Traditional Cardiovascular Risk Factors

Présenté par:

Nura Shnqir

a été évalué par un jury composé des personnes suivantes:
Dr Ramy El-Jalbout, président-rapporteur
Dr Carl Chartrand-Lefebvre, directeur de recherche
Dr Madeleine Durand, co-directeur
Dr Stéphanie Tan, membre du jury

Résumé

Objectif: Évaluer l'association des caractéristiques biomécaniques des parois carotidiennes et de l'épaisseur intima-média (EIM) « *Intima-media Thickness* » (IMT) carotidienne, telles qu'évaluées par échographie, lorsque celles-ci sont incluses dans les modèles de prédiction de la charge de plaque coronarienne évaluée par tomodensitométrie (CT) chez les personnes vivant avec le VIH (PVVIH) et les personnes contrôles séronégatives.

Méthodes : Dans notre étude transversale, 164 participants (âge moyen 57 ans ± 8 ans ; 134 hommes) présentant un risque cardiovasculaire faible/intermédiaire ont été recrutés, provenant tous de l'étude prospective Cohorte canadienne VIH et vieillissement (CHACS, *Canadian HIV an Aging Cohort Study*). Parmi les 164 participants recrutés, un total de 154 participants (âge moyen, 56.5 ans ±7.55 ans; 83 PPLWH, 54 %; 137 hommes; 88%) ont été évalués. Dix participants ont été exclus en raison de données de plaques non disponibles. L'intervalle de temps moyen entre le CT et l'élastographie carotidienne était de 7.7 ± 20.1 mois

Avec l'imagerie par ultrasons, nous avons mesuré la déformation axiale cumulée, la déformation de cisaillement cumulée, la translation axiale cumulée, la translation latérale cumulée et l'IMT des artères carotides commune et interne. Les participants ont également subi une tomodensitométrie cardiaque pour l'évaluation de la plaque coronarienne. Des analyses de régression de Poisson univariées et multivariées avec une variance robuste ont été réalisées pour identifier comment les facteurs de risque cardiovasculaire, les paramètres IMT et élastographie sont indépendamment associés à la présence de plaque coronarienne. La fonction d'efficacité du récepteur (« caractéristique de fonctionnement du récepteur ») (ROC, *receiver operating characteristic*) et l'analyse de l'aire sous la courbe (AUC, *area under the curve*) ont également été utilisées pour comparer différents modèles de prédiction de la présence de plaque coronarienne.

Résultats: Il y avait 83 PVVIH et 71 contrôles (N=154). Le score médian de risque de Framingham sur 10 ans était de 12% [IQR, 8 - 16] chez les PLWH and de 9% [IQR,7 -15] chez les témoins (p = 0.045). Dans le groupe PVVIH, des plaques coronaires étaient présentes chez 55 participants (61,1 %) contre 42 (56,8 %) dans le groupe contrôle non VIH (p = 0,46).

Après ajustement pour les facteurs de risque cardiovasculaire, on note que le tabagisme est associé à la présence de plaque coronarienne (ratio de prévalence 1.10, 95% CI 1.04 – 1.13, p < 0.001). Aucune autre association significative n'a été démontré avec d'autres facteurs de risque cardiovasculaire, ou avec le statut VIH, dans les analyses multivariées. L'analyse multivariée démontre que l'ajout des données d'IMT ou d'élastographie n'augmente pas la précision des modèles, au-delà du modèle n'incluant que les facteurs de risque traditionnels.

Les analyses des courbes ROC et AUC n'ont montré aucune différence significative dans la précision prédictive entre les modèles qui incluent les paramètres d'élastographie, d'IMT et les facteurs de risque cardiovasculaire, versus les modèles qui n'incluent que les facteurs de risque cardiovasculaire, avec des AUC allant de 0,65 à 0,68.

Conclusion: Dans notre étude, les modèles incluant l'élastographie carotidienne et l'IMT n'ont pas montré d'augmentation de la prédiction de la présence de plaque coronarienne chez les PVVIH ou les contrôles, en comparaison aux modèles incluant uniquement les facteurs de risque traditionnels.

Mots clés : VIH, tomodensitométrie, angiographie, élastographie, athérosclérose

Abstract

Aim: This study aims to assess the association of biomechanical characteristics of carotid walls and carotid intima-media thickness (IMT), as assessed by ultrasound, when incorporated into prediction models for coronary CT plaque burden in both people living with HIV (PLWH) and HIV-negative control individuals.

Methods: In this cross-sectional study, 164 participants (mean age 57 years ± 8 years; 134 males) with low to intermediate cardiovascular risk were recruited from the ongoing prospective Canadian HIV and Aging Cohort Study (CHACS). Among the 164 recruited participants, a total of 154 individuals (mean age, 56.5 years ± 7.55 years; 83 PLWH, 54%; 137 males; 88%) were evaluated. Ten participants were excluded due to unavailable coronary plaque data. The mean time interval between coronary CT and carotid ultrasound per participant was 7.69 ± 20.1 months.

Using ultrasound, cumulated axial strain, cumulated shear strain, cumulated axial translation, cumulated lateral translation, and IMT of the common and internal carotid arteries were measured. Participants also underwent cardiac CT for coronary plaque assessment. Univariate and multivariate Poisson regression analyses with robust variance were performed to identify independent associations of cardiovascular risk factors, IMT, and elastography parameters with coronary plaque presence. Receiver operating characteristic (ROC) curve analysis and the area under the curve (AUC) were used to compare different prediction models for coronary plaque presence.

Results: The study included 83 PLWH and 71 controls (N=154). The median 10-year Framingham risk score was 12% [IQR, 8 - 16] in PLWH and 9% [IQR, 7 - 15] in controls (p = 0.045). In the PLWH group, coronary plaques were observed in 55 participants (61.1%) compared to 42 (56.8%) in the non-HIV control group (p = .46). Carotid IMT and all elastography features for both the internal and common carotid arteries were similar between PLWH and healthy volunteers.

After adjusting for cardiovascular risk using multivariate Poisson regression, smoking exposure was significantly associated with coronary plaque presence on CT (prevalence ratio 1.10, 95% CI 1.04 – 1.13, $p < 0.001$). No significant associations were found with other coronary artery disease risk factors or HIV status in multivariate analysis. Carotid elastography parameters and carotid intima-media thickness were not associated with coronary atherosclerosis after adjustment.

AUC analyses did not reveal any significant differences in predictive accuracy between models when adding either elastography parameters, IMT, or both elastography parameters and IMT results to the cardiovascular risk factor model, with AUC ranging from 0.647 to 0.681 in all models.

Conclusion: In our study, models incorporating carotid elastography and IMT did not enhance the prediction of coronary plaque presence in PLWH or controls, compared to models including only traditional cardiovascular risk factors.

Key words: HIV, computed tomography, angiography, us elastography, atherosclerosis

Table of Contents

List of Tables

List of Figures

List of Abbreviations and Symbols

AIDS: Acquired Immunodeficiency Syndrome

ART: Anti-Retroviral Therapy

AUC: Area Under the Curve

CAD: Coronary Artery Disease

CAS_CCA Cumulated Axial Strain of Common Carotid Artery (%)

CAS_ICA Cumulated Axial Strain of Internal Carotid Artery (%)

CAT_CCA Cumulated Axial Translation of Common Carotid Artery (mm)

CAT_ICA Cumulated Axial Translation of Internal Carotid Artery (mm)

CCA: Common Carotid Artery

CCTA: Coronary Computed Tomography Angiography

CHACS: Canadian HIV and Aging Cohort Study

cIMT: Carotid Intima-Media-Thickness

CLT_CCA Cumulated Lateral Translation (mm) of Common Carotid Artery (mm)

CLT_ICA Cumulated Lateral Translation (mm) of Internal Carotid Artery (mm)

CShS_CCA Axial Shear Strain Magnitude of Common Carotid Artery (%)

CShS_ICA Axial Shear Strain Magnitude of Internal Carotid Artery (%)

CT: Computed Tomography

CVD: Cardiovascular Disease

HAART: Highly Aggressive Anti-Retroviral Therapy

HDL-C: High Density Lipoprotein-Cholesterol

HIV-1: Human Immunodeficiency Virus type 1

HIV-2: Human Immunodeficiency Virus type 2

IMT: Intima-Media-Thickness

IMT_CCA Intima-Media Thickness of Common Carotid Artery (mm)

IMT_ICA Intima-Media Thickness of Internal Carotid Artery (mm)

IOR: Interquartile Range IQR

MI: Myocardial Infarction

MRI: Magnetic Resonance Imaging

NIVE: Non-Invasive Vascular Elastography

PLWH: People Living with HIV

ROC: Receiver Operating Characteristic curve

SD: Standard Deviation

SE: Strain Elastography

ŧ: Chi-Square Test

©: Copyright

♦: Mann–Whitney Test

*: Student's t-Test

Acknowledgements

There are no proper words to convey my deep gratitude and utmost respect for my thesis and research supervisor, Dr. Carl Chartrand-Lefebvre. His unwavering support, invaluable advice, constant availability, and the opportunity to work on this master's project have been instrumental in my success. His scientific approach has played a pivotal role in helping me accomplish this task.

I would like to express my sincerest appreciation to Dr. Madeleine Durand, my master's co-director, for her consistent support and guidance, and her scientific expertise.

I extend heartfelt thanks to Dr. Manel Sadouni for her unfailing assistance in every aspect as needed. Her support, advice, and availability have been invaluable throughout this journey.

A special thanks is reserved for my family. To my father, Abdurahman, and my mother, Zohra, whose boundless love, prayers, and unwavering support have been a constant source of strength, even across the miles that separate us. Thank you for being in my life.

My heartfelt thanks go to my husband, Sayf, for his great support, encouragement, and patience through the challenging journey of life. I also want to thank my little sons, Elias, Eyad, and Adam, whose presence has brought me immeasurable happiness, and whose patience has been a source of inspiration throughout my academic years.

A special appreciation goes to my government, the Libyan government, for providing the scholarship that made it possible for me to complete my master's program overseas. Their financial support has been indispensable to my academic journey.

Chapter 1:

LITERATURE REVIEW

HIV-1 and HIV-2, both part of the Retroviridae family, have the capacity to infect and replicate within the human body. Notably, HIV-1 is responsible for the majority of cases of acquired immunodeficiency syndrome (AIDS). As of the end of 2020, the estimated number of newly acquired HIV cases worldwide stood at 1.5 million [1.0 million to 2.0 million], contributing to a cumulative total of 79.3 million [55.9 million to 110 million] people infected with HIV since the global outbreak began (1). Globally, the highest concentrations of infected individuals are found in Eastern and Southern Africa. At the end of 2018, Canada reported approximately 62,050 people living with HIV (PLWH). In other words, there were 167 HIV-positive individuals for every 100,000 Canadians. Among the provinces, Quebec recorded the third-highest provincial diagnosis rate at 7.4 per 100,000 population, trailing behind Saskatchewan (16.9 per 100,000) and Manitoba (8.8 per 100,000))(2).

1.1.1. Epidemiological Observations

Epidemiological studies have consistently indicated that the most common mode of HIV transmission is through unprotected sexual contact with an HIV-infected partner (3, 4). HIV can also be transmitted via contaminated blood, through transfusions or the shared use of infected needles among individuals who inject drugs or in healthcare settings (5). Vertical transmission of HIV from mothers to their infants during pregnancy, labor, delivery, or breastfeeding has also been documented in cases where mothers are not receiving antiretroviral therapy (6).Globally, an estimated 37.7 million [30.2 million–45.1 million] people were living with HIV in 2020. That same year, approximately 680 000 [480 000–1 million] people worldwide lost their life due to AIDS-related illnesses, compared to 1.9 million [1.3 million–2.7 million] recorded in 2004 and 1.3 million [910 000–1.9 million] in 2010. This represents a 47% reduction since 2004 (1).

Despite the notable increase in accessibility to antiretroviral treatment by the end of June 2021—reaching 28.2 million people compared to 7.8 million [6.9 million to 7.9 million] in 2010 (1), there remain 10.2 million [9.8 million to 10.2 million] individuals who have not

yet received any form of HIV therapy. This underscores the ongoing need for global efforts to ensure the availability of antiretroviral treatment to all infected individuals, particularly in low-income countries.

1.1.2. Origin of HIV

The origins of HIV are believed to be traced back to a species of monkeys in West Central Africa, where it evolved from the simian immunodeficiency virus (SIV). Subsequently, the virus was transmitted to humans following contact with the infected blood of these primates (7, 8).

Intriguingly, four distinct classes of HIV-1 have been identified and classified based on four separate events leading to human transmission, denoted as groups M (Main), O (Outlier), N (New), and P (possible) (9, 10) .

The M group accounts for a large proportion of HIV-1 infections worldwide and was first identified in 1981. It comprises nine different subtypes (A, B, C, D, F, G, H, J, K), with subtype B being the most prevalent in North America (11). Group O was first identified in Central Africa in 1990 (12), while the N subgroup was discovered in Cameroon in 1998, albeit in only a few cases (13). Additionally, the P group was isolated from two individuals, also in Cameroon (14).

Phylogenetically, two possible origins of HIV have been proposed. The HIV-1-related genome is believed to have originated from the chimpanzee species Pan troglodyte (troglodytes), known as SIVcpzPtt (15). Conversely, HIV-2 is likely derived from the SIV of sooty mangabey (SIVSM) lineages (7, 16). and is predominantly found in West Africa, with milder infection effects compared to HIV-1 (16).

These phylogenetic investigations have enabled researchers to estimate the time of HIV transmission to humans. The initial three groups (M, N, and O) were transmitted to humans in the early 20th century, while the precise timing of the P group's transmission remains unclear (17). Regardless of its origins, HIV spreads rapidly due to frequent mutational changes driven by the error-prone nature of the virus's reverse transcriptase enzyme and recombination events affecting its human hosts.

1.1.3. HIV Discovery

In the summer of 1981, an increase in the occurrence of rare cancers, including Kaposi's sarcoma, and specific opportunistic infections like Pneumocystis jiroveci, was reported among homosexual couples in New York and California (18). Furthermore, some of these patients exhibited significantly reduced CD4+ lymphocyte counts and persistent lymphadenopathy. These observations raised concerns among clinicians that these individuals might be suffering from a similar immunodeficiency condition, prompting them to seek an etiologic agent behind this ailment. Initially, sexual transmission was hypothesized due to its high incidence among homosexual men (19, 20). Concurrently, in the United States, similar patterns were observed among individuals for whom blood transmission was suspected (21).

In 1983, in France, Françoise Barré-Sinoussi and her colleague Luc Montagnier at *Institut Pasteur* identified the HIV-1 virus by culturing T-cells from an infected lymph node (22). Initially, this infectious agent was referred to as lymphadenopathy-associated virus (LAV). Interestingly, this virus bore similarities to the Type I and Type III Human T-Lymphotropic Viruses (HTLV-I and III) previously discovered by Robert Gallo in the United States (23). By 1986, LAV and HTLV-III were recognized as a single virus and were named the human immunodeficiency virus (HIV) (24).

1.1.4. Anti-Retroviral Therapy for HIV-1 Infection

The primary objective of antiretroviral therapy (ART) is to reduce HIV-related illnesses and mortality. This is accomplished by employing effective ART that suppresses HIV-1 viremia to low, preferably undetectable levels, as per available tests. Maintaining plasma HIV-1 RNA at undetectable levels offers several benefits to individuals with HIV. It not only extends their lifespan but also enhances their immune system and overall well-being. This reduction in viral load decreases the risk of AIDS-related comorbidities. Ultimately, it helps them achieve a life expectancy nearly equivalent to that of individuals without HIV (25).

Another goal of ART is to minimize the risk of HIV transmission between sexual partners and from HIV-positive parents to their children through vertical transmission. Increased plasma HIV RNA concentrations are a significant risk indicator for HIV transmission (26, 27, 28).

A groundbreaking advancement in HIV treatment was witnessed in the mid-1990s. Widespread use of ART in the advanced world led to a substantial decrease in illnesses and deaths (29).

Initially, in 1987, treatment began with a nucleoside reverse transcriptase inhibitor, namely zidovudine (AZT) (30). However, AZT had significant side effects, including high initial doses that were exceedingly toxic. This led to inadequate viral inhibition, resulting in the emergence of numerous drug-resistant strains (31).

Subsequently, the combination of drugs showed remarkable progress in slowing the progression of HIV disease and proved superior to monotherapy treatment (32). Nevertheless, the landscape of HIV treatment has evolved significantly over the last two decades, highlighting the changing challenges in managing HIV treatment.

Currently, approved antiretroviral (ARV) medications are categorized into seven drug classes, each affecting different stages of the viral life cycle:

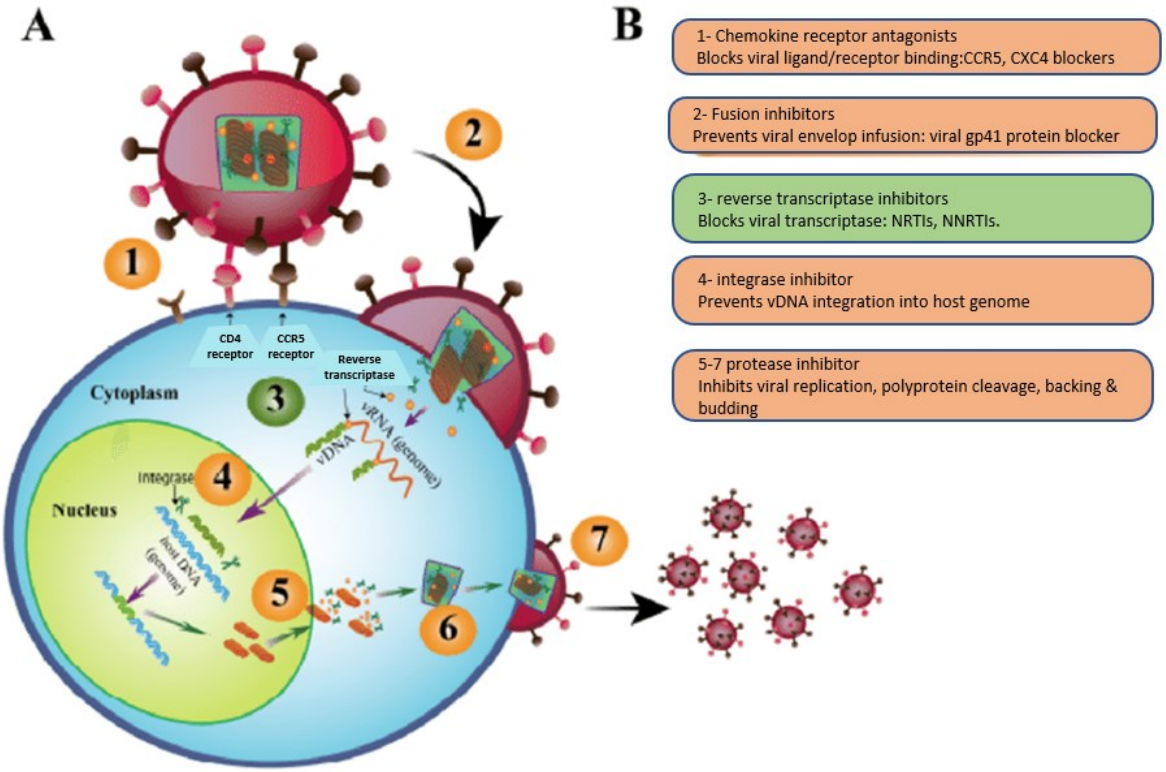

Figure 1

A) HIV-1 infection pathway and (B) Antiretroviral drug (ARV) action site. The numbers in part (A) show the ARVs target action site of part (B).

vRNA, viral RNA genome; vDNA, complimentary viral DNA(33).

1- Nucleoside Reverse Transcriptase Inhibitors

Nucleoside reverse transcriptase inhibitors (NRTIs) were the initial medications used for HIV treatment. They function by inhibiting the reverse transcriptase enzyme, which converts HIV RNA into DNA. This inhibition effectively blocks the process of reverse transcription, preventing HIV replication. This class comprises abacavir (ABC), didanosine (ddI), emtricitabine (FTC), lamivudine (3TC), stavudine (d4T), tenofovir alafenamide (TAF), tenofovir disoproxil fumarate (TDF), and zidovudine (ZDV) (34).

2-Non-Nucleoside Reverse Transcriptase Inhibitors

The introduction of the non-nucleoside reverse transcriptase inhibitors (NNRTIs) class occurred in 1996. The primary generation of NNRTIs includes nevirapine, delavirdine, and efavirenz. The subsequent generation, marked by enhanced resistance capabilities, includes etravirine and rilpivirine (35). These inhibitors bind directly to the HIV-1 reverse transcriptase at a hydrophobic site distinct from the enzyme's active site, inducing a conformational change that prevents substrate binding (36).

3-Protease Inhibitors

In contrast to reverse transcriptase inhibitors that interfere with transcription, protease inhibitors (PIs) act by suppressing the protease enzyme's activity within infected cells, thereby impeding further viral replication (37).

This class encompasses atazanavir (ATV), darunavir (DRV), fosamprenavir (FPV), indinavir (IDV), lopinavir + ritonavir (LPV/r), nelfinavir (NFV), ritonavir (RTV), saquinavir (SQV), and tipranavir (TPV).

4-Integrase Strand Transfer Inhibitors

Integrase strand transfer inhibitors halt HIV replication by blocking the action of the HIV integrase enzyme, responsible for inserting viral DNA into the host CD4 cells' DNA (38).

This category encompasses bictegravir (BIC), cabotegravir, rilpivirine, dolutegravir (DTG), elvitegravir (EVG), and raltegravir (RAL).

5-Fusion Inhibitors

Fusion inhibitors operate by preventing the fusion of the HIV envelope with the membrane of host CD4 cells. Enfuvirtide (ENF) or T-20 stands as the sole FDA-approved drug in this category (39).

6-CCR5 Antagonists

This class prevents HIV from entering immune cells, such as CD4 T-lymphocytes, by obstructing the CCR5 co-receptors located on their surface. Maraviroc serves as an example within this class and received FDA approval in 2007 for use in combination with other HIV drugs (40).

7-Post-Attachment Inhibitors

Post-attachment inhibitors attach to receptors on the surface of CD4 host cells. Consequently, they prevent the virus from binding to CCR5 and CXCR4 co-receptors and entering the cell. Ibalizumab-uiyk, approved in 2018, falls within this category (41).

1.1.5. Timing of HAART Initiation

The World Health Organization (WHO) currently recommends initiating antiretroviral therapy (ART) as soon as seroconversion is confirmed, regardless of CD4 counts (42). Early treatment reduces the risk of opportunistic infections associated with HIV and curtails substantial CD4 T cell depletion. Additionally, it diminishes the likelihood of significant HIV reservoir development (43). Furthermore, prompt treatment initiation is advised as part of comprehensive prevention measures. This recommendation is based on the findings of various studies that explored the advantages of commencing ART early, including the Strategic Timing of Anti-Retroviral Therapy (START) study and the Strategies for Management of Anti-Retroviral Therapy (SMART) trials (44). In the SMART study, which compared continuous ART with CD4+ count-guided interrupted ART, it was revealed that ongoing ART (regardless of CD4 counts) reduced the risk of opportunistic infections and lowered mortality risk (45). Moreover, the HIV Prevention Network Trial 052 (HPNT052), conducted across multiple countries, examined the efficacy of antiretroviral therapy among individuals in sero-discordant couples who had HIV-1. The study found that early initiation and management of antiretroviral treatment in this group, until they achieved viral suppression, significantly reduced the sexual transmission of HIV infection to their partners because they were no longer infectious (26).

ART has effectively lowered plasma viral load in PLWH, but it is not sufficient to completely eliminate the virus. Despite increased investment, the quest for an efficient HIV vaccine remains unfulfilled (46, 47).

1.1.6. Antiretroviral Therapy for HIV Prevention

Antiretroviral therapy can effectively prevent HIV infection in individuals who do not have the virus but are at a higher risk of contracting it. This includes serodiscordant heterosexual couples and men who have sexual intercourse with other men. This preventive strategy is known as pre-exposure prophylaxis (PrEP) (48). Research studies, such as the Proud study (which examined continuous PrEP use) and the Ipergay study (which examined intermittent PrEP use), have demonstrated that the use of PrEP before engaging in sexual contact reduces the risk of HIV transmission by 86% (49). Additionally, PrEP has been shown to be a cost-effective prevention method(50).

1.2. Atherosclerosis in HIV

1.2.1. Background

Atherosclerosis is more prevalent in PLWH, whether they receive ART or not (51). Due to improved access to antiretroviral medications, PLWH receiving regular ART now enjoy longer life expectancy but are susceptible to age-related ailments, including neurocognitive conditions associated with HIV (52) and cardiovascular diseases (CVD) (46, 47, 53). Myocardial infarction and stroke, both linked to atherosclerosis-related CVD, are currently among the leading causes of mortality in HIV-positive patients (54, 55). However, the mechanisms responsible for HIV-induced atherogenesis remain incompletely understood. The available information, which primarily stems from clinical observations, explains the pathological aspects of HIV infection, immune cell activation, and the molecular and cellular processes contributing to atherosclerosis.

1.2.2. Role of ART in Atherosclerosis-Associated CVD

Cardiovascular diseases associated to atherosclerosis, including conditions like myocardial infarction and heart failure, have been increasingly observed with the development of ART(56). In the D:A:D study (Data Collection on Adverse Effects of Anti-HIV Drugs), the use of PI or NNRTI drug classes, either individually or in combination with other ART regimens, was found to lead to dyslipidemia, elevating the risk of coronary heart disease, particularly among older participants with normal CD4 cell counts and suppressed viral load (57). Results from Strategies for Management of Antiretroviral Therapy (SMART) study revealed that HIV patients with CD4 counts below 350/µl who adhere to ART have a reduced likelihood of experiencing CVD and AIDS-related complications. Conversely, individuals who fail to adhere to their ART regimen face a 70% higher risk of developing cardiovascular disease, underscoring the importance of treatment adherence in achieving optimal outcomes in HIV management (58).

1.2.3. High-Risk Atherosclerotic Plaque Characteristics in HIV

In the general population, noncalcified coronary plaques identified through coronary computed tomography angiography (CCTA) are typically associated with a higher incidence of acute coronary syndrome when compared to calcified or mixed plaques (59, 60, 61).On the contrary, in HIV+ patients, non-calcified plaques are detected in the earliest stages of atherosclerotic changes and pose a greater risk of rupture and subsequent blood clot formation than calcified plaques (59). Consequently, HIV individuals are at an elevated risk of developing acute coronary syndrome (59).

Moreover, it has been observed that asymptomatic HIV-infected individuals without recognized cardiovascular disease are more likely to exhibit a higher burden of noncalcified coronary plaques compared to non-HIV individuals (62).
A meta-analysis study has shown a correlation between lower CD4 cell counts in HIV+ patients and the presence of noncalcified coronary artery plaques, supporting the theory that systemic inflammatory dysregulation in HIV+ patients contributes to coronary heart disease (59). All this evidence underscores the role of inflammatory processes and immune cell activation triggered by HIV in the increased prevalence of atherosclerosis in HIV+ patients.

1.2.4. Biomarkers Related to HIV-Associated Atherosclerosis

Biomarkers play a crucial role in initiating immune system responses and inflammatory processes in HIV-related cardiovascular diseases. Clinical studies have linked the activation of monocytes and specific substances in plasma macrophages to HIV-related cardiovascular diseases. For instance, there is an association between the presence of plasma-soluble CD163, a monocyte macrophage activation marker, and the existence of

non-calcified plaques in HIV+ males (63). A higher likelihood of cardiovascular conditions has also been linked to the presence of certain nonspecific immune markers, including D-dimer, IL-6, and CRP. This association was observed in the SMART trial, independent of other common causes of cardiovascular disease (64). Additionally, it has been reported that elevated D-dimer and IL-6 levels are linked to increased mortality. Atherogenesis primarily depends on the presence of inflammation (65). Cardiovascular disease has also been linked to elevated levels of IL-6, CRP, and D-dimer. Furthermore, IL-6 and D-dimer levels are elevated in PLWH, and these levels decrease with regular ART use, suggesting that discontinuing ART could lead to increased inflammatory processes and a higher risk of cardiac events (65, 66).

1.2.5. Cellular Mechanism in HIV-Associated Atherosclerosis

Atherosclerosis is an ongoing inflammatory process that initiates endothelial cell damage through both immune and non-immune mechanisms, marking the initial phase of atherosclerosis. Subsequent endothelial cell damage triggers the production of pro-thrombotic and pro-inflammatory cytokines, along with adhesive substances that promote the expansion of inflammatory reactions by recruiting T-cells and monocytes. Within the intima, oxidized low-density lipoproteins (oxLDL) are phagocytized by macrophages, forming foam cells, and eventually leading to plaque formation—the hallmark of atherosclerosis. Plaque may then rupture, and cause thrombosis and MI. Plaques may subsequently rupture, causing thrombosis and myocardial infarction (MI). An overview of this entire process is illustrated in Figure 2.

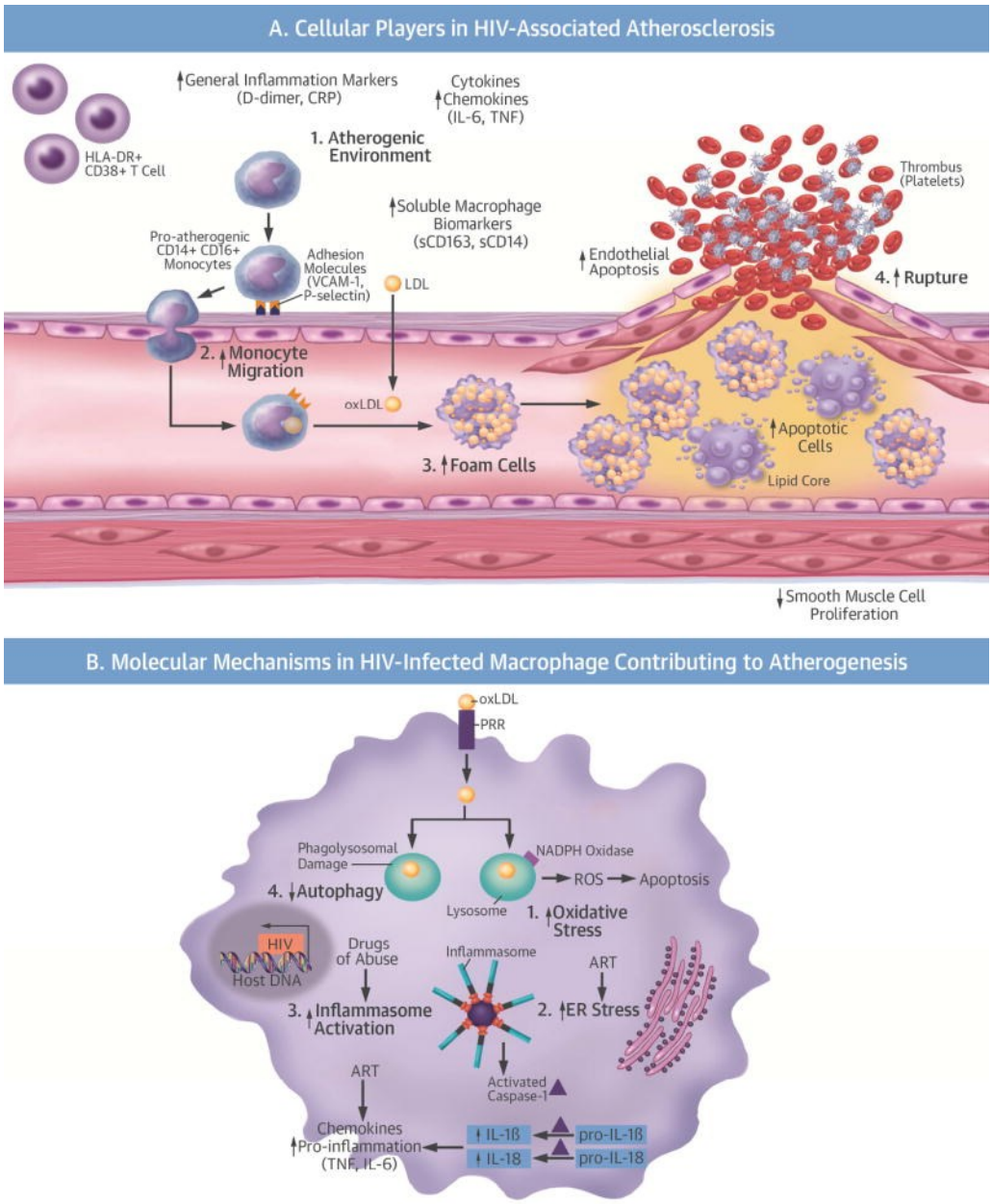

Figure 2.

A) Cellular Players in the Initiation, Progression, and Plaque Rupture of HIV-Associated Atherosclerosis

1. As part of the inflammatory process, the HIV virus increases atherogenic monocytes, HLA-DR+, CD38+ T cells, cytokines, and chemokines.
2. The elevation of atherogenic monocytes and chemokines facilitates monocyte migration into the vasculature.

3. HIV accelerates the formation of foam cells.
4. HIV reduces smooth muscle cell proliferation while increasing endothelial and foam cell apoptosis, rendering the plaque more susceptible to rupture.

B) Atherogenesis-Related Molecular Mechanisms in an HIV-Infected macrophage

1) Elevated oxidative stress (OS).
2) Increased endoplasmic reticulum (ER) stress, which activates the unfolded protein response (UPR) present at all stages of atherosclerotic lesions.
3) Heightened inflammasome activation and cytokine production.
4) Reduced autophagy.

These molecular processes reinforce each other and are further complicated by ART and HIV risk factors and comorbidities.

> ART: Antiretroviral Therapy. CRP: C-Reactive Protein. ER: Endoplasmic Reticulum. HCV: Hepatitis C Virus. HIV: Human Immunodeficiency Virus. IL: Interleukin. LDL: Low-Density Lipoprotein. NADPH: Nicotinamide Adenine Dinucleotide Phosphate. OS: Oxidative Stress. oxLDL: Oxidized Low-Density Lipoprotein. PRR: Pathogen Recognition Receptor. ROS: Reactive Oxygen Species. TNF: Tumor Necrosis Factor. VCAM-1: Vascular Cell Adhesion Molecule-1(67).

1.2.5.1 Macrophages monocytes and foam cells

The macrophage and its role in triggering inflammation and plaque development are arguably the most crucial factors in HIV-related atherosclerosis (68). While T cells are considered the primary cell reservoir for HIV, macrophages and monocytes also play a role in the HIV replication process. They remain continuously infected as the HIV virus remains latent within these cells in patients receiving ART. Tat, Nef, and other potent viral

regulatory proteins are produced at low levels in T cells and monocytes, which can affect their activity (68, 69). Furthermore, during HIV infection, chemokines and their receptors, including CCL2, CX3CR1, and CCR5, are increased and may enhance monocyte attraction to the vasculature. Nearly all monocyte movement and accumulation in sclerotic artery walls can be attributed to these chemokines and adhesive particles. The size of atherosclerotic areas has been strongly linked to the quantity of circulating monocytes, thereby facilitating HIV-associated atherogenesis (70). Additionally, HIV Nef protein impairs cholesterol efflux from infected macrophages by interfering with the normal activity of the ATP-binding cassette transporter A1 (ABCA1) (71). This inhibition leads to lipid proliferation, transforming macrophages into foam cells (71).

1.2.5.2. T-Cells

In comparison with HIV-negative participants, activated $CD38^{+}$, $HLA^{-}DR^{+}$ types of T cells were found to be twice as abundant in HIV^{+} patients with viral suppression (72, 73). These T cells release proatherogenic substances that contribute to plaque formation and local inflammation (74). Numerous studies have demonstrated the correlation between these types of activated T-cells and the progression of atherosclerosis (72, 75).

1.2.6. Molecular Mechanisms in HIV-related Atherosclerosis

The molecular processes associated with HIV-related atherosclerosis remain less understood compared to the cellular processes. Here, we elucidate some of the key molecular mechanisms involved in HIV-related atherosclerosis:

1.2.6.1 Oxidative stress (OS)

During the cellular phase, normal oxidation-reduction reactions produce reactive oxygen species (ROS) in regular amounts. When ROS production exceeds normal levels or the cell's antioxidant capacity diminishes, ROS becomes toxic. In HIV-infected patients, ROS levels increase, leading to oxidative stress (OS) (76). HIV^+ patients with high HIV viral replication, low CD4 counts, and elevated cytotoxicity experience heightened OS due to mutational processes affecting antioxidant capacity (69). Several HIV proteins, such as Nef, contribute to endothelial dysfunction by increasing ROS production.

1.2.6.2. Endoplasmic Reticulum (ER) Stress, GP120

The ER regulates calcium levels and oxidation-reduction potential.

In HIV infection, elevated ROS and other factors stimulate the ER stress response, causing vascular endothelial apoptosis (77).

Gp120, an HIV substance, induces type 1 programmed cell death through ER stress via various pathways (78). HIV ART further stimulates ER stress, releasing large amounts of inflammatory cytokines like tumor necrosis factor-alpha (TNF-α) and IL-6, enhancing programmed cell death, and promoting foam cell formation within macrophages (79).

1.2.6.3. NLRP3 inflammasome activation

The inflammasome, a multiprotein complex within cells, detects pathogens like HIV and activates highly pro-inflammatory cytokines. Excessive inflammasome activation occurs in many autoimmune and chronic inflammatory diseases, including atherosclerosis (80). NLRP3 inflammasome activation occurs in HIV-infected T cells, leading to T cell depletion.

1.2.6.4. Inhibition of autophagy

Autophagy is a programmed process that removes toxigenic proteins and degrades defective organelles by merging with lysosomes, enhancing cell survival (86). (81). Autophagy is heightened in macrophages, a key contributor to atherosclerosis progression. However, during HIV infection, these events are altered. Autophagy protects infected immune cells by reducing excess oxidative and ER stress, but it is also inhibited in macrophages of the infected host (67).

1.3. Carotid Artery Disease

1.3.1. Carotid Artery Stenosis

Stroke has emerged as the second leading cause of fatal illness and the third major contributor to disability worldwide (82). Extracranial carotid artery stenosis accounts for approximately 20% of all strokes (83), while stenosis of intracranial carotid artery results in 5 to 10% of strokes among white people (84). Atherosclerosis stands out as a primary factor leading to the narrowing of the carotid artery. As atherosclerosis progresses, atherosclerotic clots may rupture, forming thrombi that subsequently obstructs the carotid artery. Additionally, small fragments from the plaques can dislodge and block smaller branches of the carotid artery (85). Carotid artery disease accounts for roughly half of all transient ischemic attacks (TIAs) (86).

Clinical manifestations of carotid artery stenosis span from asymptomatic cases to symptomatic ones. TIAs and ischemic strokes occur when ipsilateral retinal or cerebral hypoxia takes place. Patients with carotid artery stenosis of 50% or more who exhibit no symptoms commonly suffer from peripheral arterial conditions (15%) (87). Studies have demonstrated that the risk of stroke escalates in tandem with the severity of carotid artery stenosis (88).

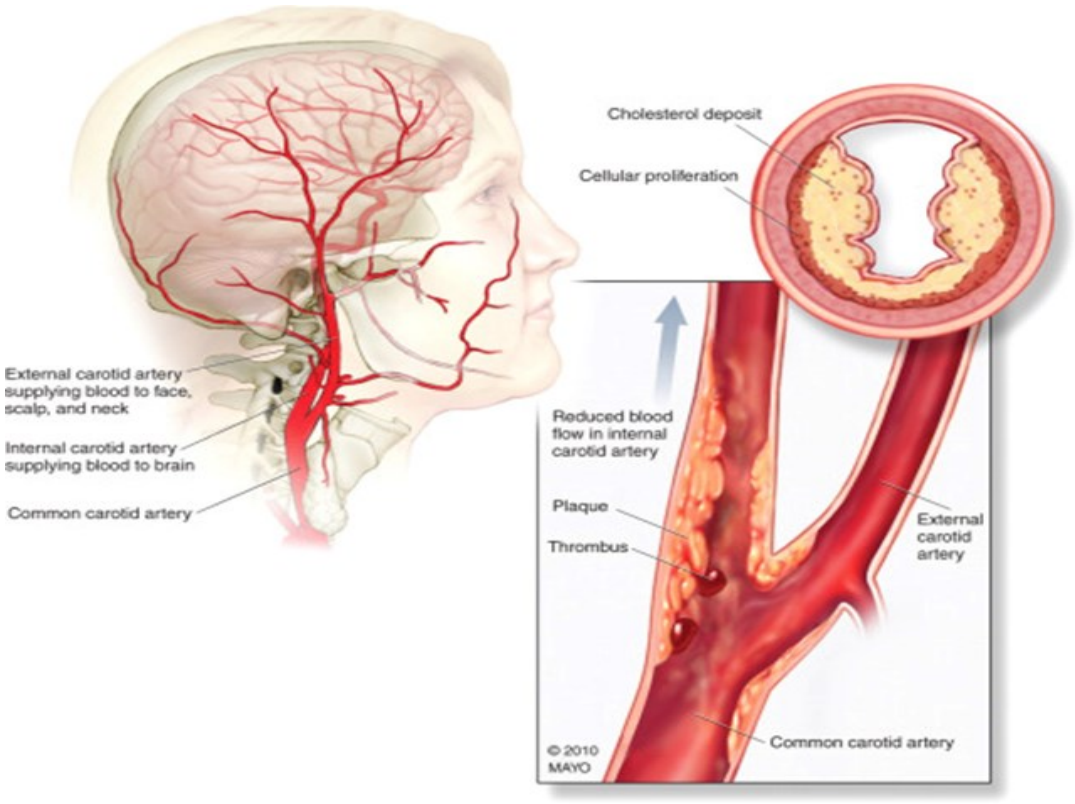

Figure 3. Carotid Artery Disease: Atherosclerotic Plaque at the Carotid Artery's Bifurcation. Plaque causes narrowing of the artery's lumen, disrupts normal blood flow, and fosters the development of thrombi and emboli. These effects result from the deposition of cholesterol and the proliferation of cellular structures(89). Reproduced with permission from copyright 2022.

Serious carotid artery disease is considered when the carotid artery is stenosed by more than 50%, either with or without symptoms. It is crucial to differentiate between asymptomatic and symptomatic carotid artery stenosis, as treatment approaches vary. Typically, asymptomatic patients are treated medically. For hypertensive patients, maintaining their blood pressure below 140/90 mm Hg is essential (90). However, diabetics or patients with renal failure should aim for blood pressure below 130/80 mm Hg (91). Currently, there's uncertainty regarding whether some antihypertensive agents are more effective than others in slowing the progression of carotid atherosclerosis (92). The target LDL cholesterol level should be below 100 mg/dL, preferably achieved with

statin therapy. Additionally, asymptomatic carotid artery stenosis patients should be treated with aspirin, while dipyridamole should be reserved for patients with aspirin sensitivity(93). Lifestyle changes are advised for all diagnosed patients with asymptomatic carotid artery stenosis**,** including regular aerobic exercise (more than 30 minutes, five or more days a week). Smoking cessation is imperative, and adopting a low-saturated-fat diet is essential to achieve a body mass index lower than 25 kg/m^2.(94). Finally, all patients with carotid artery stenosis should receive information about stroke symptoms and be educated on the importance of seeking medical attention immediately if symptoms appear. On the other hand, individuals experiencing symptoms of carotid artery stenosis exceeding 50%, as well as those without symptoms but with stenosis exceeding 60%, require invasive intervention (95, 96).

1.3.1.1. Epidemiology of **Carotid Artery Stenosis:**

Atherosclerosis most commonly affects the area where the carotid artery bifurcates into the external and internal carotid arteries, primarily impacting the internal carotid artery's ostium. Atherosclerosis has a less severe impact on the intracranial internal carotid artery and its smaller trees.(97). According to the Framingham Heart Trial, the incidence of carotid artery stenosis was 9% in males and 7% in females aged around 65 to 90 (98). Notably, approximately 15% of patients with extracranial carotid artery stenosis also had intracranial CAS (99). Several studies have reported a higher prevalence of asymptomatic carotid artery stenosis among patients with peripheral arterial disease (100, 101, 102). Furthermore, carotid atherosclerotic plaques exhibit variations in size and composition between carotid arteries. Left-sided carotid plaques are more prone to intraplaque hemorrhage, suggesting greater susceptibility to rupture compared to right-sided lesions, which tend to be more rigid due to higher calcification levels (103).

1.3.1.2. Pathogenesis of Carotid Artery Stenosis

Carotid artery stenosis involves the regional expansion of the arterial wall intima, resulting in a gradual reduction in the carotid artery's lumen due to atherosclerosis.

The typical categories of lesions include fatty streaks, fibrous caps, and complex elements that vary depending on the progression of atherosclerosis (104). Carotid atherosclerotic lesions consist of a central fatty area infiltrated by inflammatory cells, encased by a fibrous cap.

This fibrous cap consists of the following: (A) smooth muscular cells, white blood cells, thick connective tissue (including elastic tissue, collagen fibres, proteoglycans), and a basement layer (B). Just beneath it lies a cellular layer composed of macrophages, smooth muscle tissue, and T lymph cells (C). Finally, the deep necrotic core contains calcium deposits, lipids, and fat particles.

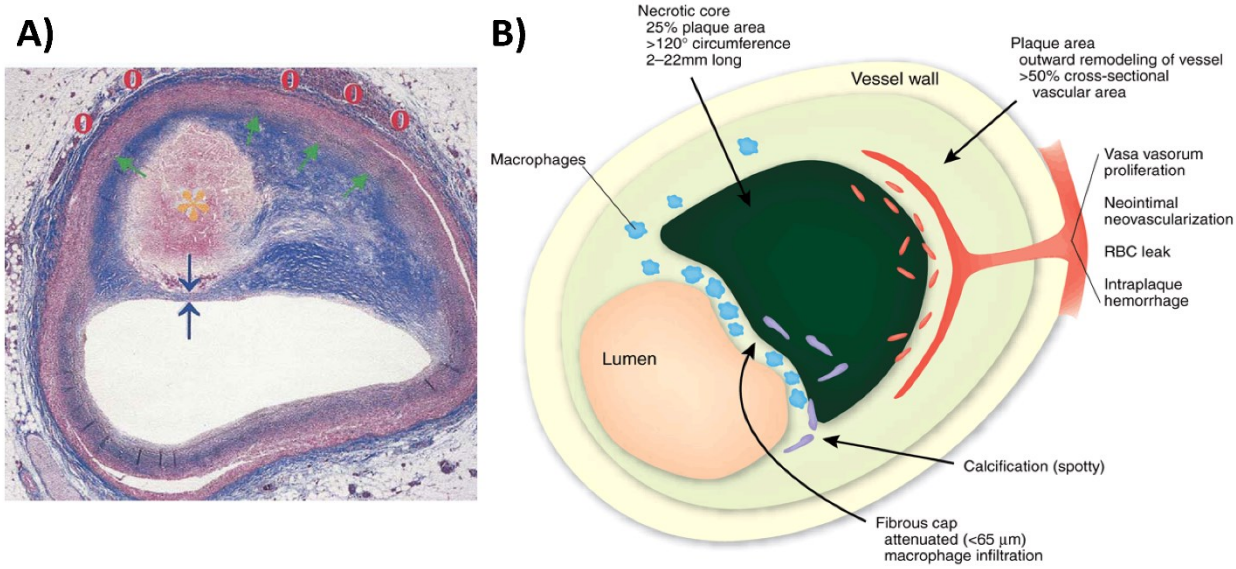

Figure 4. (A) Cross section of a coronary artery plaque prone to rupture, characterized by: (1) a large lipid-rich necrotic core (orange asterisk), (2) a thin fibrous cap (blue arrows), (3) expansive remodeling (green arrows), and (4) vasa vasorum and neovascularization (red circles). Reproduced from Falk et al., 2006(105) (B) (B) Schematic of a vulnerable plaque depicting a vulnerable plaque, showcasing the features associated with plaque instability (106).

Note: This figure is part of an open-access article from PMC and is in the public domain, allowing its use and reproduction without requesting special permission.

Over time, plaques can grow large enough to narrow the lumen of the carotid artery. These plaques may remain stable, causing no symptoms, or they may become mobile, leading to embolization. Vulnerable or unstable plaques, which are more prone to rupture, are characterized by extensive inflammation, substantial macrophage production, a thin fibrous cap surrounding a large lipid center, endothelial denudation with surface-level platelet accumulation, scars, and significant stenosis (107). Plaque rupture occurs when leukocytes within the intima secrete metalloproteinases due to extracellular matrix remodeling. This process leads to a thinning of the fibrous cap, making the plaque more susceptible to rupture (108).

1.3.2.1. Carotid Artery Stiffness

Arterial stiffness can be influenced by various factors, including aging, inflammation, and cardiovascular disease. Inflammation itself can lead to early changes that affect the structural formation of arterial walls. (109). Aging also induces alterations in arterial structure and function that may lead to arterial wall stiffening (110). Numerous studies have established a link between evidence of carotid artery stiffness and an increased incidence of stroke (109, 111, 112, 113).

However, the relationship between arterial stiffness and stroke may involve multiple mechanisms.

Increased arterial stiffness results in the early return of reflecting waves at the end of systole, leading to elevated systolic pressure and an increase in central pulse pressure. This, in turn, places more strain on the left ventricle, potentially leading to left ventricular hypertrophy and heart failure. Additionally, changes in the diameter of the arterial lumen, distensibility of the common carotid artery, and an increase in arterial volume are associated with an enlargement of the left ventricular cavity. Consequently, arterial wall stiffness can be considered a robust predictor of cardiovascular morbidity (114).

Alterations in wall diameter and stiffness, influenced by vascular endothelial function, also impact arterial compliance, contributing to the development of cardio-cerebrovascular diseases (115).

Several studies have investigated the molecular and cellular factors influencing arterial stiffness (116, 117). The stiffness of the vascular wall is primarily determined by the relative contribution of two major proteins: collagen and elastin. Vascular stiffness results from an excess of abnormal collagen and a reduction in the quantity of normal elastin. Recent immunohistochemical and ultrastructural research findings clearly indicate that arterial stiffness is not only influenced by the quantity and density of these stiff wall components but also by their spatial organization. These two components are predominantly located in the intercellular matrix of the blood vessel wall and are responsible for its strength and flexibility. Collagen has a slow hydrolytic turnover rate, leading to its accumulation during the arterial stiffness process. Elastin, normally stabilized in the matrix as desmosine and isodesmosine, experiences weakening due to deposits of minerals such as calcium and phosphorus during the inflammatory process associated with arterial stiffness (118, 119).

Elevated arterial pressure leads to arterial remodeling, which occurs concurrently with thickening of the arterial wall, the promotion of plaque formation, and the development of atherosclerosis. This process can eventually result in ulceration or rupture of atherosclerotic plaques. As arterial stiffness increases, the ability to regulate pulsatile circulation diminishes, leading to increased resistance within the aorta and arterial branches. These resistances subsequently affect cerebral microvascular function and cognitive performance. (120).

Stiffness can be assessed using a range of techniques and at different arterial segments or sites. Some techniques are: **“segmental carotid-femoral pulse wave velocity (cfPWV)”** (121), **“local carotid, femoral, or brachial artery stiffness, and systemic arterial**

compliance (SAC) assessment" (122). additionally, **"the aortic augmentation index (Aix) can be used as a wave reflection surrogate"** (122).

Given the variability in arterial stiffness across the arterial network and the distinct characteristics of elastic and muscular arteries, assessing arterial stiffness at different points is essential for a comprehensive evaluation.

1.3.2.2. Carotid Artery Stiffness in HIV

Arterial stiffening is a complex process characterized by changes in the structure and function of the arterial wall, which naturally occur with aging and are exacerbated by various conditions, including type 2 diabetes mellitus, arterial hypertension, and renal failure (123). In addition to these traditional risk factors, endothelial dysfunction induced by acute and chronic inflammation is associated with arterial stiffness (124).

This association is exemplified in chronic inflammatory diseases such as rheumatoid arthritis (125).

One explanation for this chronic inflammation is that people living with HIV exhibit elevated levels of circulating pro-inflammatory cytokines and an increased number of circulating CD4+ and CD8+ T cells, indicating ongoing activation through elements like CD38 and HLA-DR. These atypical T cell counts may only be reversed in the short term with successful antiretroviral therapy (126, 127). Subclinical carotid artery abnormalities have been linked to HIV-associated T cell alterations, which can persist even in patients who have achieved viral suppression through effective antiretroviral therapy (128).

While most studies have linked HIV-related immune-mediated consequences with increased arterial wall thickness (73, 129), it's important to note that vasculitis, a pathological vascular condition, could also account for arterial stiffness in PLWH. The pathogenesis of systemic vasculitis has been linked to viral infections, and HIV, like some other viruses, has been associated with vasculitis. In the context of HIV, various types of vasculitis affecting small, medium, and large vessels have been reported (130). Typically, it is confined to specific vessels in individuals with a progressive decline in the immune

system and may be linked to T lymphocyte infiltration (131). Recent research suggests that chronic HIV infection can lead to modifications in arterial tissue, resulting in a reduction of typical arterial elastic properties and vasoreactivity. Carotid artery biopsies from HIV-infected patients with carotid artery stenosis have revealed destruction of elastic fibers and infiltration of inflammatory cells into the vascular wall (132).

Furthermore, co-infections can trigger HIV-related vasculitis. For example, co-infection with "**CMV, Herpes zoster virus, toxoplasmosis, pneumocystis, salmonella, and Mycobacterium tuberculosis**" has been reported to cause vasculitis in PLWH (139). Infection can lead to vasculitis through two primary mechanisms: direct microbial invasion causing vessel wall damage or immune-mediated injury (both cellular and humoral).

The use of ART has also been associated with increased carotid artery stiffness. The Multicenter AIDS Cohort Study (MACS) found that rigidity increased with the introduction of ART(133).

1.4.1 Carotid Intima-Media Thickness

Carotid intima-media thickness (CIMT) is a test that measures the space between the intima and media adventitia layers of the arterial wall. It is useful for detecting changes in vessel wall thickness and the presence of arterial plaques. IMT is visualized and assessed as a double-line arrangement on the two walls of the common carotid artery longitudinal images (CCA)(134). It is a widely used indicator for assessing subclinical atherosclerosis in the general population and predicting future cardiovascular disease (CVD) events (135), as well as in HIV population (129, 136). Therefore, for the accurate

assessment and management of potential strokes, precise measurements of IMT and plaque in vessel walls are invaluable (137).

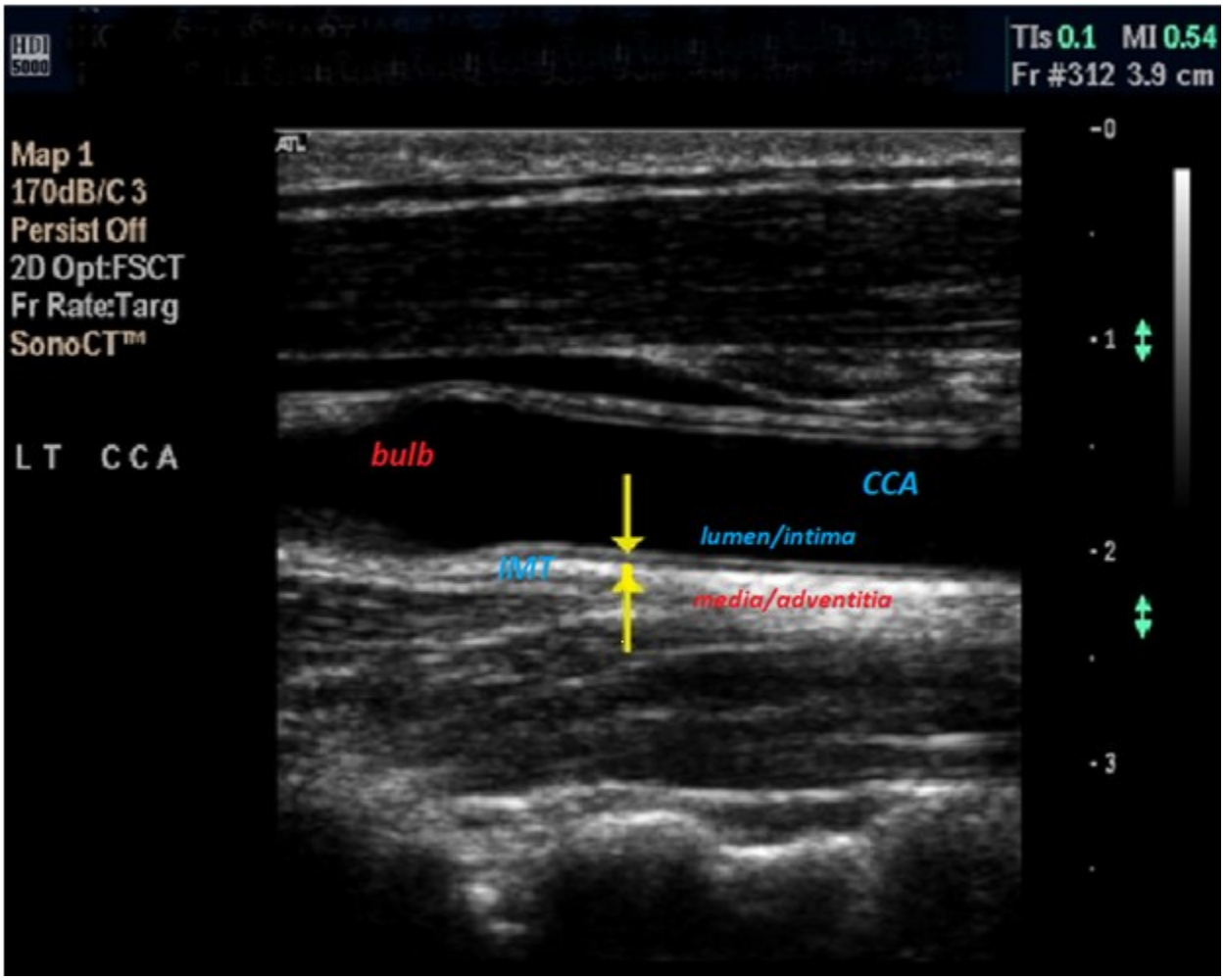

Figure 5. Intima-Media Thickness (IMT). Measurement of carotid intima-media thickness (IMT) with a double-line arrangement on the far wall of the common carotid artery (138). Note: This figure is part of an open-access article from PMC and is in the public domain, allowing its use and reproduction without requesting special permission.

In a healthy carotid artery, the intima-media thickness can reach 0.8 mm (139), It is considered abnormal when values exceed 1.20 mm (140). Moreover, CIMT increases by 0.005 to 0.010 mm annually (141). Consequently, in young adults, a CIMT measurement exceeding 1.00 mm is typically indicative of abnormal thickness (142). The thickening of IMT is associated with endothelial dysfunction, resulting in abnormal vasomotion and

smooth muscle cell hypertrophy, preceding the appearance of plaques. When the measured IMT value exceeds the specified threshold (see above), it indicates the presence of subclinical atherosclerosis. Additionally, factors such as the thickness of the vessel wall (including intima-media thickness), the degree of carotid artery narrowing, and the presence or absence of symptoms all play pivotal roles in determining whether medical or surgical treatment, such as carotid endarterectomy, is warranted (143, 144).

In a study aimed at evaluating the utility of CIMT and coronary artery calcium (CAC) score (CACS) in detecting mild arterial diseases, 86 asymptomatic middle-aged females, considered to have a low risk by the Framingham risk score but with at least one cardiovascular risk factor, were included. This study calculated the average intima thickness, the presence of plaques on CIMT, and the Agatston calcium score for CACS. For this specific population, the results suggest that CIMT, as compared to CACS and other traditional risk measures, may be a more accurate tool for evaluating cardiovascular risk. In contrast, the measurement of IMT was not found to significantly enhance the predictability of cardiovascular risk in another group of individuals. In attempts to improve cardiovascular risk stratification in the general population, the mean common CIMT measurement was used to assess whether there was any improvement over ten years in predicting the risk of first-time stroke or myocardial infarction (MI) in hypertensive patients (145). An extensive individual data meta-analysis involving 17,254 hypertensive individuals from sixteen cohort trials was conducted. In this study, the baseline model included the Framingham Risk Score risk factors of participants without symptoms, and this model was updated by adding measurements of mean common CIMT (CIMT model). The ten-year risk of having a myocardial infarction or stroke was calculated using data from both models. The results indicated that measuring mean common CIMT did not provide additional value in improving cardiovascular risk prediction for individuals with high blood pressure (140).

1.4.2. Carotid Intima-Media Thickness and HIV

Numerous studies have investigated the relationship between HIV infection and CIMT, yielding conflicting results. Some studies have reported higher CIMT values in HIV-infected individuals (146, 147, 148), while others have found associations between PLWH on HAART and higher IMT compared to uninfected individuals (149), particularly those taking protease inhibitors (150). Additionally, some studies revealed no difference in baseline IMT measurements between HIV-infected and non-HIV-infected subjects (151), nor did they observe CIMT progression over time (152).

These conflicting findings can be attributed to various factors, including limited sample sizes in some studies, differences in patient populations, and variations in CIMT measurement methods (average or highest for one assessment, average of the average or highest of multiple measurements). IMT measurements obtained at a single site may differ significantly from measurements taken at another site (153).

Therefore, measuring CIMT at a single location can reduce the accuracy of diagnosing changes in arterial walls.

Furthermore, the timing of CIMT measurements within the cardiac cycle varies across studies. Parameters measured during peak systole yielded smaller values compared to those calculated from end-diastole due to luminal size changes during systole, leading to a decrease in CIMT over systole (154).

The anatomical measurement site of CIMT may cause a difference in measurement. The carotid bifurcation area exhibited the most significant differences between HIV-infected and uninfected groups.

Researchers from the Fat Redistribution and Metabolic Change in HIV Infection (FRAM) study discovered a stronger correlation between HIV infection and carotid IMT in the internal and bifurcation regions of the carotid arteries compared to the common carotid (146).

Therefore, for accurate assessment and effective management of potential stroke risk, precise measurements of IMT are essential.

1.5. Cardiac Imaging

1.5.1. X-ray Imaging

The journey of X-ray imaging began in 1895 when Wilhelm Rontgen made the groundbreaking discovery that X-rays could be utilized to image biological tissues. Due to various optical characteristics, the quantity of radiation undergoes changes when passing through different tissues—some are scattered, while others are attenuated. When this radiation interacts with photographic film, it creates a 2D image. Initially, X-ray imaging found its first applications in the medical field for imaging bones, capitalizing on X-rays' high photon attenuation in calcium-rich bones (155).

In X-ray vascular imaging (X-ray angiography), the injection of a contrast agent becomes necessary to visualize blood flow within blood vessels. Contrast agents, often containing iodine, enhance radiation attenuation as they traverse through blood.

1.5.2. Digital Subtraction Angiography (DSA)

Digital subtraction angiography (DSA) or mask mode subtraction, is a procedure employed for visualizing the vascular lumen and blood flow within vessels under X-ray exposure. Remarkably, DSA uses a reduced amount of contrast agent compared to conventional angiography (156) . In DSA, highly contrasted images of blood vessels are generated by subtracting two X-ray images—one acquired before injecting the contrast agent (the mask) and another taken after the injection. In a comparative study involving 100 participants for carotid artery visualization, DSA demonstrated 95% sensitivity, 99% specificity, and 97% accuracy (157).

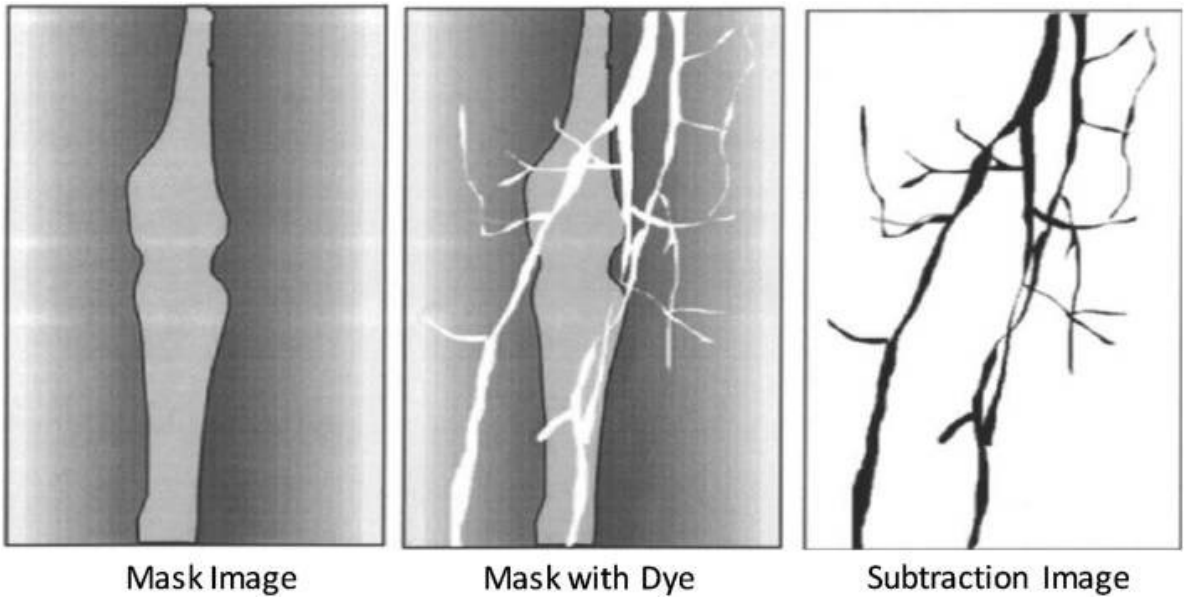

Figure 6. Subtraction image technique employed in DSA (166), utilizing mask and contrast images. Note: This figure is part of an open-access article from PMC and is in the public domain, allowing its use and reproduction without requesting special permission.

1.5.3 Computed Tomography Angiography (CTA)

Obtaining detailed anatomical information through a conventional angiography's 2D images is often limited. The CT scanner was introduced in 1973 to address this issue. This advanced equipment proved to be significantly more precise than conventional X-ray angiography (157, 158). while also reducing the volume of contrast material needed for testing when compared to traditional angiography (159). A CTA scanner comprises an X-ray radiation source aimed at a specific region of the 3D body from one side, with detectors on the opposite side to capture these signals. To create a complete 360° scan, a series of these source-detector pairs rotate around the human body, capturing slice-by-slice images. Newer CTA scanners require less contrast material compared to traditional angiography (159). Advancements in imaging analysis technology have led to the development of semi- and fully automated 3D CTA systems. In semi-automated algorithms, the crucial steps include the manual identification of a segmentation point as

a reference and the selection of appropriate upper or lower limits for contrast intensity. Conversely, in fully automated segmentation techniques, the process involves more intricate technical steps, resulting in a noteworthy 75% accuracy in detecting carotid arteries(160).

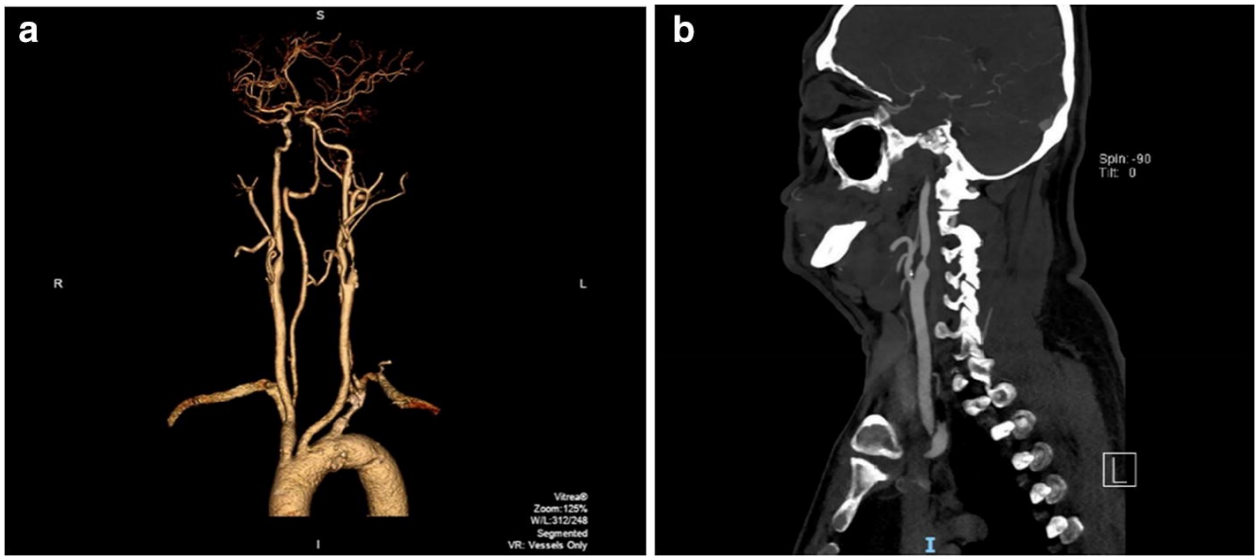

Figure 7. Carotid artery CTA with a 3D reconstruction (a) and a 2D slice image (b) (166). Note: This figure is part of an open-access article from PMC and is in the public domain, allowing its use and reproduction without requesting special permission.

Limitation

Diagnostic radiation exposure and the potential for radioactive materials, including ionizing radiation, have raised significant concerns, particularly in cases requiring long-term monitoring (161, 162). However, newer CT systems empower radiologists to employ more effective dose-saving strategies (163). CT A also presents a significant drawback due to the potential for hypersensitivity reactions to contrast agents (164). Another serious complication of angiographic procedures is contrast-induced nephropathy, which can be caused by the use of contrast agents (165).

1.5.4 MRI

Magnetic resonance imaging technique is achieved by stimulating rotation of protons inside a tissue with various chemical characteristics. by radio frequency pulses. Moving protons line up themselves with the exact direction of the applied field when they meet an externally generated stable field of magnets. However, some protons in a state that have an increased energy, line up in the reverse order to applied magnetic field.

When the radio frequencies signals are removed, the protons go back to their first position and begin to release magnetic resonance signal energies at an amount set by T1and T2 relaxation intervals(166).

When the protons of the increased energy condition begin to fall back to the decreased energy condition in the same way of the external magnetic field, this causes growing again of magnetization in the parallel direction. Measurement of this is done by the T1 relaxation time (spin–lattice relaxation). The time different T1 or T2 is assessed according to the molecular framework under study, and thus provides the basic for creating an MRI image. Such an image gives informative details about the inner structures and boundaries (167).

1.5.5. Magnetic resonance angiography (MRA)

MRA projection imaging is used to introduce image contrast related to the blood moving in the vessels and to reduce the unmoved tissue nearby. To create estimation pictures, techniques such as "**temporal subtraction, inversion excitation, stimulating adjacent regions, and phase shift are used"** (168). In temporal subtraction process, a contrast-enhanced movable tissue picture is created by subtracting a pair of pictures with the same unmoved tissue signals and the blood (different moveable tissue signals.

Time of flight (169) is another method which involves applying particular reversal magnetic field to the rotation of the passing molecules of tissue and deducting one from both pictures containing and excluding inversion are subtracted to remove the static

cellular signal. Both phase-contrast and Time of flight methods are commonly used to detect carotid artery diseases.

1.5.6. Duplex Ultrasound

Duplex ultrasound (DUS) has emerged as one of the most frequently employed techniques for evaluating carotid artery diseases, owing to its precision, non-invasive nature, and cost-effectiveness. This technique amalgamates two distinct approaches: conventional B-mode (greyscale) ultrasound, which captures static images of bodily structures and organs through transmitted sound waves during rest, and color-Doppler ultrasound, which visualizes the dynamics of mobile components or fluids (such as blood) to assess flow parameters like velocity.

B-mode, often referred to as brightness mode, is typically used to generate two-dimensional (2D) cross-sectional images by capturing the reflection of ultrasound waves (echo) from surrounding organs. This imagery is created by placing an ultrasound transducer on the body's external surface and emitting ultrasound pulses. This is commonly referred to as the pulse-echo technique. The resulting 2D image is composed of numerous B-mode lines generated by a pulse-echo sequence.

The pulse-echo pattern is generated by highlighting the bright point corresponding to the object that represents the impulse (170, 171).

In 1986, measuring intima-media thickness using B-mode ultrasound, yielding results that closely match histological details was a significant accomplishment. (172).

Since then, numerous studies have assessed intima-media thickness (IMT) through B-mode ultrasound, aiming to establish a link between the development of carotid atherosclerosis and various cardiovascular disease risk factors (173). For more in-depth information about IMT, please refer to section 1.4.1 on page 38.

1.5.7. Cardiac Computed Tomography

Cardiac computed tomography (CT) is a radiological procedure that enables the imaging of both individual cardiac structures and the heart as a whole. Commonly examined structures include the atria, ventricles, intra-cardiac valves, myocardium, pericardium, and major cardiac vessels. Standard cardiac CT can also offer insights into pulmonary and other mediastinal structures in close proximity to the heart.

A contrast-enhanced CT examination that focuses on the evaluation of the epicardial coronary arteries is known as coronary CT angiography (CCTA). CCTA provides a non-invasive alternative to traditional coronary angiography, offering a swift means to assess patients with intermediate risk for CAD, all without the associated risks of an invasive intra-arterial catheter procedure (174).

The moving epicardial coronary arteries are typically of a few millimeters in diameter. Consequently, to effectively examine them with CCTA, both good spatial and temporal resolution are essential.

Spatial resolution refers to the shortest distance at which two points can be distinguished from each other, whereas temporal resolution is defined as the ability to rapidly acquire images of a movable structure.

The temporal and spatial resolution of cardiac CT has seen significant advancements in recent years. CCTA's improved resolution now allows for the identification of even the distal-most segments of the coronary arteries. With the evolution of CT systems, spatial resolution has significantly improved. It has progressed from 0.5 mm with a 64-slice CT scanner to 0.4 mm with a 128-slice scanner, further advancing to 0.35 mm with a 320-slice CT scanner and 0.17 mm in a 640-slice CT scanner (175). Temporal resolution can now reach less than 50 ms, enabling the imaging of the heart in less than 1 second during a single breath-hold (acquisition time) (176). One clinical indication for CCTA is to assess chest pain conditions in individuals with a moderate pre-test likelihood of cardiovascular disease, especially when they face limitations in conventional testing, such as an uninterpretable ECG or difficulties in performing exercise tests (177). Under optimal

conditions, such as when there is a low pre-test probability of cardiovascular disease, CT can be employed as a screening test. This means that if the CT coronary angiography yields negative (normal) results, no further invasive investigations are required (176). However, in cases where it produces positive findings, additional tests, such as perfusion studies in nuclear medicine or conventional catheter coronary angiography, may be considered, particularly in symptomatic patients. In addition to its advantage of imaging the degree of luminal narrowing, CCTA offers the benefit of simultaneously recognizing and characterizing coronary atherosclerotic plaques. CCTA can identify calcified, mixed, and non-calcified coronary plaques (178, 179, 180). Furthermore, it enables the assessment of the number of coronary plaques, their size, composition, and any changes in the plaques over time.

Non-contrast CT can be utilized to assess the coronary artery calcium (CAC) score (178, 181) (182). The Agatston method is the most commonly employed approach for calculating the CAC score. The Agatston calcium score is determined by assessing the area of each calcified coronary lesion with a peak attenuation density exceeding 130 Hounsfield units (HU), with greater weighting factors applied to lesions exhibiting higher peak attenuation values (174, 183).

The CAC score is valuable for categorizing individuals into low, moderate, or high-risk groups for potential future cardiovascular events. The American College of Cardiology and American Heart Association (ACC/AHA) endorse CAC scoring as a suitable test for certain asymptomatic patients with an intermediate risk of CAD (184). Nevertheless, despite its favorable performance characteristics, CT has several limitations. Firstly, CT coronary angiography encounters challenges related to artifacts arising from high or irregular heart rates. Even though most modern CT scanners boast exceptional temporal resolution, patients with elevated or irregular cardiac beats may still experience suboptimal image quality (174, 185). Stepladder artifacts, as illustrated by example (186). and the presence of extensive calcified changes in arterial walls, leading to blooming artifacts, represent additional limitations. Consequently, the evaluation of coronary artery luminal narrowing can be challenging, potentially leading to incorrect assessments of stenosis severity and

false-positive CT results (187). Furthermore, dense coronary stents can also produce blooming artifacts (188)

Moreover, radiation exposure associated with cardiac CTA can induce gene changes related to the regulation of apoptosis and DNA repair processes (189). In recent years, CT techniques have made significant advancements aimed at reducing the radiation dose in cardiac CT, including prospective ECG-gating (163), axial adjustment of the x-ray tube output (190), and iterative reconstruction of CT images (191). A multicentric analysis of dose-saving strategies for CCTA in daily practice has demonstrated a 78% reduction in radiation dose from 2007 to 2017, with a median dose-length product (DLP) of 195 mGy*cm in 2017 (163).

1.5.8. Elastography

Tissue stiffness has long been acknowledged as a significant biomarker for tissue pathology. Ultrasound elastography, an innovative ultrasound technique, can assess the physical properties of tissue by observing how it responds to energy from sound waves. Common disease processes that induce alterations in tissue mechanical properties encompass fibrotic changes, inflammatory conditions, and neovascularization. Ultrasound elastography serves as an apt diagnostic tool to assess these changes, facilitating the study of various tissues and diseases.

1.5.8.1 Elastography Physics

Elastography comprises a spectrum of methods employed to gauge the elastic characteristics of tissue. Elasticity, in this context, refers to a tissue's capacity to either resist deformation when subjected to a force or return to its original state once the force is removed. The tissue's stiffness is assessed as a physical property and is referred to as Young's modulus (E). Young's modulus serves as a proportionality parameter that illustrates the correlation between the applied force per unit area (stress) and the resultant relative change in the dimensions of tissue (strain). Ultrasound elastography is

categorized into two distinct types based on the nature of the external mechanical stimulus method: "**quasi-static, or strain-based,"** and "**dynamic, or shear wave-based.”** In strain-based elastography, the mechanical force is generated by endogenous sources such as carotid pulsation or the prob force generate the force. Conversely, in shear wave elastography, the imaging system is responsible for generating a shear wave within the tissue. In both methods, the mechanical properties of the tissue are estimated based on the tissue's response to these mechanical stimuli.

Strain imaging adheres to a direct relationship, described by Hooke's Law, between the externally applied stress and strain (192, 193). Nevertheless, in clinical strain imaging systems, the calculation of Young's modulus is typically not determined because the exact force applied to the area of interest is often unknown. In contrast, Young's modulus is computed in shear wave imaging systems(192, 193).

Moreover, many vendors typically offer automatic calculation systems. Upon completing the ultrasound examination, most systems provide stiffness values in both kPa (kilopascals) and m/s (meters per second).

1.5.8.2 Strain Elastography (SE)

Strain elastography (SE) assesses tissue stiffness by applying external force to the tissue (203), which induces changes in tissue dimensions and deformations. These alterations in shape and dimensions are termed strain. Stiffer regions exhibit minimal deformation, resulting in lower strain values and a higher Young's modulus. The strain ratio is calculated by dividing the strain observed in the tissue of interest by the strain measured in a specific reference area of tissue. Furthermore, there is no requirement to know the exact applied force when calculating the strain ratio. Therefore, it is commonly employed in medical procedures and is analogous to the proportion of Young's modulus between two areas, assuming that the applied force remains consistent across these areas. Strain elastography is further divided into two subgroups based on the method used for tissue excitation, which can either involve external manual pressure or be induced by internal physiological motion (192).

In the case of external manual excitation, elasticity is primarily measured in superficial tissues, and the manual stress applied is not effectively transmitted to deeper tissues. Conversely, when using natural physiological movements such as respiration or cardiac pulsation as a means to generate tissue stress, it becomes possible to assess deeper organs as well.

Tissue deformation in strain imaging (elastograms) can be quantified by analyzing radiofrequency (RF) data collected before and after the application of pressure to the tissue using an ultrasonic transducer (194). To enhance anatomical information, translucent and colorful strain overlays can be added to B-mode images. The strain map is often depicted using colored pixels overlaid on a gray-level or red/blue-level background(195).

Typically, for deeper organs like the kidneys and liver, tissue stress is obtained from the natural movements associated with cardiac/arterial or respiratory motion. In contrast,

manual compression is employed to induce tissue stress in superficial organs, such as the thyroid.

1.5.8.3. Shear Wave Elastography (SWE)

In traditional B-mode image generation, compressive acoustic waves travel rapidly through soft tissue at speeds ranging from 1450 to 1550 m/s. In contrast, mechanical shear waves employed in shear wave elastography propagate at a significantly lower speed, typically ranging from 1 to 10 m/s. The speed at which shear waves propagate is influenced by tissue stiffness (193, 194). Most available shear wave elastography systems generate and monitor shear waves using compressed sound waves. Shear waves in acoustics move perpendicular to the compressed waves, and the displacement of tissue induced by these shear waves is measured at various points using the ultrasound probe, enabling the assessment of shear wave speed (194). Young's modulus can be algebraically calculated using the shear wave speed (SWS). SWS is employed for characterizing, evaluating, and diagnosing various tissue diseases, including the characterization of renal lesions (196), hepatic lesions (197), thyroid lesions (198), or for the evaluation of diffuse liver and renal disease (199, 200), and the examination of breast masses (201, 202). SWS is also utilized in cancer detection in the prostate (203), and in imaging tendons (204).

1.5.9. Non-Invasive Vascular Elastography (NIVE)

NIVE offers a comprehensive assessment of the elasticity of the vessel wall. It assesses the biomechanics of vessel walls by harnessing the natural cardiac pulse and generates two-dimensional images that detect any specific deformities in the vessel wall (205).

Non-invasive elastography targets a specific segment of the artery to generate 2D displacement maps across consecutive ultrasound images. These maps are used to create an elastogram that encompasses elastography parameters, including translations (axial or lateral), shear strain, and strain. "Axial" refers to the direction along the ultrasound

beam, while “lateral” indicates the direction that is opposite to the ultrasound beam. Additionally, “translations” denote changes that occur over the cardiac cycle. Axial strain demonstrates how pulsating blood pressure compresses or dilates the vessel wall, while shear strain reflects the curved deformation resulting from the mechanical heterogeneity of the vessel wall. Elastograms are averaged across the entire vessel wall at various timescales to generate time-varying slopes that depict the translation and deformity of the vessel wall throughout the cardiac cycle (206).

Chapter 2:

Rationale & Methodological Considerations

2.1. Rationale and Methodological Considerations of my Research Project

Cardiovascular disease remains a significant cause of mortality among people living with HIV (PLWH) under antiretroviral therapy (ART). Existing cardiovascular risk calculation algorithms consistently underestimate the risk in PLWH. Hence, it is imperative to achieve accurate prediction of cardiovascular risk in PLWH. Recent studies conducted in the general population have demonstrated that the atherosclerotic burden identified through coronary computed tomography (CT) angiography serves as a robust predictor of future major cardiovascular events (207, 208). Despite its reliability, coronary CT still entails radiation exposure (163) and the use of iodinated contrast agents. In contrast, carotid ultrasound elastography stands as a non-invasive tool capable of evaluating subclinical atherosclerosis. It detects deformations and strains in the arterial wall, as well as atherosclerotic plaque, prompted by the pulsating blood flow.

In a study from the prospective Canadian HIV and Aging Cohort study, ultrasound elastography demonstrated that carotid artery walls in PLWH with low or intermediate cardiovascular risk were more rigid (axial strains and displacements were smaller), in comparison to healthy volunteers (16). In the same study, IMT was not different in PLWH and non-HIV controls. Elastography also showed carotid artery premature stiffening in children with elevated body-mass index (BMI) (17). As reported by the authors of both studies (16, 17), biomechanical vessel wall assessment in these at-risk populations shows premature subclinical atherosclerosis. Based on the previous results, we hypothesize that the inclusion of carotid elastography biomarkers alongside conventional cardiovascular risk factors will enhance the predictive accuracy of coronary atherosclerosis burden in both HIV+ and HIV- individuals. Furthermore, we hypothesize that the incorporation of carotid intima-media thickness (CIMT) into the aforementioned algorithms will not result in a significant improvement in predictive power for both HIV+ and HIV- individuals (209, 210).

In this study, our objective was to evaluate models that combine carotid elastography, intima-media thickness (IMT), cardiovascular risk factors, and HIV-related factors, including

antiretroviral therapy (ART), for the prediction of coronary artery disease in both PLWH and non-HIV controls.

2.2. Hypotheses

a. We hypothesize that the inclusion of carotid elastography biomarkers alongside conventional cardiovascular risk factors will enhance the predictive accuracy of coronary atherosclerosis burden in both HIV+ and HIV- individuals.
b. Additionally, we hypothesize that the incorporation of carotid intima-media thickness (CIMT) into the aforementioned algorithms will not result in a significant improvement in predictive power for both HIV+ and HIV- individuals.

Chapter 3:
Material & Methods

3. Materials and Methods

This study has received approval from the institutional review board of ethics at the *Centre Hospitalier de l'Université de Montréal* (CHUM). Written informed consent was obtained from all participants (211).

3.1. Study design

This is a cross-sectional study, nested in the Canadian HIV and Aging Cohort Study (CHACS) (204).

CHACS is an ongoing multicenter, prospective, controlled cohort study actively following more than 1100 people living with HIV (PLWH) and non-HIV-infected participants in 10 Canadian centers.

At enrollment, HIV-infected individuals must be either 40 years old or younger or have had HIV for at least 15 years, confirmed by an anti-HIV antibody test. They should also be capable of providing informed consent and have a minimum one-year life expectancy. Participants in the control group must be under 40 years old or younger, and able to provide informed consent.

3.2. Study Population

3.2.1 Canadian HIV and Aging Cohort Study (CHACS)

CHACS recruits participants both from hospital-based and community-based clinics. In includes HIV-positive individuals diagnosed through a positive HIV serology test who are receiving follow-up care in HIV clinics. Additionally, recently diagnosed HIV- positive individuals who meet the inclusion criteria are also recruited into this cohort, as well as non-HIV participants who are defined as HIV-seronegative individuals. Hospital-based recruitment includes PLWH aged 40 years or older enrolled from the HIV clinics of the University of Montreal Hospital. Non-HIV healthy volunteers of similar ages are recruited from outpatient internal medicine clinics at the same hospital. Community recruitment for PLWH is conducted within family medicine clinics in

Montreal. In the case of healthy volunteers, recruitment is conducted among non-HIV friends and family members (proximity recruitment) to minimize disparities in socioeconomic variables between the two groups.

3.2.2 Participants in the Imaging Subcohort of the CHACS and Present Study

The CHACS includes a prospective imaging subcohort initially formed for cardiac CT imaging, later expanded to include carotid ultrasound imaging. These two imaging examinations were offered to participants in the CHACS.

Imaging Subcohort of the CHACS

All PLWH and control participants in the imaging subcohort were recruited from the CHACS between 2013 and 2019.

Participants in the imaging subcohort were consecutively included based on the following criteria: low or intermediate cardiovascular risk (10-year Framingham score of 5% to 20%) and no history or symptoms of coronary artery disease. The Framingham Risk Score calculates the 10-year risk of coronary heart disease (CHD) as a percentage. Low-risk participants have a CHD risk of 10% or less after 10 years, intermediate-risk participants have a risk of 10% to 20% to develop CHD after 10 years, and high-risk participants have a risk of 20% or greater (212).

Other exclusion criteria are a history of contrast media allergy, creatinine clearance of less than 50 mL/min and pregnancy.

Present Study

The present study included all participants from the imaging subcohort who had undergone both carotid ultrasound with elastography and cardiac CT prospectively. Exclusions were made in cases of unavailable data, for example imaging artifacts, unavailable postprocessing results, missing values, etc. Participants who underwent only non-enhanced cardiac CT without contrast-enhanced CT (coronary CT angiography) were not included.

3.2.3 Data Collection

CHACS participants are followed for three consecutive years (first visit, one year after, and two years after), followed by visits in years five and eight based on their initial enrollment date. During each study visit, participants complete questionnaires, undergo a comprehensive medical history and physical examination by a doctor, and have a series of blood tests. At the initial visit, all necessary data, including previous and present treatments, as well as any prior and current health issues such as high blood pressure, diabetes, lipid disorders, family history of premature cardiovascular disease (CVD), and lifestyle habits like smoking and physical activity levels, are collected and recorded in an electronic case report form. However, diagnoses are primarily based on study questionnaires rather than made during the visits.

During study visits, nurses measure blood pressure using an electronic sphygmomanometer with the participant's arm at heart level while seated with feet touching the floor. They also record weight, height, and waist circumference. High waist circumference is defined as over 102 cm in males or 88 cm in females.

Smokers are participants who currently smoke cigarettes, while ex-smokers are individuals who reported smoking cigarettes in the past but have quit at the time of the study visits. Pack-years is calculated as the product of the number of packs of cigarettes smoked per day multiplied by the number of years the person has smoked. For additional information about the CHACS study, refer to The Canadian HIV and Aging Cohort Study - Determinants of Increased Risk of Cardiovascular Diseases in HIV-Infected Individuals: Rationale and Study Protocol (213).

3.3. Ultrasound Imaging

Carotid ultrasound assessed the arterial walls of the right and left common and internal carotid arteries. For each patient, four cine-loops were acquired. Longitudinal views of each vessel were obtained using an Aixplorer system (SuperSonic Imagine) equipped with a 256-element linear array probe (SuperLinear™ SL15-4) operating at a central frequency of 7.5 MHz. The examinations were conducted with the patient at rest in a supine position, with the head tilted at a 45° angle opposite to the direction of the scanned artery. Beamforming was performed by the Aixplorer, and the specific angles used are unknown.

The vessel was positioned parallel to the probe. Cine-loops were recorded at a frame rate of 50 frames per second, with each loop lasting approximately 5 seconds. The examinations were conducted by a technologist with over 20 years of experience.

3.4. Image Analysis

B-mode cine-loops were generated from radiofrequency images using the NIVE platform, employing Hilbert transform and logarithmic compression techniques. The reconstructed B-mode images had pixel dimensions of 20.5 µm axially × 200 µm laterally. A semiautomated segmentation method was applied to all frames of the B-mode cine-loops in order to detail a normal portion of the carotid far wall, excluding calcium or plaque.

Plaques were defined as a CIMT greater than 1 mm or a portion of the vessel wall thicker than 1 mm protruding into the lumen, or IMT > 1.5 mm, following the Mannheim recommendations. Manual segmentation of carotid wall contours was performed on a single B-mode image by an experienced technologist and reviewed by a radiologist (GS) with over 20 years of experience.

The carotid IMT was defined as the mean distance between two segmented carotid wall contours, specifically the lumen-intima and media-adventitia interfaces. It was calculated from automated segmentations for all frames within each 5-second cine-loop and then averaged. Measurements for the CCA walls were taken at a segment located at least 5 mm before the bulb, with a minimum length of 10 mm. For the ICA walls, measurements were taken above the flow divider. If this was not feasible due to geometric constraints or image quality issues,

measurements were made as far above the bulb widening as possible. The average values for IMT from both the right and left sides were used for analysis, and all analyses in this study were conducted using the average values. All segmentations were performed independently of elastography analysis.

Elastograms were generated for each pair of time-varying radiofrequency images to assess the mechanical properties of carotid artery walls and plaques (209). Elastography cine-loops of lateral and axial translation motions (in mm), axial strains (in %), and axial shear strains (in %) were computed. Translations represent rigid displacements within the cardiac cycle. Axial strain reflects compression or dilation of the arterial wall due to pulsating blood flow, while shear strain indicates angular deformation resulting from the mechanical heterogeneity of the arterial wall(210).

For each mechanical parameter, the spatial average over the segmented region was calculated over consecutive cardiac cycles and displayed over time. Our analysis focused on the average over the entire cardiac cycle, and we did not isolate data from diastole to investigate potential differences in results(209).

3.5. Coronary CT Angiography

All participants underwent both non-contrast and contrast-enhanced cardiac CT. Before the CT scan, participants received sublingual nitroglycerin (0.4 mg) and oral metoprolol (50–75 mg) if their pre-scan heart rate exceeded 60 beats per minute, unless contraindicated. Contrast-enhanced coronary CT angiography (ECG-gated) was conducted using a 256-slice CT scanner (Brilliance iCT; Philips Healthcare). Iopamidol at a concentration of 370 mg/mL (Bracco Imaging) was administered at a rate of 5 mL/sec. The gantry had a rotation time of 270 msec, with an axial slice thickness of 0.625 mm and a slice interval of 0.45 mm.

3.6. Exposure of Interest

- **US Elastography Parameters**

Imaging biomarkers were derived from elastography time-varying curves, including cumulated axial translation (CAT), cumulated lateral translation (CLT), maximum and cumulated axial strains (CAS), and maximum and cumulated axial shear strain magnitudes (CShS). The term 'cumulated' used for each biomarker quantifies the total strain or translation occurring during the cardiac cycle, representing the range of variation in the cumulated curve over one cycle. The cumulated range is calculated for each complete cardiac cycle within the 5-second acquisition. The cumulated parameter is the average range of the cumulated curves across all available cardiac cycles.

The ultrasound radiofrequency data processing and B-mode image segmentation methods were implemented in-house using the Visual-NIVE commercial imaging platform from Object Research Systems.

- **Intima-media thickness,** also measured by NIVE.

3.7. Outcome of Interest: Coronary Plaque Presence

Plaque presence on the CT angiograms was determined by a board-certified radiologist (CCL) with 17 years of experience.

All image assessors were blinded to the HIV status and clinical data.

3.8. Main Confounding Variables

Cardiovascular risk factors including age, sex, high blood pressure, family history of premature coronary artery disease, smoking exposure, low-density lipoprotein or high-density lipoprotein cholesterol levels, body mass index, statin use, and HIV serostatus.

3.9. Statistical Analysis

Descriptive statistics are presented as means ± standard deviations (SDs) or median [25th – 75th interquartile range (IQR)], while categorical variables are shown as counts and percentages. Between-group comparisons utilized Student's t-tests for normally distributed data, Mann–Whitney tests for non-normally distributed data, and Chi-square tests for categorical data.

Data normality was assessed using histograms for each characteristic variable. A histogram estimates the probability of a continuous variable. A roughly bell-shaped and symmetric histogram suggests normal distribution (214).

Univariate and multivariate Poisson regression analyses with robust variance were conducted to determine the independent associations of cardiovascular risk factors, IMT, and elastography parameters with coronary plaque presence. All multivariate analyses were adjusted for HIV serostatus and cardiovascular risk factors, including age, sex, high blood pressure, family history of premature coronary artery disease, smoking exposure, low-density lipoprotein or high-density lipoprotein cholesterol levels, body mass index, and statin use. Variables with a univariate association with coronary plaque presence and a p-value of 0.1 or less were included. A p-value of 0.1 indicates a 10% or lower likelihood that the results are due to chance.

In the multivariate analysis, we tested the association between cardiovascular risk factors, IMT, elastography parameters, and coronary plaque presence using a total of 19 models. The first model included only the cardiovascular risk factors significantly associated with coronary plaque presence: age, statin use, and smoking exposure. Subsequent models added individual elastography parameters from either CCA or ICA, both with and without IMT of CCA or ICA, to the cardiovascular risk factors model. Missing data for smoking exposure among patients with incomplete continuous covariable data were imputed using the median value (0.9 pack-years). Statistical significance was defined as a p-value less than 0.05, and no adjustments were made for multiple testing.

Receiver operating characteristic (ROC) curve and area under the curve (AUC) analysis were used to compare various prediction models for coronary plaque presence.

Statistical analysis was conducted using R software, version R i386 4.0.3, provided by the R Foundation for Statistical Computing (https://www.r-project.org).

Chapter 4:

Results

4.1. Participant Characteristics

Out of the 164 CHACS participants who underwent carotid elastography analysis and cardiac CT, 154 participants with complete data were included, while ten were excluded due to missing coronary plaque data. The mean time interval between coronary CT and carotid ultrasound per participant was 7.69 ± 20.1 months (230.97 ± 607.24 days).

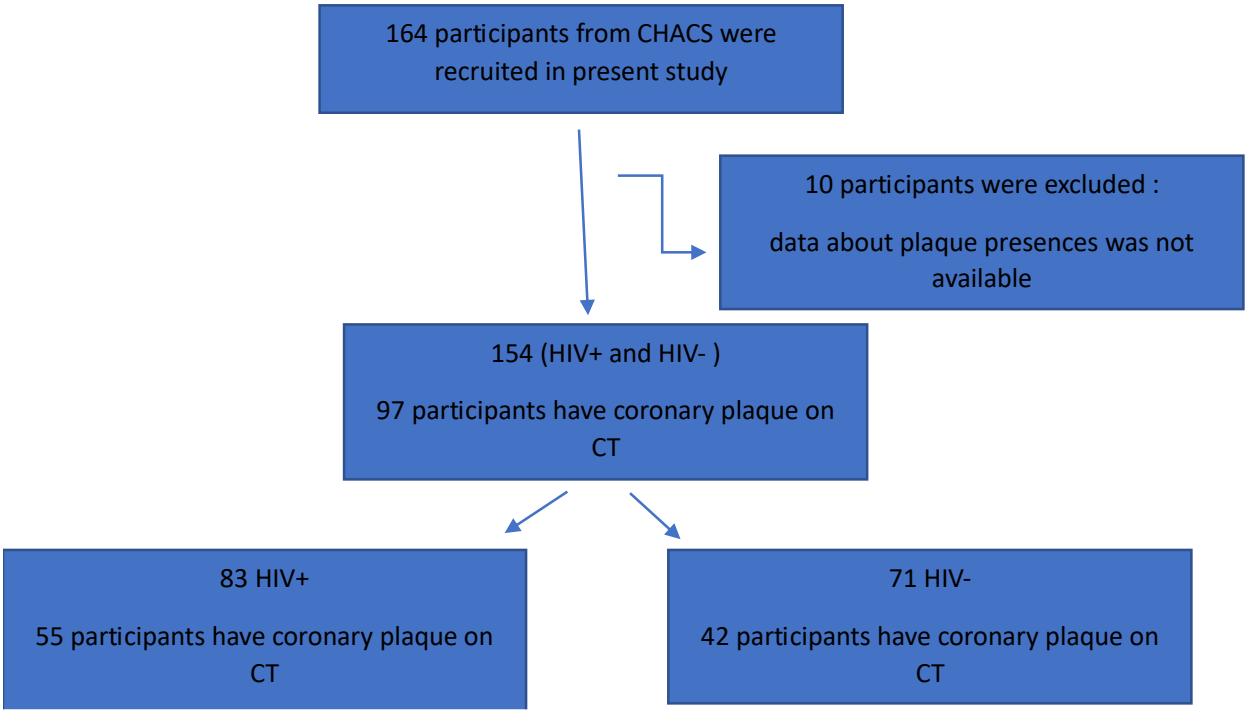

Figure 8: Participant Flow Diagram. Out of 164 recruited participants, 154 with complete carotid ultrasound and cardiac CT data were evaluated, including 83 HIV+ and 71 HIV-.

Participant characteristics stratified by HIV Status are summarized in Table 1. Of the 154 participants, 83 were PLWH (53.8%), and 71 were healthy volunteers (47.4%). Participants with HIV had a mean age of 57.2 ± 7.3 years, while controls had a mean age of 55.7 ± 7.8 years (p = 0.22). PLWH included a higher proportion of men compared to healthy volunteers (95.2% vs. 81.7%, respectively; p = 0.01). The median Framingham risk score was 12% [IQR, 8 - 16] in PLWH and 9% [IQR, 7 - 15] in controls (p = 0.045). PLWH had a lower BMI than controls, with mean body

mass indices of 25.3 ± 3.69 kg/m2 and 27.2 ± 4.69 kg/m2, respectively (p = 0.01). More PLWH had a history of tobacco smoking, with a median of 6.00 [IQR, 0 -18.0 pack-years], compared to controls with a median of 0 pack-years [IQR, 0 - 7.20 pack-years] (p < 0.001), and a higher proportion of smokers were among PLWH (21.7% [18 of 83] compared to 9.9% [7 of 71], p = 0.05). In the PLWH group, there were slightly more statin users (30% [25 of 83]) compared to the non-HIV group (16% [11 of 71]; p = 0.051). Additionally, the mean HDL cholesterol level was 1.25 ± 0.331 in the HIV-positive group and 1.42 ± 0.386 in the non-HIV group (p = 0.006). In the HIV group, the mean LDL cholesterol was 2.87 ± 0.911, and in the non-HIV group, it was 3.20 ± 0.862 (p = 0.024). The mean total cholesterol was 4.84 ± 1.13 in the HIV-positive group and 5.27 ± 1.03 in the non-HIV group (p = 0.01). No statistical differences were found for other clinical characteristics.

In the PLWH group, the median HIV infection duration was 20.0 years [IQR, 15.0 - 26.0 years]. Among them, 90.3% [75 of 83] were on antiretroviral therapy, with a median duration of 15.9 years [IQR, 7.83 - 19.7 years]. Detectable viral load (>40 copies/ml) was observed in 4.8% [4 of 84] of PLWH. Details of exposure to different antiretroviral therapy classes are provided in Table 1.

Table 1. Clinical Characteristics of Participants, N = 154

	HIV+ (N=83)	HIV- (N=71)	Total (N=154)	P Value
Age (years)*	57.2 ±7.31	55.7 ±7.81	56.5 ±7.55	0.229
Sex, number (%)†				**0.02**
Male	79 (95.2%)	58 (81.7%)	137 (98.0%)	
Female	4 (4.8%)	13 (18.3%)	17 (11.0%)	
Missing data	0 (0%)	0 (0%)	0 (0%)	
Race†				0.46
Asian	2 (2.4%)	0 (0%)	2 (1.3%)	
Black (African)	1 (1.2%)	0 (0%)	1 (0.6%)	
Black (Haitian)	2 (2.4%)	1 (1.4%)	3 (1.9%)	
Caucasian	74 (89.2%)	67 (94.4%)	141 (91.6%)	
Hispanic	3 (3.6%)	3 (4.2%)	6 (3.9%)	

Missing	1 (1.2%)	0 (0%)	1 (0.6%)	
10-year Framingham Risk Score (%) ♦ **Median [Q25, Q75]** **Missing**	 12.0 [8.00, 16.0] 2 (2.4%)	 9.00 [7.00, 15.0] 3 (4.2)	 11.0 [7.00, 16.0] 5 (3.2%)	**0.04**
BMI (kg/m²) ♦ **Mean ±SD** **Missing**	 25.3 ±3.69 3 (3.6%)	 27.2 ±4.69 2 (2.8%)	 26.2 ±4.28 5 (3.2%)	**0.02**
High waist circumference (cm)* [1] **Mean ±SD** **Missing (%)**	 94.6 ±10.5 1 (1.2%)	 96.0 ±11.2 7 (9.9%)	 95.2 ±10.8 8 (5.2%)	0.44
Diabetes† **Yes** **No** **Missing**	 4 (4.8%) 79 (95.2%) 0 (0%)	 0 (0%) 71 (100%) 0 (0%)	 4 (2.6%) 150 (97.4%) 0 (0%)	0.17
Hypertension† **Yes** **No** **Missing**	 27 (32.5%) 56 (67.5%) 0 (0%)	 16 (22.5%) 55 (77.5%) 0 (0%)	 43 (27.9%) 111 (72.1%) 0 (0%)	0.23
Smoking status† **Current smoker** **Ex-smoker** **Never smoked** **Missing**	 18 (21.7%) 35 (42.2%) 27 (32.5%) 3 (3.6%)	 7 (9.9%) 29 (40.8%) 35 (49.3%) 0 (0%)	 25 (16.2%) 64 (41.6%) 62 (40.3%) 3 (1.9%)	0.05
Smoking history (Pack-year) ♦ [2] **Median [Q25, Q75]** **Missing**	 6.00 [0, 18.0] 6 (7.2%)	 0 [0, 7.20] 2 (2.8%)	 0.900 [0, 14.9] 8 (5.2%)	**0.01**
Family history of CVD† **Yes** **No** **Missing**	 38 (45.8%) 45 (54.2%) 0 (0%)	 30 (42.3%) 41 (57.7%) 0 (0%)	 68 (44.2%) 68 (44.2%) 0 (0%)	0.78

HDL_Cholesterol(mmol/L) ♦ **Mean ±SD** **Missing**	1.25 ±0.331 2(2.4%)	1.42 ±0.386 0(0%)	1.33 ±0.366 2(1.3%)	**0.01**
LDL_Cholesterol(mmol/L) * **Mean ±SD** **Missing**	2.87 ±0.911 6 (6.0%)	3.20 ±0.862 2 (2.8%)	3.02 ±0.901 7 (4.5%)	**0.02**
Total Cholesterol(mmol/L) * **Mean ±SD** **Missing**	4.84 ±1.13 2(2.4%)	5.27 ±1.03 1(1.4%)	5.04 ±1.10 3(1.9%)	**0.01**
Triglyceride (mmol/L) ♦ **Median [Q25, Q75]** **Missing**	1.40[1.02, 2.02] 2(2.4%)	1.30[0.940, 1.84] 2(2.8%)	1.34[0.945,1.98] 4(2.6%)	0.31
Statin use[†] **Yes** **No** **Missing**	 25 (30.1%) 58 (69.9%) 0 (0%)	 11 (15.5%) 60 (84.5%) 0 (0%)	 36 (23.4%) 118 (76.6%) 0 (0%)	0.051
HIV duration(years) **Median [Q25, Q75]** **Missing**	20.0 [15.0, 26.0] 1 (1.2%)			
Exposure to ART **Missing**	75 (90.3%) 6 (7.2%)			
Exposure to INSTI **Missing**	31 (37.3%) 6 (7.2%)			
Exposure to NNRT **Missing**	37(44.5%) 6 (7.2%)			
Exposure to NRTI **Missing**	70 (84.3%) 6 (7.2%)			
Exposure to PI **Missing**	55 (66.2) 6 (7.2%)			
Exposure to EI **Missing**	3 (3.5) 6 (7.2%)			
ARV duration (years) ♦ **Median [Q25, Q75]** **Missing**	15.9 [7.83, 19.7] 6 (7.2%)			
Detectable viral load [3] **Missing**	4 (4.8%) 8 (9.6%)			

CD4 (cells/mm3) ♦ **Median [Q25, Q75]** **Missing**	 590 [460, 809] 7 (7.8%)			
CD8 (cells/mm3) * **Mean ±SD** **Missing**	800±404 7 (7.8%)			

* Student's t tests

♦Mann–Whitney test

[†] Chi-square test (Bold P-value refers to a significant p-value <0.05). Analysis of comparisons between groups was done using Student's t-tests when data were normally distributed or Mann–Whitney test when data were not normally distributed. Chi-square tests were used when data were categorical.

CVD: Cardiovascular risk factors,

ART: Antiretroviral therapy,

NRTI: Nucleoside reverse transcriptase inhibitor,

NNRTI: Nonnucleoside reverse transcriptase inhibitor,

PI: Protease inhibitor,

INSTI: Integrase strand transfer inhibitor

EI: Entry inhibitors.

[1] High waist circumference is defined as exceeding 102 cm in males or 88 cm in females.

[2] Pack-years is calculated by multiplying the number of packs of cigarettes smoked per day by the number of years a person has smoked.

[3] Defined as viral load =<40 copies/mL.

4.2. IMT, Elastography and Coronary Plaque Data

Carotid IMT and all elastography features for both internal and common carotid arteries were similar between PLWH and healthy volunteers. Comparisons between groups were conducted using Student's t-tests for normally distributed data and Mann–Whitney tests for non-normally distributed data. The analysis used the average of left and right-sided measurements, and we did not differentiate between the right and left sides in our study. Additionally, we analyzed only the average over the entire cardiac cycle, without specific focus on diastolic data (Table 2)

At coronary CT angiography, coronary artery plaque prevalence for all participants was 63.0% [97 out of 164], with 66.3% [55 out of 84] in PLWH and 59.2% [42 out of 71] in non-HIV participants (p = 0.46) (Table 2).

Table 2. Cardiac CT Results, IMT and Elastography Parameters of Participants, N = 154

	HIV+ (N=83)	HIV- (N=71)	Total (N=164)	P Value
IMT and elastography results				
IMT_ CCA (mm)* Mean ±SD	0.55 ±0.079	0.53 ±0.05	0.54 ±0.07	0.10
IMT_ ICA (mm)* Mean ±SD	0.54 ±0.06	0.53 ±0.05	0.54 ±0.06	0.28
CAT_CCA (mm)* Mean ±SD	0.26 ±0.09	0.27 ±0.10	0.26 ±0.09	0.54
CAT_ICA (mm) ♦ Mean ±SD	0.17±0.07	0.185 ±0.07	0.18 ±0.07	0.37
CLT_CCA (mm)* Mean ±SD	0.41 ±0.18	0.44±0.16	0.43 ±0.17	0.37
CLT_ICA (mm)* Mean ±SD	0.29 ±0.15	0.31±0.13	0.304 ±0.14	0.25
CAS_CCA (%) ♦ Median [Q25, Q75]	2.83 [1.99, 3.65]	2.64[2.15, 3.14]	2.67 [2.04, 3.50]	0.53
CAS _CCI (%) ♦ Mean ±SD	2.39 ±1.20	2.59 ±0.92	2.48 ±1.08	0.06
CShS_CCA (%) * Mean ±SD	0.19 ±0.09	0.19 ±0.07	0.19±0.08	0.70
CShS_CCI (%) ♦ Mean ±SD	0.21 ±0.09	0.22 ±0.07	0.22 ±0.08	0.37
Cardiac CT results				
Coronary plaque presence on CT[†]				0.46
Yes	55 (66.3%)	42 (59.2%)	97 (63.0%)	
No	28 (33.7%)	29 (40.8%)	57 (37.0%)	
Missing	0 (0%)	0 (0%)	0 (0%)	

IMT_CCA Intima-media thickness of common carotid artery (mm)
IMT_ICA Intima-media thickness of internal carotid artery (mm)

CAS_CCA Cumulated axial strain of common carotid artery (%)
CAS_ICA Cumulated axial strain of internal carotid artery (%)
CAT_CCA Cumulated axial translation of common carotid artery (mm)
CAT_ICA Cumulated axial translation of internal carotid artery (mm)
CLT_CCA Cumulated lateral translation (mm)of common carotid artery (mm)
CLT_ICA Cumulated lateral translation (mm) of internal carotid artery (mm)
CShS_CCA Axial shear strain magnitude of common carotid artery (%)
CShS_ICA Axial shear strain magnitude of internal carotid artery (%)
P-values are considered significant if they are less than 0.05. We used Student's t-tests for normally distributed data, Mann–Whitney tests for non-normally distributed data, and Chi-square tests for categorical data.
* Student's t tests
♦Mann–Whitney test
ǂ Chi-square test

4.3. Association of Cardiovascular Risk Factors, HIV Status, Elastography Parameters, and Carotid IMT with Coronary Plaque on CT

Univariate Poisson regression analysis with robust variance showed associations of smoking exposure ($p < 0.001$) and IMT of the common carotid artery ($p = 0.02$) with coronary plaque presence ($p < 0.001$).

After adjusting for cardiovascular risk factors by multivariate Poisson regression, only smoking exposure remained significantly associated with coronary plaque presence on CT (prevalence ratio 1.10, 95% CI 1.04 – 1.13, $p < 0.001$). This association persisted even after further adjustment for common carotid artery IMT (prevalence ratio 1.08, 95% CI 1.04 – 1.13, $p < 0.001$) and internal carotid artery IMT (prevalence ratio 1.09, 95% CI 1.04 – 1.10, $p < 0.001$). No significant associations were found with other coronary artery disease risk factors or HIV status in the multivariate analysis. Additionally, carotid elastography parameters and carotid intima-media thickness were not associated with coronary atherosclerosis after adjustment (Table 3).

Table 3. Association of Cardiovascular Risk Factors, IMT and Elastography Parameters of CCA and ICA with Coronary Plaque Presence - Univariate Poisson Regression Analysis with Robust Variance, N=154.

Variables	Univariable Analysis	
	RR and 95 % CI	**P Value**
Age (cof^10)	1.13(0.98 _ 1.31)	0.08
BMI	0.99(0.98_1.01)	0.83
Sex	1.01(0.84_1.21)	0.87
Hypertension	0.91(0.80_1.03)	0.13
Family history of premature CVD	0.96(0.83_1.12)	0.66
SmokingPack-year (cof^10)	1.10 (1.05 _1.14)	**<0.001**
Statin use	1.26 (0.99_1.60)	0.07
HDL Cholesterol	1.07 (0.92_ 1.25)	0.35
LDL Cholesterol	1.01 (0.95_1.08)	0.68
HIV status	1.05 (0.94_1.18)	0.36
IMT_CCA	0.45 (0.22_0.90)	**0.02**
IMT_ICA	1.06 (0.43_ 2.60)	0.90
CAT_CCA	1.08 (0.61_1.89)	0.79
CAT_ICA	1.33 (0.64_2.72)	0.44
CLT_CCA	0.95 (0.69_1.29)	0.75
CLT_ICA	1.13 (0.78_1.64)	0.51
CAS_CCA	1.02 (0.96_ 1.07)	0.53
CAS_ICA	1.01 (0.96 _1.06)	0.72
CShS_CCA	0.95 (0.91_1.00)	0.06
CShS_ICA	1.05 (0.97_ 1.13)	0.17

IMT_CCA Intima-media thickness of common carotid artery (mm)
IMT_ICA Intima-media thickness of internal carotid artery (mm)
CAS_CCA Cumulated axial strain of common carotid artery (%)
CAS_ICA Cumulated axial strain of internal carotid artery (%)
CAT_CCA cumulated axial translation of common carotid artery (mm)

CAT_ICA cumulated axial translation of internal carotid artery (mm)
CLT_CCA cumulated lateral translation (mm)of common carotid artery (mm)
CLT_ICA cumulated lateral translation (mm) of internal carotid artery (mm)
CShS_CCA Axial shear strain magnitude of common carotid artery (%)
CShS_ICA Axial shear strain magnitude of internal carotid artery (%)
Averages from the right carotid and left sides IMT were obtained
P value results have gotten by using from univariate Poisson regression analysis after adjusting of cardiovascular risk factors

Table 4. Association of Cardiovascular Risk Factors, IMT and Elastography Parameters of CCA and ICA with Coronary Plaque Presence using Multivariate* Poisson Regression with Robust Variance. N=154

Variables	Multivariable model 1 = Cardiovascular risk		Multivariable model 2 A= Cardiovascular risk factors and CCA_IMT		Multivariable model 2 B= Cardiovascular risk factors and ICA_IMT	
	RR and 95 % CI	P value	RR and 95 % CI	P value	RR and 95 % CI	P value
Age (cof^10)	1.10 (0.96 _1.26)	0.16	1.08 (0.93_1.24)	0.27	1.11 (0.95 _1.34)	0.16
Smoking Pack-year (cof^10)	1.10 (1.04 _1.13)	**<0.001**	1.08 (1.04_ 1.13)	**<0.001**	1.09 (1.04_ 1.10)	**<0.001**
Statin use	1.15 (0.90_1.46)	0.26	1.13 (0.89_1.43)	0.29	1.15 (0.90_1.46)	0.25
IMT_CCA	/	/	2.77(0.75_10.2)	0.12	/	/
IMT_ICA	/	/	/	/	0.81 (0.13_ 4.91)	0.82

IMT_CCA Intima-media thickness of common carotid artery (mm)
IMT_ICA Intima-media thickness of internal carotid artery (mm)
Averages from both right and left carotid IMT were obtained.
P-value results were obtained using multivariate Poisson regression analysis after adjusting for cardiovascular risk factors
RR (Relative Risk): Relative risk represents the prevalence ratio for Poisson regression with robust variance.
*: Multivariate analyses were conducted for predictors with a univariate association with coronary plaque presence and a p-value 0.1 or less (see Table 3).

The additional multivariate models are provided in Chapter 8, Appendices, Page 131.

4.4. Assessment of Predictive Models

We used ROC analyses to assess the predictive accuracy of our multivariate Poisson regression models. ROC curves and area under the ROC curves (AUC) were generated. AUC is a measure of the predictive ability of the model, with values ranging from 0.5 to 1. An AUC of 0.5 corresponds

to a model no better than chance, while an AUC of 1 represents 100% accuracy. However, adding IMT or elastography data to the cardiovascular risk factors model did not improve prediction accuracy. The AUC results in all models ranged from 0.66 to 0.68, as shown in Table 5.

To visualize the performance of the multivariate models, ROC curves for six models were plotted. Figures 9 to 12 illustrate these curves as follows:

Figure 9: Cardiovascular risk factors with IMT and elastography parameters related to the common carotid artery;

Figure 10: Cardiovascular risk factors with IMT and elastography parameters related to the internal carotid artery;

Figure 11 Cardiovascular risk factors with elastography parameters related to the common carotid artery;

Figure 12: Cardiovascular risk factors, with elastography parameters related to the internal carotid artery.

Figures 9 to 12 show that all six curves of the models are moderately distant from the diagonal line, and similar to each other.

Table 5. Predictive Value of Cardiovascular Risk, IMT, and Elastography Parameters of CCA and ICA for Detecting Coronary Plaques – AUC Analyses of ROC Curves

	ICA		**CCA**	
	AUC	95% CI	AUC	95%CI
Model 1: CVRF	0.66 (0.57_0.74)			
Model 2: CVRF + IMT	0.66	0.57-0.74	0.67	0.589-0.76
Model 3: CVRF +IMT+ Elastography parameters				
CAT	0.66	0.57-0.74	0.6	0.58-0.75

CAS	0.67	0.58-0.75	0.67	0.59-0.76
CLT	0.67	0.58-0.75	0.67	0.58-0.75
CShS	0.68	0.59-0.76	0.68	0.59-0.76
Model 4: CVRF + Elastography parameters				
CAT	0.66	0.57-0.75	0.65	0.57-0.743
CAS	0.67	0.58-0.75	0.67	0.58-0.75
CLT	0.67	0.58-0.75	0.66	0.57-0.74
CShS	0.6	0.59-0.76	0.67	0.58-0.75

CVRF Cardiovascular risk factors
IMT Intima-media thickness
CAS Cumulated axial strain
CAT Cumulated axial translation
CLT Cumulated lateral translation
CShS Axial shear strain magnitude

Figure 9. ROC Curves: CDV Risk, IMT of CCA and Elastography Parameters of CCA for Detecting Coronary Plaques.

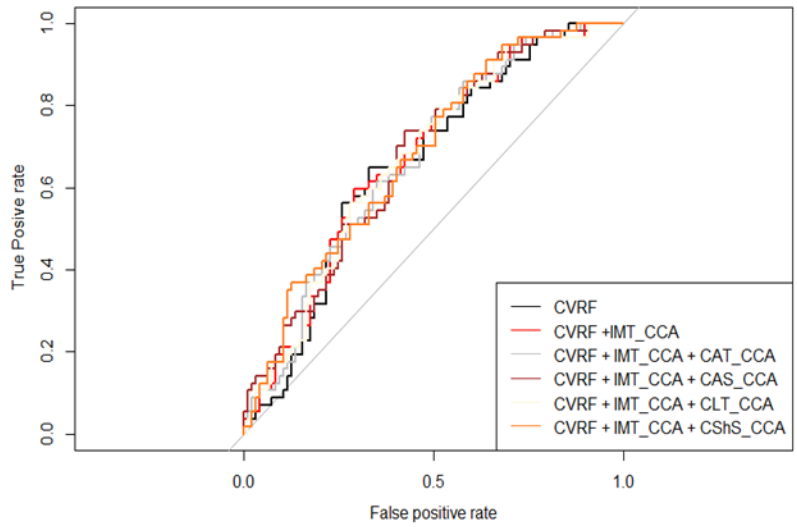

CVFR cardiovascular risk factors
IMT_CCA Intima-media thickness of common carotid artery
CAT_CCA cumulated axial translation of common carotid artery
CAS_CCA Cumulated axial strain of common carotid artery

CLT_CCA cumulated lateral translation (mm)of common carotid artery
CShS_CCA Axial shear strain magnitude of common carotid artery

Figure 10. ROC Curves: CDV Risk, IMT of ICA and Elastography Parameters of ICA for Detecting Coronary Plaques.

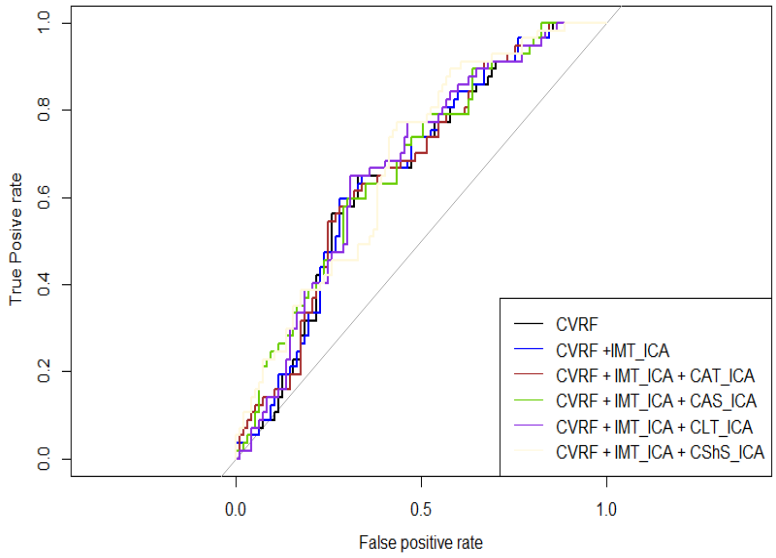

CFRF cardiovascular risk factors
IMT_ICA Intima-media thickness of internal carotid artery
CAT_ICA cumulated axial translation of internal carotid artery
CAS_ICA Cumulated axial strain of internal carotid artery
CLT_ICA cumulated lateral translation (mm) of internal carotid artery
CShS_ICA Axial shear strain magnitude of internal carotid artery

Figure 11. ROC Curves: CDV Risk and Elastography Parameters of CCA for Detecting Coronary

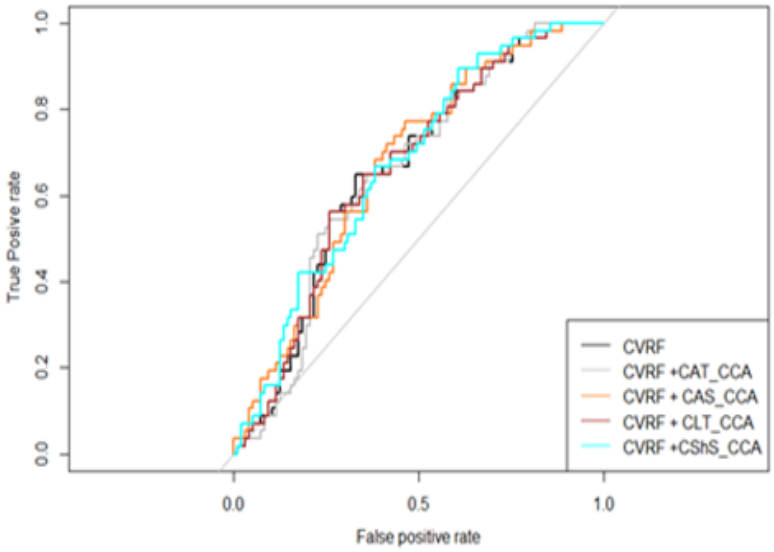

Plaques**.**

CVFR cardiovascular risk factors
CAT_CCA cumulated axial translation of common carotid artery
CAS_CCA Cumulated axial strain of common carotid artery
CLT_CCA cumulated lateral translation (mm)of common carotid artery
CShS_CCA Axial shear strain magnitude of common carotid artery

Figure 12. ROC Curves: CDV risk and Elastography Parameters of ICA for Detecting Coronary Plaques.

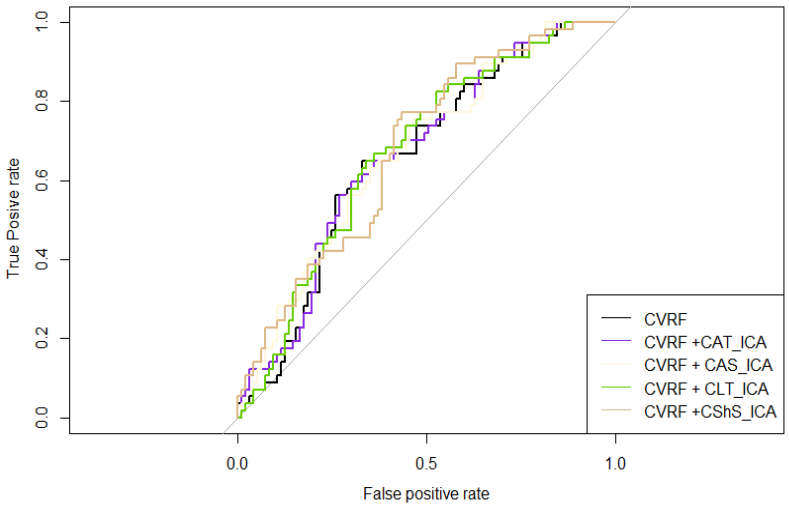

CFRF cardiovascular risk factors
CAT_ICA cumulated axial translation of internal carotid artery

CAS_ICA Cumulated axial strain of internal carotid artery
CLT_ICA cumulated lateral translation (mm) of internal carotid artery
CShS_ICA Axial shear strain magnitude of internal carotid artery

Chapter 5:

Discussion & Conclusion

5.1. Discussion

Compared to the general population, PLWH face an elevated risk of experiencing myocardial infarction (215, 216).

In this study, our objective was to evaluate the added predictive value of models incorporating carotid elastography parameters and IMT in predicting the development of coronary artery disease, beyond the scope of conventional risk factors. Our research prospectively enrolled 154 participants, comprising PLWH and HIV-negative healthy volunteers. All participants underwent coronary CT angiography and carotid US elastography to assess subclinical coronary atherosclerosis. At the time of recruitment, all enrolled participants were asymptomatic for cardiovascular issues and had mild to moderate cardiovascular risk scores. In the coronary CT angiography analysis, there was no difference in the overall prevalence of coronary artery plaque between PLWH and non-HIV participants ($p = 0.46$). Furthermore, there was no statistically significant disparity observed in either IMT or any elastography features of the internal and common carotid arteries between the two groups.

Canadian HIV and Aging Cohort Study (CHACS)

Firstly, this project is nested within the Canadian HIV and Aging Cohort Study (CHACS). CHACS is an ongoing, multicenter, prospective, controlled cohort study that currently monitors over 1,100 individuals, comprising people living with HIV (PLWH) and non-HIV-infected participants, across ten Canadian centers.

The advantage of a project nested within a large prospective controlled cohort is the ability to longitudinally track groups of individuals who share similarities in relevant variables (control variables), while also possessing a specific distinguishing characteristic (exposure of interest). Researchers can then compare the outcomes (outcomes of interest) within these groups, and crucially, between them, facilitating the investigation of causative relationships between specific characteristics and their corresponding results. Furthermore, within a prospective cohort,

researchers can delineate temporal sequences between an exposure and an outcome. Another notable advantage of employing a prospective cohort design is its inherent ability to mitigate selection bias. Since the outcome remains unknown at the time of establishing the initial status, data points are selected for evaluation without prior knowledge of the eventual outcome, reducing the potential for biased data selection. Conversely, one of the drawbacks associated with such studies is the necessity to track a substantial number of subjects over extended time periods. This undertaking can prove to be both expensive and time-consuming. Additionally, the potential for differential loss to follow-up between groups poses a risk, as it may introduce bias.

Our study employs an observational cross-sectional design, nested in a prospective study. While this type of study (with a cross-sectional design) does not yield conclusive insights into cause-and-effect relationships or temporal sequences of events, it does offer the advantage of simultaneously comparing multiple factors. Moreover, it serves as a basis for subsequent studies, facilitating the assessment of specific issues in greater depth.

Summary of Our Main Results

Following adjustment for cardiovascular risk factors, only smoking exposure retained a significant association with the presence of coronary plaque, demonstrating a prevalence ratio of 1.10 (95%CI 1.04 – 1.13; $p < 0.001$) for plaque presence (see discussion below). Neither carotid elastography parameters nor carotid intima-media thickness showed any significant association with coronary atherosclerosis. Our ROC analyses revealed that adding IMT or elastography data to the model, which initially included only cardiovascular risk factors, did not enhance the prediction accuracy of these multi-source models.

Ultrasound Non-Invasive Vascular Elastography

Utilizing non-invasive vascular elastography (NIVE) based on our data, we found that elastography parameters did not exhibit statistically significant differences PLWH and the group of healthy volunteers. This finding contradicts the observations made by Roy Cardinal et al. (209), who reported that NIVE, based on radio-frequency data, was capable of detecting differences in

axial strain and translation motion PLWH and control subjects. In this study, the findings indicated that HIV-infected subjects exhibited lower cumulated lateral translations in both common and internal carotid arteries. Additionally, lower cumulated axial strains were observed in the internal carotid arteries of PLWH. This contradiction with the findings of Roy Cardinal et al. (209) may be attributed to differences in methodology and sample size.

In our analysis, the total sample size comprised 154 participants, with 83 being HIV+ and 71 being HIV-. Comparatively, in Roy Cardinal's study, the total number of participants was 149, consisting of 74 HIV-infected individuals and 75 control subjects. In contrast, our sample included a higher proportion of males, comprising 137 participants (98.0%). Among these, 79 (95.2%) were HIV+, and 58 (81.7%) were HIV-. Conversely, in Roy Cardinal's study, there were 128 males (86%) of which 70 (95%) were HIV+, and 58 (77%) were HIV-. Furthermore, in our statistical analysis, we employed Student's t-tests for between-group comparisons when the data followed a normal distribution. For non-normally distributed data, we utilized the Mann–Whitney test. In contrast, in Roy Cardinal's study, the comparison between infected and control subjects was conducted using Mann–Whitney tests.

In the previously mentioned study by Roy Cardinal et al., which was also part of the Canadian HIV and Aging Cohort Study, ultrasound elastography findings indicated that carotid artery walls in PLWH who had low or intermediate risk factors for cardiovascular disease exhibited greater rigidity, smaller axial strains, and more displacements compared to non-HIV controls (209). In the study by Tjan et al. wall stiffness measured using US elastography emerged as a robust predictor of cerebrovascular accidents (217). This research entailed a pair-matched case-control study involving 40 case subjects and 40 controls from the general population. Strain elastography ultrasound was employed to assess carotid arteries, and the findings revealed that carotid artery stiffness constituted a significant risk factor for stroke, with an odds ratio of 351 (p-value < 0.001) (217). Numerous studies have consistently demonstrated an association between the presence of carotid artery stiffness and the incidence of stroke (109, 112, 218). Additionally, this stiffness has been linked to the extent of atherosclerosis and the presence of carotid artery plaque (219). Furthermore, elastography assessments unveiled early carotid artery stiffening in children with high body mass index (BMI) (210). In line with the findings of two studies by the authors (209,

210), biomechanical vessel wall assessments in these high-risk populations revealed the presence of premature subclinical atherosclerosis.

In our study, CIMT did not exhibit significant differences between PLWH and non-HIV controls. Moreover, our research demonstrated that the inclusion of CIMT alongside elastography parameters and cardiovascular models did not enhance the predictive capacity of these models. A similar observation was made in a meta-analysis encompassing 14 population-based cohorts, comprising data from 45,828 individuals. In the meta-analysis, studies were eligible for inclusion if they comprised participants from the general non-HIV population, measured common CIMT at baseline, and subsequently followed individuals for the occurrence of first-time myocardial infarction or stroke. The results of this study indicated that the augmentation of common CIMT measurements to the 10-year Framingham Risk Score in the general population had minimal added value (0.8% according to the prediction model). Such a finding is unlikely to have clinical significance (220). Additionally, another meta-analysis, comprising 15 articles aimed at evaluating the association of CIMT with future cardiovascular events, concluded that the inclusion of CIMT in cardiovascular risk prediction models did not enhance their performance compared to models incorporating only conventional risk factors (221). Similar findings were also reported in other studies involving different populations (220, 222).

It is noteworthy that the absence of added prognostic value in models incorporating CIMT could be attributed to the observation that early carotid atherosclerosis primarily develops in the bulb. This region may not be as readily detected using B-mode ultrasound, as indicated by Fin et al. in 2009 (223). B-mode ultrasound's capability for detecting plaques with features such as lipid-rich necrotic cores, intraplaque hemorrhage, and thin fibrous caps, which are closely associated with plaque vulnerability and cardiovascular risk, is likely limited (224).

While PLWH are experiencing a rising incidence of coronary artery disease (54), accurately predicting cardiovascular risk within this population continues to be a challenging endeavor (225, 226, 227, 228).

Our study confirms the strong association between smoking and heightened cardiovascular risk, as previously demonstrated by other researchers (see discussion below). Nevertheless, our data

did not reveal a significant improvement in predictive power when incorporating biomechanical assessments of the carotid artery wall into models for CAD prediction.

Smoking

Our prospective study encompassed participants characterized by low to intermediate cardiovascular risk, all of whom had no prior history of cardiovascular disease. One of our key findings is the confirmation of a significant association between smoking and subclinical coronary atherosclerosis within this low cardiovascular risk group. Specifically, we observed a prevalence ratio of 1.10 (50% confidence interval: 1.04 – 1.13; $p < 0.001$).

Smoking is widely acknowledged as a significant contributing factor to cardiovascular diseases and mortality in the general population (229). Toxic compounds present in cigarette smoke, such as nicotine and nitric oxide, have been observed to accelerate the rate of endothelial cell destruction, suggesting that they may indeed promote vascular damage (230, 231). Smoking exerts its influence on atherogenic inflammatory pathways, for instance, through the interleukin-6 pathway (232), local recruitment of leukocytes (232), and monocyte adherence to endothelial cells (233).

PLWH have a higher exposure to smoking compared to individuals without HIV. In a systematic review, Johnston et al. reported pooled odds of smoking among PLWH to be 1.64 (95% CI: 1.45–1.85) when compared to the general population (234). Helleberg et al. conducted a population-based study in Denmark, revealing that the risk of mortality associated with smoking was significantly higher in PLWH compared to the general population (235). When smokers were compared to non-smokers, the excess mortality rate among PLWH was 17.6 per 1000 person-years (95% CI, 13.3–21.9), while it was 4.8 (95% CI, 3.2–6.4) for individuals without HIV (235).

Our study had several limitations. Firstly, it employed a cross-sectional design, which precludes the establishment of cause-and-effect relationships based solely on the associations observed. Secondly, our study had a higher proportion of male participants than females. Notably, gender has been noted to exert an influence on carotid elasticity, with females exhibiting greater vascular elasticity compared to males (236). Interestingly, Riley et al. (237) similarly observed

disparities in carotid artery wall elasticity between men and women. Consequently, it remains uncertain whether our findings can be generalized to women. Furthermore, it's worth noting that diabetes mellitus did not emerge as a significant confounding factor in our present study, given the minimal number of diabetic participants among our cohort. Nonetheless, examining the potential confounding influence of diabetes should be a crucial consideration in future studies of a similar nature. We also excluded participants with renal failure. While this exclusion might have led to an underestimation of CAD, it doesn't introduce bias into our results. However, it does constrain the generalizability of our findings to populations with renal failure. The limited sample size within our HIV group, coupled with the presence of HIV-related confounders like co-infections (cytomegalovirus, hepatitis), variations in ART regimens, ART durations, nadir CD4+ and CD4+ T-cell counts, and the CD4+/CD8+ ratio, posed constraints on our ability in the current study to comprehensively evaluate the association between HIV-related factors and arterial wall stiffness. A larger dataset may be necessary to uncover any potential associations. Additionally, in our current study, elastography parameters were measured only once. However, the inclusion of repeated measures over several years could provide valuable insights into the relationship between elastography and either the incidence of new coronary plaques or the progression of existing ones. It is possible that a study employing such a design may offer more power compared to our current approach. However, due to the analysis of 2D longitudinal images of the carotid artery, it was inevitable to encounter out-of-plane motion artifacts. The measurement of CIMT specifically during diastole, as opposed to averaging measurements over systole and diastole, and considering the average of both carotid artery sides, were also limitations. Finally, we employed coronary atherosclerosis as a surrogate endpoint; in future longitudinal studies, our models could be assessed against clinical cardiovascular and non-cardiovascular events.

5.2. Conclusion

In summary, our comprehensive study involved 154 consecutive PLWH and non-HIV controls, all nested within a large prospective cohort. Our primary aim was to determine the additional predictive value of incorporating carotid ultrasound elastography into existing models for the assessment of subclinical coronary atherosclerosis, beyond the use of conventional risk factors. Carotid intima-media thickness was not associated with coronary atherosclerosis. Furthermore, the inclusion of elastography or other ultrasound parameters did not result in an enhanced ability to predict subclinical coronary artery disease. Further research is warranted to explore how imaging modalities or other surrogate markers could improve cardiovascular risk assessment within the HIV population.

Chapter 6.

Manuscript

6.Carotid artery biomechanical parameters as measured with ultrasound elastography in HIV individuals – An assessment of the association to coronary atherosclerosis and comparison to traditional cardiovascular risk factors.

Nura Shnqir 1-2, M Sadouni 1-2, MH Cardinal 2, G Soulez 1-2, C Tremblay 2-3, G Cloutier 1-2, M Durand 2-4, C Chartrand-Lefebvre 1-4

1: Département de radiologie, radio-oncologie et médecine nucléaire, Université de Montréal
2 : CRCHUM
3 : Département de microbiologie et infectiologie, Université de Montréal
4 : Département de médecine, Université de Montréal

6.1. Abstract

Purpose: To assess the association and use of biomechanical characteristics of carotid walls and carotid intima-media thickness (IMT), as evaluated by ultrasound, when included in prediction models of coronary CT plaque burden in people living with HIV (PLWH) and HIV-negative population individuals.

Methods: In this cross-sectional study, 164 participants (mean age 57 years ±8 years; 134 men) with low/intermediate cardiovascular risk were recruited from the ongoing prospective Canadian HIV and Aging Cohort Study (CHACS). Among the 164 recruited participants, a total of 154 participants (mean age, 56.5 years ±7.55 years; 83 PPLWH, 54 %; 137 men; 88%) were evaluated. Ten participants were excluded because their coronary plaque data were not available. The mean time interval between coronary CT and carotid ultrasound per participant is 7.69 ± 20.1 months.

By using ultrasound, we measured cumulated axial strain, cumulated shear strain, cumulated axial translation, cumulated lateral translation and IMT of the common and internal carotid arteries. Participants also underwent cardiac CT for the assessment of coronary plaque. Univariate and multivariate Poisson regression analyses with robust variance were performed to identify how cardiovascular risk factors, IMT and elastography parameters are independently associated with coronary plaque presence. Receiver operating characteristic (ROC) curve and area under the curve (AUC) analysis were also used to compare different prediction models for coronary plaque presence.

Results: There were 83 PLWH and 71 controls (N=154). The median 10-year Framingham risk score was 12% [IQR, 8 - 16] in PLWH and 9% [IQR,7 -15] in controls ($p = 0.045$). In PLWH group, coronary plaques were presented in 55 participants (61.1%) compared with 42 (56.8%) in non-HIV control ($p = .46$). Carotid IMT and all elastography features for both internal and common carotid arteries were similar between PLWH and healthy volunteers.

After adjustment for cardiovascular risk by multivariate Poisson regression, smoking exposure was significantly associated for coronary plaque presence on CT (prevalence ratio 1.10, 95%CI 1.04 – 1.13, $p < 0.001$). No significant association with other coronary artery disease risk factors nor with HIV status was shown at multivariate analysis. Carotid elastography parameters and

carotid intima-media thickness were not associated with coronary atherosclerosis, after adjustment.

AUC analyses did not show any significant difference in predictive accuracy between models when adding either elastography parameters, IMT, or adding both elastography parameters and IMT results to cardiovascular risk factor model, with AUCs results in all models ranging from 0.647 to 0.681.

Conclusion: In our study, models including carotid elastography and IMT did not increase the prediction for the presence of coronary plaque in PLWH or controls, over models including only traditional cardiovascular risk factors.

Key words: HIV, computed tomography, angiography, us elastography, atherosclerosis

6.2. INTRODUCTION

Cardiovascular disease is as an important cause of death in people living with HIV infection (PLWH) under antiretroviral therapy (ART) (1). Increased risk of coronary artery disease (CAD) in this population has been demonstrated in several large cohort studies (2, 3). However, accurate prediction of cardiovascular risk in PLWH remains a significant unmet medical need. Currently used cardiovascular risk calculation algorithms still systematically underestimate the risk in PLWH, such as the Framingham risk score (4, 5). Also, underprediction of the American College of Cardiology/American Heart Association pooled cohort cardiovascular risk equations (PCEs) (6), which includes traditional risk factors, has been reported in PLWH with low to-moderate cardiovascular risk or in women with HIV. Moreover, attempts to improve risk models adding HIV-variables to the algorithms remained unsuccessful (7, 8). Consequently, clinical teams fail to identify PLWH who could benefit from aggressive cardiovascular risk reduction.

In the light of this low accuracy of current cardiovascular risk equations in PLWH, developing and tailoring risk models incorporating a) traditional risk variables, b) HIV-specific variables and ultimately c) novel variables is of prime importance.

Recent insights gained from studies performed in the general population demonstrated that atherosclerotic burden identified at coronary computed tomography (CT) angiography is a strong predictor of future major events (9, 10). Coronary CT, although robust, still involves radiation exposure and use of iodinated contrast agents. In comparison, carotid ultrasound elastography is a novel non-invasive tool that can be used to assess subclinical atherosclerosis. It detects deformations and strains in arterial wall and atherosclerotic plaque, as induced by the pulsating blood flow (11-13).

In the present controlled study, nested in a large prospective cohort, we assessed models that integrate carotid elastography and intima-media thickness (IMT), cardiovascular risk factors and HIV-related factors, including antiretroviral therapy (ART), for coronary artery disease prediction in PLWH and non-HIV controls.

6.3.MATERIALS AND METHODS

This study has received approval from the institutional review board on ethics at the *Centre Hospitalier de l'Université de Montréal*. Written informed consent was obtained from all participants (14).

6.3.1. Study design and population

This is a cross-sectional study, nested in the Canadian HIV and Aging Cohort Study (CHACS) (14). CHACS is an ongoing multicenter, prospective, controlled cohort, actively following more than 1100 people living with HIV (PLWH) and non-HIV-infected participants in 10 Canadian centers.

In the CHACS, recruitment is hospital-based as well as community-based, for both HIV and non-HIV participants. Hospital-based recruitment involves PLWH aged 40 years or older, enrolled from the HIV clinics of the University of Montreal Hospital. Non-HIV healthy volunteers with similar ages are recruited from outpatient internal medicine clinics of the same hospital. Community recruitment for the PLWH is performed within family medicine clinics in Montreal. For healthy volunteers, it is performed within non-HIV friends and family (proximity recruitment), in order to ensure with similar socioeconomic status between the two groups.

All PLWH and healthy volunteer participants in the present study were recruited from the CHACS, between 2013 and 2019. They were consecutively included in an imaging subcohort if their cardiovascular risk was low or intermediate (10-year Framingham score 5% to 20%) and they had no history or symptoms of coronary artery disease. Exclusion criteria included history of contrast media allergy and creatinine clearance of less than 50 mL/min.

Participants underwent both carotid ultrasound elastography and cardiac computed tomography.

6.3.2. Ultrasound imaging

For carotid ultrasound, arterial walls of right and left common and internal carotids were assessed, and 4 cine-loops were acquired for every patient. Longitudinal views of each vessel were acquired with an Aixplorer system (SuperSonic Imagine) using a 256-element linear array probe (SuperLinear™ SL15-4) at 7.5 MHz. The set of the frame rate was 50 frames per s, and cine-loops were documented for a duration of approximately 5 s. Examinations were performed by a technologist (> 20 year-experience).

6.3.3. Image analysis

By utilizing a Hilbert transform and logarithm compression, B-mode cine-loops were reproduced from radiofrequency pictures. The size of pixels of reconstructed B-mode images was 20.5 µm axially × 200 µm laterally. A semiautomated segmentation method was used on all frames of B-mode cine-loops in order to detail a normal portion of the carotid far wall (without calcium or plaque) (15).

Plaques were defined as an intima-media thickness (IMT) more than 1 mm. Manual segmentation of carotid wall contours was done on a single B-mode image by an expert technologist, then reviewed by a radiologist (GS) (> 20 year-experience).

The carotid IMT was defined as the mean distance between two segmented carotid wall contours (lumen-intima and media-adventitia interfaces). It was calculated from automated segmentations, on all segmented frames and then averaged for each 5-s cine-loop; averages from the right and left sides IMT were obtained. All segmentations were performed blindly to elastography analysis.

Elastograms were generated for each pair of time-varying radiofrequency images, in order to assess the mechanical properties of both carotid artery walls and existing plaques (16). Elastography cine-loops of lateral and axial translation motions, axial strains, and axial shear strains were computed. Translations refer to rigid displacements within the cardiac cycle. The axial strain corresponds to compression or dilation of the arterial wall produced by the pulsating

blood. The shear strain refers to the angular deformation caused by the mechanical heterogeneity of the arterial wall (17).

For each mechanical parameter and over consecutive cardiac cycles, the spatial average over the segmented region was calculated and displayed as a function of time (16).

6.3.4. Coronary CT angiography

All participants underwent both non-contrast and contrast-enhanced cardiac CT. Prior to CT, 0.4 mg nitroglycerin was given sublingually, as well as metoprolol 50–75 mg orally if prescan heart rate was more than 60 beats per minute, unless contraindicated. Contrast-enhanced cardiac CT with electrocardiographic gating was performed using a 256-slice CT scanner (Brilliance iCT; Philips Healthcare), using370 mg/mL iopamidol (Bracco Imaging) at a rate of 5 mL/sec. Gantry rotation time was 270 msec, axial slice thickness 0.625 mm, and slice interval 0.45 mm.

6.3.5. Exposure of interest:

US Elastography parameters

Imaging biomarkers were extracted from the elastography time-varying curves. These were cumulated axial translation (CAT), cumulated lateral translation (CLT), maximum and cumulated axial strains (CAS), and maximum and cumulated axial shear strain magnitudes (CShS). The term “cumulated” used for each biomarker quantifies the total strain or translation occurring during the cardiac cycle and referred to the range of variation of the cumulated curve over a that cycle.

The ultrasound radiofrequency data processing and B-mode image segmentation methods were implemented inhouse in a commercial imaging platform (Visual-NIVE, Object Research Systems).

Intima-media-thickness which was also measured by us elastography.

6.3.6. Outcome of interest:

Coronary Plaque presence

Plaques were identified on the CT angiograms by one board-certified radiologist (CCL, 17-year experience).

All image assessors were blinded to the HIV status and clinical data.

6.3.7. Statistical analysis

Descriptive statistics are reported as means ± standard deviations (SDs), or median [25th –75th interquartile range (IQR)] and categorical variables are presented as count and percentage. Comparisons between-group were done using Student's t tests when data was normally distributed, or Mann–Whitney test when data was not normally distributed. Chi-square test was used when data was categorical.

Univariate and multivariate Poisson regression analysis with robust variance were performed to identify how cardiovascular risk factors, IMT and elastography parameters are independently associated with coronary plaque presence. All multivariate analyses were performed with adjustment for HIV serostatus and cardiovascular risk factors including age, sex, high blood pressure, family history of premature coronary artery disease, smoking exposure, low-density lipoprotein or high-density lipoprotein cholesterol, body mass index, and statin use if they showed a univariate association with coronary plaque presence with a p value 0.1 or less. In multivariate analysis, there are 19 multivariate models in order to test the association between cardiovascular risk factors, IMT, elastography parameters and coronary plaque presence. The first model included only cardiovascular risk factors significantly associated with coronary plaque presence, namely: age, statin use, and smoking exposure. In further models, each elastography parameters of either CCA or ICA with and without IMT of CCA or ICA were added to the cardiovascular risk factors model. For patients with incomplete continuous covariable data of smoking exposure, the median value was used to impute the missing data. A p value less than 0.05 was considered statistically significant.

Receiver operating characteristic (ROC) curve and area under the curve (AUC) analysis were used to compare different prediction models for coronary plaque presence.

Statistical analysis was performed using R software (version R i386 4.0.3R Foundation for Statistical Computing, https://www.r-project.org).

6.4. RESULTS:

6.4.1. Participant characteristics

Among 164 recruited participants, a total of 154 participants (mean age, 57 years ±8 years; 137 men; 88%) were evaluated. The mean time interval between coronary CT and carotid ultrasound per participant is 8 ± 20 months. Ten participants were excluded because their coronary plaque data were not available.

Participant's characteristics stratified by HIV status are described in Table 1. PLWH were 83, and healthy volunteers were 73. Participants with HIV had a mean age of 57 ±7 years, whereas controls had a mean age of 56 ± 8 years (p = 0.23). PLWH included more men compared with healthy volunteers (95% vs 82%, respectively; p = 0.02). The median Framingham risk score was 12% [IQR, 8 - 16] in PLWH and 9% [IQR,7 -15] in controls (p = 0.045). PLWH had lower BMI than controls (mean body mass index, 25.3 ±3.69 kg/m2 vs 27.2 ±4.69 kg/m2, respectively, p = 0.02). More PLWH were exposed to tobacco smoking (median 6.00 [IQR, 0 -18.0 pack-years] vs 0 pack-years [IQR, 0 - 7.20 pack-years] in controls (p < 0.001), and more smokers were among PLWH (21.7% [18 of 83] vs 9.9% [7 of 71], p = 0.051) respectively. There were marginally more statin users (30% [25 of 83] vs 16% [11 of 71]; p = 0.051) in the PLWH group, and average lipid values were different between groups, accordingly. No statistical differences were found for other clinical characteristics.

In the PLWH group, median HIV infection duration was 20.0 years [IQR,15.0 - 26.0 years]. Among them, 90.3% [75 of 83] were exposed to antiretroviral therapy, and median duration of antiretroviral therapy was 15.9 years [IQR,7.83 - 19.7years]. Viral load was detectable (>40

copies/ml) in 4.8% [4 of 84] of PLWH. Exposure to the different antiviral therapy classes is shown in Table 1.

Table 1. Clinical characteristics of participants, N = 154

	HIV+ (N=83)	**HIV- (N=71)**	**Total (N=154)**	**P Value**
Age (years)*	57.2 ±7.31	55.7 ±7.81	56.5 ±7.55	0.23
Sex, number (%)ǂ				**0.02**
Male	79 (95.2%)	58 (81.7%)	137 (98.0%)	
Female	4(4.8%)	13(18.3%)	17(11.0%)	
Missing	0(0%)	0(0%)		
Raceǂ				0.46
Asian	2(2.4%)	0(0%)	2(1.3%)	
Black (African)	1(1.2%)	0(0%)	1(0.6%)	
Black (Haitian)	2(2.4%)	1(1.4%)	3(1.9%)	
Caucasian	74(89.2%)	67(94.4%)	141(91.6%)	
Hispanic	3(3.6%)	3(4.2%)	6(3.9%)	
Missing	1(1.2%)	0(0%)	1(0.6%)	
10-year Framingham Risk Score (%) ♦				**0.045**
Median [Q25, Q75]	12.0 [8.00, 16.0]	9.00 [7.00, 15.0]	11.0 [7.00, 16.0]	
Missing	2(2.4%)	3(4.2)	5(3.2%)	
BMI (kg/m²) ♦				**0.019**
Mean ±SD	25.3 ±3.69	27.2 ±4.69	26.2 ±4.28	
Missing	3(3.6%)	2(2.8%)	5(3.2%)	
High waist circumference (cm)* ¹				0.44
Mean ±SD	94.6 ±10.5	96.0 ±11.2	95.2 ±10.8	
Missing	1(1.2%)	7(9.9%)	8(5.2%)	
Diabetesǂ				0.17
Yes	4(4.8%)	0(0%)	4(2.6%)	
No	79 (95.2%)	71 (100%)	150 (97.4%)	
Missing	0(0%)	0(0%)	0(0%)	
Hypertensionǂ				0.23

Yes **No** **Missing**	27 (32.5%) 56(67.5%) 0(0%)	16 (22.5%) 55(77.5%) 0(0%)	43 (27.9%) 111(72.1%) 0(0%)	
Smoking status[ł] **Current Smoker** **Ex Smoker** **Never Smoked** **Missing**	 18(21.7%) 35(42.2%) 27(32.5%) 3(3.6%)	 7(9.9%) 29(40.8%) 35(49.3%) 0(0%)	 25(16.2%) 64(41.6%) 62(40.3%) 3(1.9%)	0.051
Smoking history (Pack_year) ♦ [2] **Median [Q25, Q75]** **Missing**	6.00 [0, 18.0] 6(7.2%)	0 [0, 7.20] 2(2.8%)	0.900 [0, 14.9] 8(5.2%)	**0.006**
Family history of CVD[ł] **Yes** **No** **Missing**	 38 (45.8%) 45(54.2%) 0(0%)	 30 (42.3%) 41(57.7%) 0(0%)	 68 (44.2%) 68(44.2%) 0(0%)	0.78
HDL_Cholesterol(mmol/L) ♦ **Mean ±SD** **Missing**	1.25 ±0.331 2(2.4%)	1.42 ±0.386 0(0%)	1.33 ±0.366 2(1.3%)	**0.006**
LDL_Cholesterol(mmol/L) * **Mean ±SD** **Missing**	2.87 ±0.911 6(6.0%)	3.20 ±0.862 2(2.8%)	3.02 ±0.901 7(4.5%)	**0.02**
Total Cholesterol(mmol/L) * **Mean ±SD** **Missing**	4.84 ±1.13 2(2.4%)	5.27 ±1.03 1(1.4%)	5.04 ±1.10 3(1.9%)	**0.01**
Triglyceride (mmol/L) ♦ **Median [Q25, Q75]** **Missing**	1.40 [1.02, 2.02] 2(2.4%)	1.30 [0.940, 1.84] 2(2.8%)	1.34 [0.945, 1.98] 4(2.6%)	0.31
Statin use[ł] **Yes** **No**	 25 (30.1%) 58(69.9%)	 11 (15.5%) 60(84.5%)	 36 (23.4%) 118(76.6%)	0.051

Missing	0(0%)	0(0%)	0(0%)	
HIV duration(years) **Median [Q25, Q75]** **Missing**	20.0 [15.0, 26.0] 1 (1.2%)			
Exposure to ART **Missing**	75 (90.3%) 6 (7.2%)			
Exposure to INSTI **Missing**	31 (37.3%) 6 (7.2%)			
Exposure to NNRT **Missing**	37(44.5%) 6(7.2%)			
Exposure to NRTI **Missing**	70(84.3%) 6(7.2%)			
Exposure to PI **Missing**	55(66.2) 6(7.2%)			
Exposure to EI **Missing**	3(3.5) 6(7.2%)			
ARV duration(years) ♦ **Median [Q25, Q75]** **Missing**	15.9 [7.83, 19.7] 6(7.2%)			
Detectable viral load ǂ **Missing**	4(4.8%) 8 (9.6%)			
CD4 (cells/mm3) ♦ **Median [Q25, Q75]** **Missing**	590 [460, 809] 7 (7.8%)			
CD8 (cells/mm3) * **Mean ±SD** **Missing**	800 ±404 7(7.8%)			

* Student's t test

♦ Mann–Whitney test

ǂ Chi-square test

Bold P-value refers to significant p value (<0.05)

CVD: cardiovascular risk factors,

ART: antiretroviral therapy,

NRTI: nucleoside reverse transcriptase inhibitor,

NNRTI: nonnucleoside reverse transcriptase inhibitor,

PI: protease inhibitor,

INSTI: integrase strand transfer inhibitor

EI: entry inhibitors.

[1] High waist circumference is defined as over 102 cm in males or 88 cm in females

[2] pack-years is the product of the number of packs of cigarettes smoked per day by the number of years the person has smoked

[3] Defined as viral load =<40 copies/mL.

6.4.2. IMT and elastography, coronary plaques data

Carotid IMT and all elastography features for both internal and common carotid arteries were similar between PLWH and healthy volunteers (Table 2).

At coronary CT angiography, coronary artery plaque prevalence for all participants (N=154) was 63.0% [97 of 154], with 66.3% [55 of 83] in PLWH and 59.2% [42 of 71] in non-HIV participants (p = 0.46) (Table 2).

Table 2. Cardiac CT results, IMT and elastography parameters of participants, N = 154

	HIV+ (N=83)	**HIV- (N=71)**	**Total (N=154)**	**P Value**
IMT and elastography results				
IMT_ CCA (mm)* Mean ±SD	0.557 ±0.0796	0.538 ±0.0579	0.548 ±0.0708	0.10
IMT_ ICA (mm)* Mean ±SD	0.546 ±0.0681	0.535 ±0.0520	0.541 ±0.0612	0.29
CAT_CCA (mm)* Mean ±SD	0.265 ±0.0919	0.274 ±0.107	0.269 ±0.0990	0.55
CAT_ICA (mm) ♦ Mean ±SD	0.175 ±0.0764	0.185 ±0.0744	0.180 ±0.0754	0.38
CLT_CCA (mm)* Mean ±SD	0.419 ±0.187	0.444 ±0.164	0.431 ±0.177	0.38

CLT_ICA (mm)* Mean ±SD	0.292 ±0.158	0.319 ±0.134	0.304 ±0.147	0.25
CAS_CCA (%) ♦ Median [Q25, Q75]	2.83 [1.99, 3.65]	2.64 [2.15, 3.14]	2.67 [2.04, 3.50]	0.53
CAS _CCI (%) ♦ Mean ±SD	2.39 ±1.20	2.59 ±0.926	2.48 ±1.08	0.06
CShS_CCA (%) * Mean ±SD	0.194 ±0.0900	0.193 ±0.0770	0.193 ±0.0840	0.70
CShS_CCI (%) ♦ **Mean ±SD**	0.215 ±0.0927	0.228 ±0.0794	0.221 ±0.0868	0.37
Cardiac CT results				
Plaque presence				0.46
Yes	55 (66.3%)	42 (59.2%)	97 (63.0%)	
No	28(33.7%)	29 (40.8%)	57 (37.0%)	
Missing	0(0%)	0(0%)	0(0%)	

6.4.3. Association of cardiovascular risk factors, HIV status, elastography parameters, and carotid IMT with coronary plaque

Univariable Poisson regression analysis with robust variance revealed an association of smoking exposure ($p < 0.001$) and IMT of common carotid artery ($p = 0.02$) with coronary plaque presence ($p < 0.001$) (Table 3).

After adjustment for cardiovascular risk by multivariable Poisson regression, only smoking exposure remained significantly associated for coronary plaque presence on CT (prevalence ratio 1.10, 95%CI 1.04 – 1.13, $p < 0.001$ after adjustment for cardiovascular risk factors; 1.08, 95%CI 1.04 – 1.13, $p < 0.001$ after adjustment for cardiovascular risk factors and common carotid artery IMT; 1.09, 95%CI 1.04 – 1.10, $p < 0.001$ after adjustment for cardiovascular risk factors and internal carotid artery IMT). No significant association with other coronary artery disease risk factors nor with HIV status was shown at multivariate analysis. Carotid elastography parameters and carotid intima-media thickness were not associated with coronary atherosclerosis, after adjustment (Table 3).

Table 3. Association* of cardiovascular risk factors, IMT and elastography parameters of CCA and ICA with coronary plaque presence, N=154

Variables	**Univariable analysis**		**Multivariable ** model 1 = Cardiovascular risk**		**Multivariable ** model 2 A= Cardiovascular risk factors and CCA_IMT**		**Multivariable ** model 2B = Cardiovascular risk factors and ICA_IMT**	
	RR and 95 % CI	**P value**	**RR and 95 % CI**	**P value**	**RR and 95 % CI**	**P value**	**RR and 95 % CI**	**P value**
Age (cof^10)	1.13(0.98 - 1.31)	0.08	1.10 (0.96 -1.26)	0.16	1.08 (0.93-1.24)	0.27	1.11 (0.95 -1.34)	0.16
BMI	0.99(0.98-1.01)	0.83						
SEX	1.01(0.84-1.21)	0.88						
Hypertension	0.91(0.80-1.03)	0.13						
Family history of premature CVD	0.96(0.83-1.12)	0.66						
Smoking Pack year (cof^10)	1.10 (1.05 -1.14)	<0.001	1.10 (1.04 -1.13)	<0.001	1.08(1.04- 1.13)	<0.001	1.09 (1.04- 1.10)	<0.001
Statin use	1.26 (0.99-1.60)	0.07	1.15 (0.90-1.46)	0.26	1.13 (0.89-1.43)	0.29	1.15 (0.90-1.46)	0.25
HDL Cholesterol	1.07 (0.92- 1.25)	0.36						
LDL Cholesterol	1.01 (0.95-1.08)	0.68						
HIV status	1.05 (0.94_1.18)	0.36						
IMT_CCA	0.45 (0.22_0.90)	0.02			2.77(0.75_10.2)	0.12		
IMT_ICA	1.06 (0.43_ 2.60)	0.90					0.81 (0.13_ 4.91)	0.82
CAT_CCA	1.08 (0.61_1.89)	0.79						
CAT_ICA	1.33 (0.64_2.72)	0.44						
CLT_CCA	0.95 (0.69_1.29)	0.75						

CLT_ICA	1.13 (0.78-1.64)	0.51						
CAS-CCA	1.02 (0.96- 1.07)	0.54						
CAS-ICA	1.01 (0.96 -1.06)	0.72						
CShS-CCA	0.95 (0.91-1.00)	0.07						
CShS-ICA	1.05 (0.97- 1.13)	0.17						

*: Univariable and multivariable Poisson regression analysis with robust variance

**: Multivariate analyses were performed for a given predictor if this predictor showed a univariate association with coronary plaque presence with a p value 0.1 or less.

6.4.4. Assessment of predictive models

Using ROC analyses to assess the predictive accuracy of our multivariate Poisson's regression models, we generated ROC curves and Area Under the ROC curves (AUC), as AUC is a measure of the predictive ability of the model and typically ranges between 0.5 to 1, with 0.5 corresponding to a model that is no better than chance and 1 corresponding to 100% accuracy. In our analyses, adding IMT or elastography data to cardiovascular risk factors model did not increase the prediction accuracy of models. The AUCs results in all models ranging from 0.66 to 0.68 as shown in Table 4.

Table 4. Predictive value of CDV risk, IMT and elastography parameters of CCA and ICA for detecting coronary plaques

	ICA		CCA	
	AUC	95% CI	AUC	95%CI
Model 1: CVRF	0.66		0.574-0.747	
Model 2: CVRF + IMT	0.663	0.577-0.749	0.674	0.589-0.76
Model 3: CV FR +IMT+ Elastography parameters				
CAT	0.663	0.576-0.749	0.67	0.585-0.756
CAS	0.673	0.587-0.759	0.677	0.592-0.762
CLT	0.672	0.586-0.758	0.674	0.589-0.759
CShS	0.682	0.598-0.766	0.681	0.597-0.766
Model 4: CVRF + Elastography parameters				
CAT	0.665	0.578-0.751	0.657	0.57-0.743
CAS	0.671	0.585-0.757	0.670	0.585-0.756
CLT	0.674	0.588-0.759	0.662	0.576-0.748
CShS	0.68	0.595-0.764	0.672	0.587-0.757

Furthermore, in order to visualize the performance of the multivariate models, all models were plotted using ROC curves. Six models are illustrated on Figures 1 to 4 (see below). Figure 1 illustrates the curves related to the cardiovascular risk factors, with the IMT and the elastography parameters related to the internal carotid artery; Figure 2 illustrates the curves related to the cardiovascular risk factors, with the IMT and the elastography parameters related to the common carotid artery; Figure 3 illustrates the curves related to the cardiovascular risk factors, with the elastography parameters related to the internal carotid artery; Figure 4 illustrates the curves related to the cardiovascular risk factors, with the elastography parameters related to the common carotid artery.

Figures 1 to 4 show that all 6 curves of the models are moderately distant from the diagonal line, and similar one to another.

Figure 1. ROC curves CDV risk, IMT of ICA and elastography parameters of ICA for detecting coronary plaques

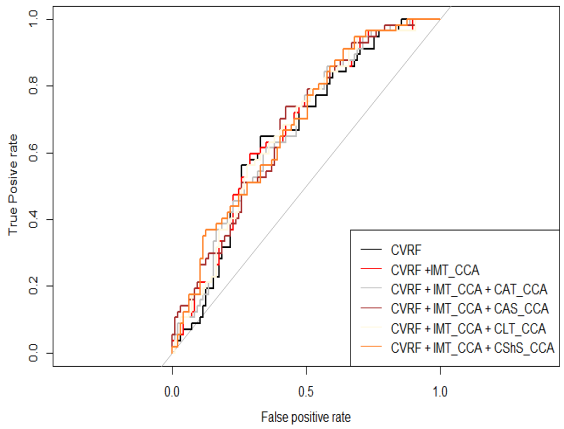

Figure 2. ROC curves CDV risk, IMT of CCA and elastography parameters of CCA for detecting coronary plaques

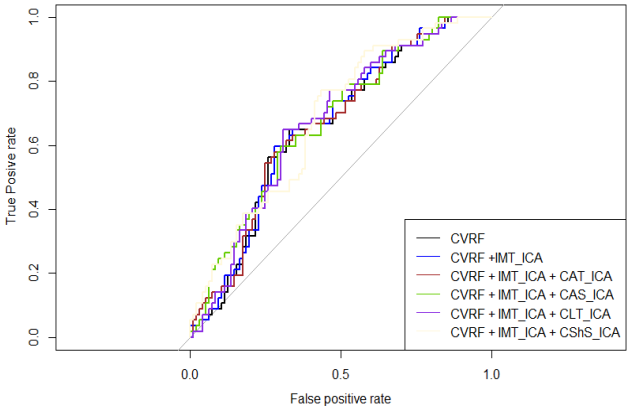

Figure 3. ROC curves CDV risk, and elastography parameters of ICA and for detecting coronary plaques

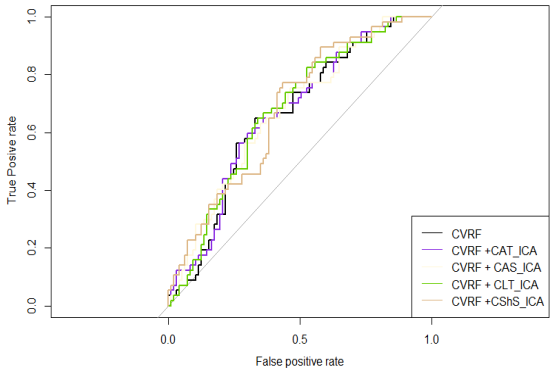

Figure 4. ROC curves CDV risk, and elastography parameters of CCA and for detecting coronary plaques

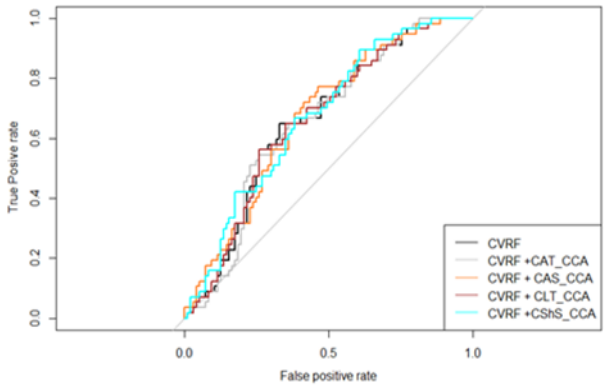

6.5. DISCUSSION AND CONCLUSION

Our study involved 154 consecutive PLWH and non-HIV controls, nested in a large prospective cohort, and assessed the incremental value of models that includes carotid ultrasound elastography for the prediction of subclinical coronary atherosclerosis as assessed with cardiac CT, further from traditional risk factors. Participants were asymptomatic, well-characterized and selected with mild to moderate cardiovascular risk score. The median time interval per participant between cardiac CT and carotid ultrasound was 8 days.

After adjustment for cardiovascular risk, only smoking exposure was significantly associated with coronary plaque presence, with a prevalence ratio of 1.10 (95% CI 1.04 – 1.13; $p < 0.001$) for plaque presence (Table 3). Carotid elastography parameters and carotid intima-media thickness were not associated with coronary atherosclerosis. Using ROC analyses, adding intima-media thickness (IMT) or elastography data to cardiovascular risk factors model did not increase the prediction accuracy of the models.

The finding of an association of smoking with subclinical coronary atherosclerosis in participants even with low to intermediate cardiovascular risk is worth to be emphasized. Smoking is well-known as an important cause for cardiovascular morbidity and mortality in the general population. Smoking exposure promotes vasomotor dysfunction through an impairment of the nitric oxide regulatory availability (18, 19). It has an impact on atherogenic inflammatory pathways, e.g through interleukin-6 pathway (20), local recruitment of leukocytes (20), and monocyte adherence to endothelial cells (21).

PLWH have an increased exposure to smoking that non-HIV individuals. In a systematic review, Johnston et al. showed the pooled odds of smoking to be 1.64 [(95% confidence interval, 95% CI: 1.45–1.85) for PLWH, compared to the general population (22). Moreover, the risk of death associated with smoking is increased in PLWH, in comparison to the general population. In a nation-wide population-based study in Denmark, Helleberg et al. (23) assessed mortality attributable to smoking among PLWH. When smokers were compared to non-smokers, excess mortality rates in PLWH was 17.6 per 1000 person-years (95% CI, 13.3–21.9), versus 4.8 (95% CI, 3.2–6.4) for non-HIV individuals.

Carotid ultrasound elastography enables to evaluate the deformation of carotid walls under stress (11, 24), ie the deformations of the arterial wall and plaque induced by the pulsating blood flow. None of the carotid elastography parameters assessed in the present study was significantly associated with the presence of subclinical coronary plaque, when included in models altogether with cardiovascular risk factors, either with or without IMT, respectively. In another study nested in our prospective cohort, ultrasound elastography previously showed that carotid artery walls in PLWH having low or intermediate cardiovascular risk were stiffer as axial strains and displacements were smaller, in comparison to non-HIV controls (16), whereas IMT was not different in PLWH and non-HIV controls. Elastography also showed carotid artery premature stiffening in children with elevated body-mass index (BMI) (17). As reported by the authors of both studies (16, 17), biomechanical vessel wall assessment in these at-risk populations shows premature subclinical atherosclerosis.

PLWH are increasingly subject to coronary artery disease (1), but still, prediction of the cardiovascular risk in this population remains inaccurate (4, 7, 8, 25). Our study confirms the strong cardiovascular risk associated to smoking, as previously shown. Our data did not show a significant incremental value of models that included biomechanics of the carotid artery wall for the prediction of CAD. The number of participants in our prospective study was moderate, which can be a limitation to our study. Another limitation is that HIV-related factors, such as antiretroviral therapy and immune status were not included in our models. Finally, we used coronary atherosclerosis as a surrogate end-point; in future longitudinal studies, our models could be assessed against clinical cardiovascular and non-cardiovascular events.

In conclusion, our study involved 154 consecutive PLWH and non-HIV controls, nested in a large prospective cohort, and assessed the incremental value of models that includes carotid ultrasound elastography for the prediction of subclinical coronary atherosclerosis as assessed with cardiac CT, further from traditional risk factors. None of the carotid wall elastography parameters was associated with coronary atherosclerosis, neither was carotid intima-media thickness. Further work should be performed to evaluate how imaging or other surrogate markers could improve cardiovascular risk assessment in the HIV population.

6.6. References

1. Farahani M, Mulinder H, Farahani A, Marlink R. Prevalence and distribution of non-AIDS causes of death among HIV-infected individuals receiving antiretroviral therapy: a systematic review and meta-analysis. Int J STD AIDS. 2017;28(7):636-50.
2. Durand M, Sheehy O, Baril JG, Lelorier J, Tremblay CL. Association between HIV infection, antiretroviral therapy, and risk of acute myocardial infarction: a cohort and nested case-control study using Québec's public health insurance database. J Acquir Immune Defic Syndr. 2011;57(3):245-53.
3. Freiberg MS, Chang C-CH, Kuller LH, Skanderson M, Lowy E, Kraemer KL, et al. HIV infection and the risk of acute myocardial infarction. JAMA Internal Medicine. 2013;173(8):614-22.
4. D'Agostino RB, Sr., Vasan RS, Pencina MJ, Wolf PA, Cobain M, Massaro JM, et al. General cardiovascular risk profile for use in primary care: the Framingham Heart Study. Circulation. 2008;117(6):743-53.
5. Raggi P, De Francesco D, Manicardi M, Zona S, Bellasi A, Stentarelli C, et al. Prediction of hard cardiovascular events in HIV patients. Journal of Antimicrobial Chemotherapy. 2016;71(12):3515-8.
6. Goff DC, Jr., Lloyd-Jones DM, Bennett G, Coady S, D'Agostino RB, Gibbons R, et al. 2013 ACC/AHA guideline on the assessment of cardiovascular risk: a report of the American College of Cardiology/American Heart Association Task Force on Practice Guidelines. Circulation. 2014;129(25 Suppl 2):S49-73.
7. Feinstein MJ, Nance RM, Drozd DR, Ning H, Delaney JA, Heckbert SR, et al. Assessing and Refining Myocardial Infarction Risk Estimation Among Patients With Human Immunodeficiency Virus: A Study by the Centers for AIDS Research Network of Integrated Clinical Systems. JAMA Cardiol. 2017;2(2):155-62.
8. Friis-Møller N, Ryom L, Smith C, Weber R, Reiss P, Dabis F, et al. An updated prediction model of the global risk of cardiovascular disease in HIV-positive persons: The Data-collection on

Adverse Effects of Anti-HIV Drugs (D:A:D) study. European journal of preventive cardiology. 2016;23(2):214-23.

9. Ahmadi N, Nabavi V, Hajsadeghi F, Flores F, French WJ, Mao SS, et al. Mortality incidence of patients with non-obstructive coronary artery disease diagnosed by computed tomography angiography. Am J Cardiol. 2011;107(1):10-6.

10. Nerlekar N, Ha FJ, Cheshire C, Rashid H, Cameron JD, Wong DT, et al. Computed Tomographic Coronary Angiography-Derived Plaque Characteristics Predict Major Adverse Cardiovascular Events: A Systematic Review and Meta-Analysis. Circ Cardiovasc Imaging. 2018;11(1):e006973.

11. Maurice RL, Ohayon J, Frétigny Y, Bertrand M, Soulez G, Cloutier G. Noninvasive vascular elastography: theoretical framework. IEEE Trans Med Imaging. 2004;23(2):164-80.

12. Mercure E, Cloutier G, Schmitt C, Maurice RL. Performance evaluation of different implementations of the Lagrangian speckle model estimator for non-invasive vascular ultrasound elastography. Med Phys. 2008;35(7):3116-26.

13. Cardinal MH, Meunier J, Soulez G, Maurice RL, Therasse E, Cloutier G. Intravascular ultrasound image segmentation: a three-dimensional fast-marching method based on gray level distributions. IEEE Trans Med Imaging. 2006;25(5):590-601.

14. Durand M, Chartrand-Lefebvre C, Baril J-G, Trottier S, Trottier B, Harris M, et al. The Canadian HIV and aging cohort study-determinants of increased risk of cardio-vascular diseases in HIV-infected individuals: rationale and study protocol. BMC Infectious Diseases. 2017;17(1):611.

15. Destrempes F, Meunier J, Giroux MF, Soulez G, Cloutier G. Segmentation of Plaques in Sequences of Ultrasonic B-Mode Images of Carotid Arteries Based on Motion Estimation and a Bayesian Model. IEEE Transactions on Biomedical Engineering. 2011;58(8):2202-11.

16. Roy Cardinal MH, Durand M, Chartrand-Lefebvre C, Fortin C, Baril JG, Trottier B, et al. Increased carotid artery wall stiffness and plaque prevalence in HIV infected patients measured with ultrasound elastography. Eur Radiol. 2020;30(6):3178-87.

17. El Jalbout R, Cloutier G, Roy-Cardinal MH, Henderson M, Levy E, Lapierre C, et al. The value of non-invasive vascular elastography (NIVE) in detecting early vascular changes in overweight and obese children. Eur Radiol. 2019;29(7):3854-61.

18. Mayhan WG, Sharpe GM. Effect of cigarette smoke extract on arteriolar dilatation in vivo. J Appl Physiol (1985). 1996;81(5):1996-2003.

19. Ota Y, Kugiyama K, Sugiyama S, Ohgushi M, Matsumura T, Doi H, et al. Impairment of endothelium-dependent relaxation of rabbit aortas by cigarette smoke extract--role of free radicals and attenuation by captopril. Atherosclerosis. 1997;131(2):195-202.

20. Bermudez EA, Rifai N, Buring JE, Manson JE, Ridker PM. Relation between markers of systemic vascular inflammation and smoking in women. Am J Cardiol. 2002;89(9):1117-9.

21. Kalra VK, Ying Y, Deemer K, Natarajan R, Nadler JL, Coates TD. Mechanism of cigarette smoke condensate induced adhesion of human monocytes to cultured endothelial cells. J Cell Physiol. 1994;160(1):154-62.

22. Johnston PI, Wright SW, Orr M, Pearce FA, Stevens JW, Hubbard RB, et al. Worldwide relative smoking prevalence among people living with and without HIV. Aids. 2021;35(6):957-70.

23. Helleberg M, Afzal S, Kronborg G, Larsen CS, Pedersen G, Pedersen C, et al. Mortality attributable to smoking among HIV-1-infected individuals: a nationwide, population-based cohort study. Clinical infectious diseases : an official publication of the Infectious Diseases Society of America. 2013;56(5):727-34.

24. Naim C, Cloutier G, Mercure E, Destrempes F, Qin Z, El-Abyad W, et al. Characterisation of carotid plaques with ultrasound elastography: feasibility and correlation with high-resolution magnetic resonance imaging. Eur Radiol. 2013;23(7):2030-41.

25. Raggi P, De Francesco D, Manicardi M, Zona S, Bellasi A, Stentarelli C, et al. Prediction of hard cardiovascular events in HIV patients. J Antimicrob Chemother. 2016;71(12):3515-8.

Chapter 7:

Bibliography

Bibiography

1. UNAIDS. UNAIDS DATA 2022 2022 [Available from: https://www.unaids.org/en/topic/data.
2. L C. The Epidemiology of HIV in Canada CATIE Canada's source of HIV and Hepatitis C information2021 [Available from: https://www.catie.ca/the-epidemiology-of-hiv-in-canada.
3. Shaw GM, Hunter E. HIV transmission. Cold Spring Harbor perspectives in medicine. 2012;2(11).
4. INFO.HIV.GOV C. Offering Information on HIV/AIDS Treatment, Prevention, and Research

2020 [updated September 2020. Available from: https://clinicalinfo.hiv.gov/en.
5. Day T, Mideo N, Alizon S. Why is HIV not vector-borne? Evolutionary Applications. 2008;1(1):17-27.
6. King C, Ellington S, Kourtis A. The role of co-infections in mother-to-child transmission of HIV. Current HIV research. 2013;11(1):10-23.
7. Sharp PM, Hahn BH. The evolution of HIV-1 and the origin of AIDS. Philosophical Transactions of the Royal Society B: Biological Sciences. 2010;365(1552):2487-94.
8. CDC. HIV CDC centers of diseas control and prevention 2021 [Available from: https://www.cdc.gov/hiv/basics/whatishiv.html#:~:text=HIV%20infection%20in%20humans%20came,contact%20with%20their%20infected%20blood.
9. Charneau P, Borman AM, Quillent C, Guétard D, Chamaret S, Cohen J, et al. Isolation and envelope sequence of a highly divergent HIV-1 isolate: definition of a new HIV-1 group. Virology. 1994;205(1):247-53.
10. Wainberg MA. HIV-1 subtype distribution and the problem of drug resistance. AIDS. 2004;18 Suppl 3:S63-8.
11. Plantier J-C, Leoz M, Dickerson J, Oliveira F, Cordonnier F, Lemée V, et al. A new human immunodeficiency virus derived from gorillas. Nature medicine. 2009;15(8):871.
12. De Leys R, Vanderborght B, Haesevelde MV, Heyndrickx L, Van Geel A, Wauters C, et al. Isolation and partial characterization of an unusual human immunodeficiency retrovirus from two persons of west-central African origin. Journal of Virology. 1990;64(3):1207-16.
13. Simon F, Mauclere P, Roques P, Loussert-Ajaka I, Muller-Trutwin MC, Saragosti S, et al. Identification of a new human immunodeficiency virus type 1 distinct from group M and group O. Nature Medicine. 1998;4(9):1032.
14. Plantier JC, Lemee V, Dorval I, Gueudin M, Braun J, Hutin P, et al. HIV-1 group M superinfection in an HIV-1 group O-infected patient. AIDS. 2004;18(18):2444-6.
15. Gao F, Bailes E, Robertson DL, Chen Y, Rodenburg CM, Michael SF, et al. Origin of HIV-1 in the chimpanzee Pan troglodytes troglodytes. Nature. 1999;397(6718):436-41.
16. Sharp PM, Hahn BH. Origins of HIV and the AIDS pandemic. Cold Spring Harbor perspectives in medicine. 2011;1(1):a006841.
17. Wertheim JO, Worobey M. Dating the Age of the SIV Lineages That Gave Rise to HIV-1 and HIV-2. PLOS Computational Biology. 2009;5(5):e1000377.
18. Gottlieb MS, Schroff R, Schanker HM, Weisman JD, Fan PT, Wolf RA, et al. Pneumocystis carinii pneumonia and mucosal candidiasis in previously healthy homosexual men: evidence of a new acquired cellular immunodeficiency. New England Journal of Medicine. 1981;305(24):1425-31.
19. Brennan R, Durack D. Gay compromise syndrome. The Lancet. 1981;318(8259):1338-9.

20. Friedman-Kien A, Laubenstein L, Marmor M, Hymes K, Green J, Ragaz A, et al. Kaposis sarcoma and Pneumocystis pneumonia among homosexual men--New York City and California. Morbidity and Mortality Weekly Report. 1981;30(25):305-8.
21. Masur H, Michelis MA, Greene JB, Onorato I, Vande Stouwe RA, Holzman RS, et al. An Outbreak of Community-Acquired Pneumocystis carinii Pneumonia. New England Journal of Medicine. 1981;305(24):1431-8.
22. Barré-Sinoussi F, Chermann J-C, Rey F, Nugeyre MT, Chamaret S, Gruest J, et al. Isolation of a T-lymphotropic retrovirus from a patient at risk for acquired immune deficiency syndrome (AIDS). Science. 1983;220(4599):868-71.
23. Gallo R, Sarin P, Gelmann E, Robert-Guroff M, Richardson E, Kalyanaraman V, et al. Isolation of human T-cell leukemia virus in acquired immune deficiency syndrome (AIDS). Science. 1983;220(4599):865-7.
24. Coffin J, Haase A, Levy JA, Montagnier L, Oroszlan S, Teich N, et al. Human immunodeficiency viruses. Science. 1986;232(4751):697.
25. 2017 LH. Survival of HIV-positive patients starting antiretroviral therapy between 1996 and 2013: a collaborative analysis of cohort studies. Lancet HIV. 2017;4(8):e349-e56.
26. Cohen MS, Chen YQ, McCauley M, Gamble T, Hosseinipour MC, Kumarasamy N, et al. Antiretroviral Therapy for the Prevention of HIV-1 Transmission. The New England journal of medicine. 2016;375(9):830-9.
27. Quinn TC, Wawer MJ, Sewankambo N, Serwadda D, Li C, Wabwire-Mangen F, et al. Viral load and heterosexual transmission of human immunodeficiency virus type 1. Rakai Project Study Group. The New England journal of medicine. 2000;342(13):921-9.
28. Warszawski J, Tubiana R, Le Chenadec J, Blanche S, Teglas JP, Dollfus C, et al. Mother-to-child HIV transmission despite antiretroviral therapy in the ANRS French Perinatal Cohort. Aids. 2008;22(2):289-99.
29. Palella FJ, Jr., Delaney KM, Moorman AC, Loveless MO, Fuhrer J, Satten GA, et al. Declining morbidity and mortality among patients with advanced human immunodeficiency virus infection. HIV Outpatient Study Investigators. The New England journal of medicine. 1998;338(13):853-60.
30. Broder S. The development of antiretroviral therapy and its impact on the HIV-1/AIDS pandemic. Antiviral research. 2010;85(1):1-18.
31. Land S, McGavin C, Lucas R, Birch C. Incidence of zidovudine-resistant human immunodeficiency virus isolated from patients before, during, and after therapy. J Infect Dis. 1992;166(5):1139-42.
32. Hammer SM, Katzenstein DA, Hughes MD, Gundacker H, Schooley RT, Haubrich RH, et al. A trial comparing nucleoside monotherapy with combination therapy in HIV-infected adults with CD4 cell counts from 200 to 500 per cubic millimeter. AIDS Clinical Trials Group Study 175 Study Team. The New England journal of medicine. 1996;335(15):1081-90.
33. Holec A, Mandal S, Prathipati PK, Destache C. Nucleotide Reverse Transcriptase Inhibitors: A Thorough Review, Present Status and Future Perspective as HIV Therapeutics. Current HIV Research. 2017;15.
34. Patel PH ZH. Reverse Transcriptase Inhibitors. 2022 May8.
35. Usach I, Melis V, Peris JE. Non-nucleoside reverse transcriptase inhibitors: a review on pharmacokinetics, pharmacodynamics, safety and tolerability. Journal of International AIDS Society. 2013;16:1-14.
36. Sluis-Cremer N, Temiz NA, Bahar I. Conformational changes in HIV-1 reverse transcriptase induced by nonnucleoside reverse transcriptase inhibitor binding. Current HIV Research. 2004;2(4):323-32.
37. Lv Z, Chu Y, Wang Y. HIV protease inhibitors: a review of molecular selectivity and toxicity. HIV/AIDS (Auckland, NZ). 2015;7:95-104.

38. Han Y, Mesplède T, Wainberg MA. Investigational HIV integrase inhibitors in phase I and phase II clinical trials. Expert Opinion on Investigational Drugs. 2017;26(11):1207-13.
39. Ding X, Zhang X, Chong H, Zhu Y, Wei H, Wu X, et al. Enfuvirtide (T20)-Based Lipopeptide Is a Potent HIV-1 Cell Fusion Inhibitor: Implications for Viral Entry and Inhibition. Journal of virology. 2017;91(18):e00831-17.
40. Sayana S, Khanlou H. Maraviroc: a new CCR5 antagonist. Expert Rev Anti Infect Ther. 2009;7(1):9-19.
41. Markham A. Ibalizumab: First Global Approval. Drugs. 2018;78(7):781-5.
42. WHO. HIV Treatment August 16, 2021 [Available from: https://hivinfo.nih.gov/understanding-hiv/fact-sheets/hiv-treatment-basics#:~:text=treatment%20for%20HIV%3F-,The%20treatment%20for%20HIV%20is%20called%20antiretroviral%20therapy%20(ART).,HIV%20live%20longer%2C%20healthier%20lives.
43. Thorner A, Rosenberg E. Early versus delayed antiretroviral therapy in patients with HIV infection : a review of the current guidelines from an immunological perspective. Drugs. 2003;63(13):1325-37.
44. Siedner MJ. START or SMART? Timing of Antiretroviral Therapy Initiation and Cardiovascular Risk for People With Human Immunodeficiency Virus Infection. In Open Forum Infectious Diseases. 2016;3(1):ofw032.
45. Smart-Study-Group, El-Sadr WM, Lundgren JD, Neaton JD, Gordin F, Abrams D, et al. CD4+ count–guided interruption of antiretroviral treatment. The New England journal of medicine. 2006;355(22):2283-96.
46. McCluskey MM, Alexander SB, Larkin BD, Murguia M, Wakefield S. An HIV vaccine: as we build it, will they come? Health Aff (Millwood). 2005;24(3):643-51.
47. Harris JE. Why we don't have an HIV vaccine, and how we can develop one. Health Aff (Millwood). 2009;28(6):1642-54.
48. Baeten JM, Grant R. Use of antiretrovirals for HIV prevention: what do we know and what don't we know? Current HIV/AIDS Reports. 2013;10(2):142-51.
49. Spinner CD, Boesecke C, Zink A, Jessen H, Stellbrink HJ, Rockstroh JK, et al. HIV pre-exposure prophylaxis (PrEP): a review of current knowledge of oral systemic HIV PrEP in humans. Infection. 2016;44(2):151-8.
50. Ouellet E, Durand M, Guertin JR, LeLorier J, Tremblay CL. Cost effectiveness of 'on demand'HIV pre-exposure prophylaxis for non-injection drug-using men who have sex with men in Canada. Canadian Journal of Infectious Diseases and Medical Microbiology. 2015;26(1):23-9.
51. Chan P, Spudich S. Investigating vascular diseases in people living with HIV by nuclear imaging. Journal of Nuclear Cardiology. 2021.
52. Chan P, Valcour V. Neurocognition and the Aging Brain in People With HIV: Implications for Screening. Top Antivir Med. 2022;29(5):423-9.
53. Aberg JA. Aging and HIV infection: focus on cardiovascular disease risk. Top Antivir Med. 2020;27(4):102-5.
54. Farahani M, Mulinder H, Farahani A, Marlink R. Prevalence and distribution of non-AIDS causes of death among HIV-infected individuals receiving antiretroviral therapy: a systematic review and meta-analysis. Int J STD AIDS. 2017;28(7):636-50.
55. Causes of death in HIV-1-infected patients treated with antiretroviral therapy, 1996-2006: collaborative analysis of 13 HIV cohort studies. Clinical infectious diseases : an official publication of the Infectious Diseases Society of America. 2010;50(10):1387-96.
56. Vachiat A, McCutcheon K, Tsabedze N, Zachariah D, Manga P. HIV and Ischemic Heart Disease. Journal of the American College of Cardiology. 2017;69(1):73-82.

57. Friis-Møller N, Weber R, Reiss P, Thiébaut R, Kirk O, d'Arminio Monforte A, et al. Cardiovascular disease risk factors in HIV patients--association with antiretroviral therapy. Results from the DAD study. Aids. 2003;17(8):1179-93.
58. El-Sadr WM, Lundgren J, Neaton JD, Gordin F, Abrams D, Arduino RC, et al. CD4+ count-guided interruption of antiretroviral treatment. The New England journal of medicine. 2006;355(22):2283-96.
59. D'Ascenzo F, Cerrato E, Calcagno A, Grossomarra W, Ballocca F, Omedè P, et al. High prevalence at computed coronary tomography of non-calcified plaques in asymptomatic HIV patients treated with HAART: a meta-analysis. Atherosclerosis. 2015;240(1):197-204.
60. Post WS, Budoff M, Kingsley L, Palella FJ, Jr., Witt MD, Li X, et al. Associations between HIV infection and subclinical coronary atherosclerosis. Ann Intern Med. 2014;160(7):458-67.
61. Kral BG, Becker LC, Vaidya D, Yanek LR, Qayyum R, Zimmerman SL, et al. Noncalcified coronary plaque volumes in healthy people with a family history of early onset coronary artery disease. Circ Cardiovasc Imaging. 2014;7(3):446-53.
62. Boldeanu I, Sadouni M, Mansour S, Baril JG, Trottier B, Soulez G, et al. Prevalence and Characterization of Subclinical Coronary Atherosclerotic Plaque with CT among Individuals with HIV: Results from the Canadian HIV and Aging Cohort Study. Radiology. 2021;299(3):571-80.
63. Burdo TH, Lo J, Abbara S, Wei J, DeLelys ME, Preffer F, et al. Soluble CD163, a novel marker of activated macrophages, is elevated and associated with noncalcified coronary plaque in HIV-infected patients. J Infect Dis. 2011;204(8):1227-36.
64. Duprez DA, Neuhaus J, Kuller LH, Tracy R, Belloso W, De Wit S, et al. Inflammation, coagulation and cardiovascular disease in HIV-infected individuals. PLoS One. 2012;7(9):e44454.
65. Hsu DC, Ma YF, Hur S, Li D, Rupert A, Scherzer R, et al. Plasma IL-6 levels are independently associated with atherosclerosis and mortality in HIV-infected individuals on suppressive antiretroviral therapy. Aids. 2016;30(13):2065-74.
66. Kuller LH, Tracy R, Belloso W, De Wit S, Drummond F, Lane HC, et al. Inflammatory and coagulation biomarkers and mortality in patients with HIV infection. PLoS Med. 2008;5(10):e203.
67. Kearns A, Gordon J, Burdo TH, Qin X. HIV-1-Associated Atherosclerosis: Unraveling the Missing Link. J Am Coll Cardiol. 2017;69(25):3084-98.
68. Crowe SM, Westhorpe CL, Mukhamedova N, Jaworowski A, Sviridov D, Bukrinsky M. The macrophage: the intersection between HIV infection and atherosclerosis. Journal of leukocyte biology. 2010;87(4):589-98.
69. Klatt NR, Chomont N, Douek DC, Deeks SG. Immune activation and HIV persistence: implications for curative approaches to HIV infection. Immunol Rev. 2013;254(1):326-42.
70. Combadière C, Potteaux S, Rodero M, Simon T, Pezard A, Esposito B, et al. Combined inhibition of CCL2, CX3CR1, and CCR5 abrogates Ly6C(hi) and Ly6C(lo) monocytosis and almost abolishes atherosclerosis in hypercholesterolemic mice. Circulation. 2008;117(13):1649-57.
71. Pushkarsky T, Shilov E, Kruglova N, Naumann R, Brichacek B, Jennelle L, et al. Short Communication: Accumulation of Neutral Lipids in Liver and Aorta of Nef-Transgenic Mice. AIDS Res Hum Retroviruses. 2017;33(1):57-60.
72. Karim R, Mack WJ, Kono N, Tien PC, Anastos K, Lazar J, et al. T-cell activation, both pre- and post-HAART levels, correlates with carotid artery stiffness over 6.5 years among HIV-infected women in the WIHS. J Acquir Immune Defic Syndr. 2014;67(3):349-56.
73. Kaplan RC, Sinclair E, Landay AL, Lurain N, Sharrett AR, Gange SJ, et al. T cell activation and senescence predict subclinical carotid artery disease in HIV-infected women. J Infect Dis. 2011;203(4):452-63.
74. Hansson GK, Robertson AK, Söderberg-Nauclér C. Inflammation and atherosclerosis. Annu Rev Pathol. 2006;1:297-329.

75. Merlini E, Luzi K, Suardi E, Barassi A, Cerrone M, Martínez JS, et al. T-cell phenotypes, apoptosis and inflammation in HIV+ patients on virologically effective cART with early atherosclerosis. PLoS One. 2012;7(9):e46073.
76. Ivanov AV, Valuev-Elliston VT, Ivanova ON, Kochetkov SN, Starodubova ES, Bartosch B, et al. Oxidative Stress during HIV Infection: Mechanisms and Consequences. Oxid Med Cell Longev. 2016;2016:8910396.
77. Ma R, Yang L, Niu F, Buch S. HIV Tat-Mediated Induction of Human Brain Microvascular Endothelial Cell Apoptosis Involves Endoplasmic Reticulum Stress and Mitochondrial Dysfunction. Mol Neurobiol. 2016;53(1):132-42.
78. Shah A, Kumar A. HIV-1 gp120-Mediated Mitochondrial Dysfunction and HIV-Associated Neurological Disorders. Neurotox Res. 2016;30(2):135-7.
79. Chen L, Jarujaron S, Wu X, Sun L, Zha W, Liang G, et al. HIV protease inhibitor lopinavir-induced TNF-alpha and IL-6 expression is coupled to the unfolded protein response and ERK signaling pathways in macrophages. Biochem Pharmacol. 2009;78(1):70-7.
80. Strowig T, Henao-Mejia J, Elinav E, Flavell R. Inflammasomes in health and disease. Nature. 2012;481(7381):278-86.
81. Kiffin R, Bandyopadhyay U, Cuervo AM. Oxidative stress and autophagy. Antioxid Redox Signal. 2006;8(1-2):152-62.
82. Feigin VL, Brainin M, Norrving B, Martins S, Sacco RL, Hacke W, et al. World Stroke Organization (WSO): Global Stroke Fact Sheet 2022. International Journal of Stroke. 2022;17(1):18-29.
83. Ooi YC, Gonzalez NR. Management of extracranial carotid artery disease. Cardiol Clin. 2015;33(1):1-35.
84. Holmstedt CA, Turan TN, Chimowitz MI. Atherosclerotic intracranial arterial stenosis: risk factors, diagnosis, and treatment. The Lancet Neurology. 2013;12(11):1106-14.
85. Khare S. Risk factors of transient ischemic attack: An overview. J Midlife Health. 2016;7(1):2-7.
86. Alpert JN. Extracranial carotid artery. Current concepts of diagnosis and management. Tex Heart Inst J. 1991;18(2):93-7.
87. Goessens BM, Visseren FL, Algra A, Banga JD, van der Graaf Y. Screening for asymptomatic cardiovascular disease with noninvasive imaging in patients at high-risk and low-risk according to the European Guidelines on Cardiovascular Disease Prevention: the SMART study. J Vasc Surg. 2006;43(3):525-32.
88. de Weerd M, Greving JP, Hedblad B, Lorenz MW, Mathiesen EB, O'Leary DH, et al. Prevalence of asymptomatic carotid artery stenosis in the general population: an individual participant data meta-analysis. Stroke. 2010;41(6):1294-7.
89. Erickson KM, Cole DJ. Carotid artery disease: stenting vs endarterectomy. Br J Anaesth. 2010;105 Suppl 1:i34-49.
90. Chobanian AV, Bakris GL, Black HR, Cushman WC, Green LA, Izzo JL, Jr., et al. The Seventh Report of the Joint National Committee on Prevention, Detection, Evaluation, and Treatment of High Blood Pressure: the JNC 7 report. Jama. 2003;289(19):2560-72.
91. Chobanian AV, Bakris GL, Black HR, Cushman WC, Green LA, Izzo JL, Jr., et al. Seventh report of the Joint National Committee on Prevention, Detection, Evaluation, and Treatment of High Blood Pressure. Hypertension. 2003;42(6):1206-52.
92. Daskalopoulou SS, Daskalopoulos ME, Perrea D, Nicolaides AN, Liapis CD. Carotid artery atherosclerosis: what is the evidence for drug action? Curr Pharm Des. 2007;13(11):1141-59.
93. Lanzino G, Rabinstein AA, Brown RD, Jr. Treatment of carotid artery stenosis: medical therapy, surgery, or stenting? Mayo Clin Proc. 2009;84(4):362-87; quiz 7-8.
94. Sacco RL, Adams R, Albers G, Alberts MJ, Benavente O, Furie K, et al. Guidelines for prevention of stroke in patients with ischemic stroke or transient ischemic attack: a statement for healthcare

professionals from the American Heart Association/American Stroke Association Council on Stroke: co-sponsored by the Council on Cardiovascular Radiology and Intervention: the American Academy of Neurology affirms the value of this guideline. Stroke. 2006;37(2):577-617.
95. Barnett HJ, Taylor DW, Eliasziw M, Fox AJ, Ferguson GG, Haynes RB, et al. Benefit of carotid endarterectomy in patients with symptomatic moderate or severe stenosis. North American Symptomatic Carotid Endarterectomy Trial Collaborators. The New England journal of medicine. 1998;339(20):1415-25.
96. Endarterectomy for asymptomatic carotid artery stenosis. Executive Committee for the Asymptomatic Carotid Atherosclerosis Study. Jama. 1995;273(18):1421-8.
97. Prasad K. Pathophysiology and Medical Treatment of Carotid Artery Stenosis. Int J Angiol. 2015;24(3):158-72.
98. Fine-Edelstein JS, Wolf PA, O'Leary DH, Poehlman H, Belanger AJ, Kase CS, et al. Precursors of extracranial carotid atherosclerosis in the Framingham Study. Neurology. 1994;44(6):1046-50.
99. Griffiths PD, Worthy S, Gholkar A. Incidental intracranial vascular pathology in patients investigated for carotid stenosis. Neuroradiology. 1996;38(1):25-30.
100. Klop RB, Eikelboom BC, Taks AC. Screening of the internal carotid arteries in patients with peripheral vascular disease by colour-flow duplex scanning. Eur J Vasc Surg. 1991;5(1):41-5.
101. Alexandrova NA, Gibson WC, Norris JW, Maggisano R. Carotid artery stenosis in peripheral vascular disease. J Vasc Surg. 1996;23(4):645-9.
102. Ahmed B, Al-Khaffaf H. Prevalence of significant asymptomatic carotid artery disease in patients with peripheral vascular disease: a meta-analysis. Eur J Vasc Endovasc Surg. 2009;37(3):262-71.
103. Larson AS, Brinjikji W, Savastano L, Scharf E, Huston J, 3rd, Benson JC. Left-sided carotid arteries have a higher prevalence of intraplaque hemorrhage than right-sided: An asymmetric conundrum. Neuroradiol J. 2020;33(6):494-500.
104. Lusis AJ. Atherosclerosis. Nature. 2000;407(6801):233-41.
105. Falk E. Pathogenesis of Atherosclerosis. Journal of the American College of Cardiology. 2006;47(8, Supplement):C7-C12.
106. Phinikaridou A, Andia ME, Lacerda S, Lorrio S, Makowski MR, Botnar RM. Molecular MRI of atherosclerosis. Molecules. 2013;18(11):14042-69.
107. Yamazaki M, Uchiyama S. [Pathophysiology of carotid stenosis]. Brain Nerve. 2010;62(12):1269-75.
108. Galis ZS, Sukhova GK, Lark MW, Libby P. Increased expression of matrix metalloproteinases and matrix degrading activity in vulnerable regions of human atherosclerotic plaques. J Clin Invest. 1994;94(6):2493-503.
109. van Sloten TT, Sedaghat S, Laurent S, London GM, Pannier B, Ikram MA, et al. Carotid Stiffness Is Associated With Incident Stroke: A Systematic Review and Individual Participant Data Meta-Analysis. Journal of the American College of Cardiology. 2015;66(19):2116-25.
110. Ungvari Z, Tarantini S, Kiss T, Wren JD, Giles CB, Griffin CT, et al. Endothelial dysfunction and angiogenesis impairment in the ageing vasculature. Nat Rev Cardiol. 2018;15(9):555-65.
111. Dijk JM, Graaf Yvd, Grobbee DE, Bots ML. Carotid Stiffness Indicates Risk of Ischemic Stroke and TIA in Patients With Internal Carotid Artery Stenosis. Stroke. 2004;35(10):2258-62.
112. van Sloten TT, Schram MT, van den Hurk K, Dekker JM, Nijpels G, Henry RMA, et al. Local Stiffness of the Carotid and Femoral Artery Is Associated With Incident Cardiovascular Events and All-Cause Mortality: The Hoorn Study. Journal of the American College of Cardiology. 2014;63(17):1739-47.
113. Chen Y, Shen F, Liu J, Yang G-Y. Arterial stiffness and stroke: de-stiffening strategy, a therapeutic target for stroke. Stroke and Vascular Neurology. 2017;2(2):65.

114. Boutouyrie P, Laurent S, Girerd X, Benetos A, Lacolley P, Abergel E, et al. Common carotid artery stiffness and patterns of left ventricular hypertrophy in hypertensive patients. Hypertension. 1995;25(4 Pt 1):651-9.
115. Gao L, Lu D, Xia G, Zhang H. The relationship between arterial stiffness index and coronary heart disease and its severity. BMC Cardiovasc Disord. 2021;21(1):527.
116. Avolio A, Butlin M, Liu Y-Y, Viegas K, Avadhanam B, Lindesay G. Regulation of arterial stiffness: Cellular, molecular and neurogenic mechanisms. Artery Research. 2011;5(4):122-7.
117. Bézie Y, Daniel-Lamazière JM, Gabella G, Koffi I, Laurent S, Lacolley P. [Molecular and cellular determinants of arterial stiffness: role of cell-matrix connections]. Pathol Biol (Paris). 1999;47(7):669-76.
118. Wagenseil JE, Mecham RP. Elastin in large artery stiffness and hypertension. J Cardiovasc Transl Res. 2012;5(3):264-73.
119. Zieman SJ, Melenovsky V, Kass DA. Mechanisms, Pathophysiology, and Therapy of Arterial Stiffness. Arteriosclerosis, Thrombosis, and Vascular Biology. 2005;25(5):932-43.
120. van Sloten TT, Stehouwer CDA. Carotid Stiffness: A Novel Cerebrovascular Disease Risk Factor. Pulse. 2016;4(1):24-7.
121. Hu FS, Zhang YL, Ma ZC, Cao QQ, Xu YB, He ZJ, et al. A region-matching method for pulse transit time estimation: potential for improving the accuracy in determining carotid femoral pulse wave velocity. Journal of Human Hypertension. 2015;29(11):675-82.
122. Syeda B, Gottsauner-Wolf M, Denk S, Pichler P, Khorsand A, Glogar D. Arterial compliance: a diagnostic marker for atherosclerotic plaque burden? American Journal of Hypertension. 2003;16(5):356-62.
123. Zieman SJ, Melenovsky V, Kass DA. Mechanisms, pathophysiology, and therapy of arterial stiffness. Arterioscler Thromb Vasc Biol. 2005;25(5):932-43.
124. Hingorani AD, Cross J, Kharbanda RK, Mullen MJ, Bhagat K, Taylor M, et al. Acute systemic inflammation impairs endothelium-dependent dilatation in humans. Circulation. 2000;102(9):994-9.
125. Kumeda Y, Inaba M, Goto H, Nagata M, Henmi Y, Furumitsu Y, et al. Increased thickness of the arterial intima-media detected by ultrasonography in patients with rheumatoid arthritis. Arthritis Rheum. 2002;46(6):1489-97.
126. Palella FJ, Jr., Gange SJ, Benning L, Jacobson L, Kaplan RC, Landay AL, et al. Inflammatory biomarkers and abacavir use in the Women's Interagency HIV Study and the Multicenter AIDS Cohort Study. Aids. 2010;24(11):1657-65.
127. Hunt PW, Brenchley J, Sinclair E, McCune JM, Roland M, Page-Shafer K, et al. Relationship between T cell activation and CD4+ T cell count in HIV-seropositive individuals with undetectable plasma HIV RNA levels in the absence of therapy. J Infect Dis. 2008;197(1):126-33.
128. Kaplan RC, Kingsley LA, Gange SJ, Benning L, Jacobson LP, Lazar J, et al. Low CD4+ T-cell count as a major atherosclerosis risk factor in HIV-infected women and men. Aids. 2008;22(13):1615-24.
129. Hsue PY, Lo JC, Franklin A, Bolger AF, Martin JN, Deeks SG, et al. Progression of atherosclerosis as assessed by carotid intima-media thickness in patients with HIV infection. Circulation. 2004;109(13):1603-8.
130. Chetty R. Vasculitides associated with HIV infection. Journal of Clinical Pathology. 2001;54(4):275-8.
131. Chetty R. Vasculitides associated with HIV infection. J Clin Pathol. 2001;54(4):275-8.
132. Regina G, Impedovo G, Angiletta D, Martiradonna F, Lillo A, Perilli F, et al. Surgical experience with carotid stenosis in young HIV-1 positive patients under antiretroviral therapy: an emerging problem? Eur J Vasc Endovasc Surg. 2005;29(2):167-70.
133. Seaberg EC, Muñoz A, Lu M, Detels R, Margolick JB, Riddler SA, et al. Association between highly active antiretroviral therapy and hypertension in a large cohort of men followed from 1984 to 2003. Aids. 2005;19(9):953-60.

134. Touboul PJ, Hennerici MG, Meairs S, Adams H, Amarenco P, Bornstein N, et al. Mannheim carotid intima-media thickness and plaque consensus (2004-2006-2011). An update on behalf of the advisory board of the 3rd, 4th and 5th watching the risk symposia, at the 13th, 15th and 20th European Stroke Conferences, Mannheim, Germany, 2004, Brussels, Belgium, 2006, and Hamburg, Germany, 2011. Cerebrovasc Dis. 2012;34(4):290-6.
135. Polak JF, Szklo M, Kronmal RA, Burke GL, Shea S, Zavodni AE, et al. The value of carotid artery plaque and intima-media thickness for incident cardiovascular disease: the multi-ethnic study of atherosclerosis. J Am Heart Assoc. 2013;2(2):e000087.
136. Grunfeld C, Delaney JA, Wanke C, Currier JS, Scherzer R, Biggs ML, et al. Preclinical atherosclerosis due to HIV infection: carotid intima-medial thickness measurements from the FRAM study. Aids. 2009;23(14):1841-9.
137. Loizou CP, Nicolaides A, Kyriacou E, Georghiou N, Griffin M, Pattichis CS. A Comparison of Ultrasound Intima-Media Thickness Measurements of the Left and Right Common Carotid Artery. IEEE J Transl Eng Health Med. 2015;3:1900410.
138. Sibal L, Agarwal SC, Home PD. Carotid intima-media thickness as a surrogate marker of cardiovascular disease in diabetes. Diabetes Metab Syndr Obes. 2011;4:23-34.
139. Smitha B, Yadav D, Joseph PK. Evaluation of carotid intima media thickness measurement from ultrasound images. Medical & Biological Engineering & Computing. 2022;60(2):407-19.
140. Jacoby DS, Mohler IE, Rader DJ. Noninvasive atherosclerosis imaging for predicting cardiovascular events and assessing therapeutic interventions. Curr Atheroscler Rep. 2004;6(1):20-6.
141. O'Leary DH, Bots ML. Imaging of atherosclerosis: carotid intima-media thickness. Eur Heart J. 2010;31(14):1682-9.
142. Mukherjee D, Yadav JS. Carotid artery intimal-medial thickness: indicator of atherosclerotic burden and response to risk factor modification. Am Heart J. 2002;144(5):753-9.
143. Loizou CP. A review of ultrasound common carotid artery image and video segmentation techniques. Medical & Biological Engineering & Computing. 2014;52(12):1073-93.
144. Wilhjelm JE, Grønholdt ML, Wiebe B, Jespersen SK, Hansen LK, Sillesen H. Quantitative analysis of ultrasound B-mode images of carotid atherosclerotic plaque: correlation with visual classification and histological examination. IEEE Trans Med Imaging. 1998;17(6):910-22.
145. Bots ML, Groenewegen KA, Anderson TJ, Britton AR, Dekker JM, Engström G, et al. Common Carotid Intima-Media Thickness Measurements Do Not Improve Cardiovascular Risk Prediction in Individuals With Elevated Blood Pressure. Hypertension. 2014;63(6):1173-81.
146. Grunfeld C, Delaney JAC, Wanke C, Currier JS, Scherzer R, Biggs ML, et al. Preclinical atherosclerosis due to HIV infection: carotid intima-medial thickness measurements from the FRAM study. AIDS. 2009;23(14).
147. Hsue PY, Ordovas K, Lee T, Reddy G, Gotway M, Schnell A, et al. Carotid intima-media thickness among human immunodeficiency virus-infected patients without coronary calcium. Am J Cardiol. 2012;109(5):742-7.
148. Sainz T, Álvarez-Fuente M, Navarro ML, Díaz L, Rojo P, Blázquez D, et al. Subclinical atherosclerosis and markers of immune activation in HIV-infected children and adolescents: the CaroVIH Study. J Acquir Immune Defic Syndr. 2014;65(1):42-9.
149. Lorenz MW, Stephan C, Harmjanz A, Staszewski S, Buehler A, Bickel M, et al. Both long-term HIV infection and highly active antiretroviral therapy are independent risk factors for early carotid atherosclerosis. Atherosclerosis. 2008;196(2):720-6.
150. Johnsen S, Dolan SE, Fitch KV, Kanter JR, Hemphill LC, Connelly JM, et al. Carotid intimal medial thickness in human immunodeficiency virus-infected women: effects of protease inhibitor use, cardiac risk factors, and the metabolic syndrome. J Clin Endocrinol Metab. 2006;91(12):4916-24.

151. Currier JS, Kendall MA, Zackin R, Henry WK, Alston-Smith B, Torriani FJ, et al. Carotid artery intima–media thickness and HIV infection: traditional risk factors overshadow impact of protease inhibitor exposure. AIDS. 2005;19(9).
152. Currier JS, Kendall MA, Henry WK, Alston-Smith B, Torriani FJ, Tebas P, et al. Progression of carotid artery intima–media thickening in HIV-infected and uninfected adults. AIDS. 2007;21(9).
153. Naqvi TZ, Lee M-S. Carotid Intima-Media Thickness and Plaque in Cardiovascular Risk Assessment. JACC: Cardiovascular Imaging. 2014;7(10):1025-38.
154. Polak JF, Johnson C, Harrington A, Wong Q, O'Leary DH, Burke G, et al. Changes in carotid intima-media thickness during the cardiac cycle: the multi-ethnic study of atherosclerosis. J Am Heart Assoc. 2012;1(4):e001420.
155. Spiegel PK. The first clinical X-ray made in America--100 years. AJR Am J Roentgenol. 1995;164(1):241-3.
156. Brody WR. Digital Subtraction Angiography. IEEE Transactions on Nuclear Science. 1982;29(3):1176-80.
157. Chilcote WA, Modic MT, Pavlicek WA, Little JR, Furlan AJ, Duchesneau PM, et al. Digital subtraction angiography of the carotid arteries: a comparative study in 100 patients. Radiology. 1981;139(2):287-95.
158. Hounsfield GN. Computerized transverse axial scanning (tomography). 1. Description of system. Br J Radiol. 1973;46(552):1016-22.
159. Claves JL, Wise SW, Hopper KD, Tully D, Ten Have TR, Weaver J. Evaluation of contrast densities in the diagnosis of carotid stenosis by CT angiography. AJR Am J Roentgenol. 1997;169(2):569-73.
160. Saxena A, Ng EYK, Lim ST. Imaging modalities to diagnose carotid artery stenosis: progress and prospect. Biomed Eng Online. 2019;18(1):66.
161. Brenner DJ, Hall EJ. Computed tomography--an increasing source of radiation exposure. The New England journal of medicine. 2007;357(22):2277-84.
162. Nickoloff EL, Alderson PO. Radiation exposures to patients from CT: reality, public perception, and policy. AJR Am J Roentgenol. 2001;177(2):285-7.
163. Stocker TJ, Deseive S, Leipsic J, Hadamitzky M, Chen MY, Rubinshtein R, et al. Reduction in radiation exposure in cardiovascular computed tomography imaging: results from the PROspective multicenter registry on radiaTion dose Estimates of cardiac CT angIOgraphy iN daily practice in 2017 (PROTECTION VI). Eur Heart J. 2018;39(41):3715-23.
164. Cashman JD, McCredie J, Henry DA. Intravenous contrast media: use and associated mortality. Med J Aust. 1991;155(9):618-23.
165. Tao SM, Wichmann JL, Schoepf UJ, Fuller SR, Lu GM, Zhang LJ. Contrast-induced nephropathy in CT: incidence, risk factors and strategies for prevention. Eur Radiol. 2016;26(9):3310-8.
166. Edelman RR, Warach S. Magnetic resonance imaging (1). The New England journal of medicine. 1993;328(10):708-16.
167. Edelman RR, Warach S. Magnetic Resonance Imaging. New England Journal of Medicine. 1993;328(10):708-16.
168. Macovski A. Selective projection imaging: applications to radiography and NMR. IEEE Trans Med Imaging. 1982;1(1):42-7.
169. Graves MJ. Magnetic resonance angiography. Br J Radiol. 1997;70:6-28.
170. Martin KT, editor Diagnostic Ultrasound: Introduction to B-mode imaging2010.
171. Martin K. Introduction to B-mode imaging. In: Thrush A, Martin K, Hoskins PR, editors. Diagnostic Ultrasound: Physics and Equipment. 2 ed. Cambridge: Cambridge University Press; 2010. p. 1-3.
172. Pignoli P, Tremoli E, Poli A, Oreste P, Paoletti R. Intimal plus medial thickness of the arterial wall: a direct measurement with ultrasound imaging. Circulation. 1986;74(6):1399-406.

173. Howard G, Sharrett AR, Heiss G, Evans GW, Chambless LE, Riley WA, et al. Carotid artery intimal-medial thickness distribution in general populations as evaluated by B-mode ultrasound. ARIC Investigators. Stroke. 1993;24(9):1297-304.
174. Chartrand-Lefebvre C, Cadrin-Chênevert A, Bordeleau E, Ugolini P, Ouellet R, Sablayrolles JL, et al. Coronary computed tomography angiography: overview of technical aspects, current concepts, and perspectives. Can Assoc Radiol J. 2007;58(2):92-108.
175. Benjamin MM, Shaker M, Rabbat MG. Chapter 5 - Assessing coronary artery disease using coronary computed tomography angiography. In: El-Baz AS, Suri JS, editors. Cardiovascular and Coronary Artery Imaging: Academic Press; 2022. p. 129-45.
176. Nikolaou K, Alkadhi H, Bamberg F, Leschka S, Wintersperger BJ. MRI and CT in the diagnosis of coronary artery disease: indications and applications. Insights Imaging. 2011;2(1):9-24.
177. Hendel RC, Patel MR, Kramer CM, Poon M, Hendel RC, Carr JC, et al. ACCF/ACR/SCCT/SCMR/ASNC/NASCI/SCAI/SIR 2006 appropriateness criteria for cardiac computed tomography and cardiac magnetic resonance imaging: a report of the American College of Cardiology Foundation Quality Strategic Directions Committee Appropriateness Criteria Working Group, American College of Radiology, Society of Cardiovascular Computed Tomography, Society for Cardiovascular Magnetic Resonance, American Society of Nuclear Cardiology, North American Society for Cardiac Imaging, Society for Cardiovascular Angiography and Interventions, and Society of Interventional Radiology. J Am Coll Cardiol. 2006;48(7):1475-97.
178. Boldeanu I, Sadouni M, Mansour S, Baril J-G, Trottier B, Soulez G, et al. Prevalence and Characterization of Subclinical Coronary Atherosclerotic Plaque with CT among Individuals with HIV: Results from the Canadian HIV and Aging Cohort Study. Radiology. 2021;299(3):571-80.
179. Chen Z, Boldeanu I, Nepveu S, Durand M, Chin AS, Kauffmann C, et al. In vivo coronary artery plaque assessment with computed tomography angiography: is there an impact of iterative reconstruction on plaque volume and attenuation metrics? Acta Radiologica. 2016;58(6):660-9.
180. Leber AW, Becker A, Knez A, von Ziegler F, Sirol M, Nikolaou K, et al. Accuracy of 64-slice computed tomography to classify and quantify plaque volumes in the proximal coronary system: a comparative study using intravascular ultrasound. J Am Coll Cardiol. 2006;47(3):672-7.
181. Rau P, Durand M, Mansour S, Tremblay C, Chartrand-Lefebvre C. Coronary calcium assessment with computed tomography in HIV-infected patients. Atherosclerosis. 2016;249.
182. Wang W, Yang L, Wang S, Wang Q, Xu L. An automated quantification method for the Agatston coronary artery calcium score on coronary computed tomography angiography. Quant Imaging Med Surg. 2022;12(3):1787-99.
183. Berman DS, Arnson Y, Rozanski A. Coronary Artery Calcium Scanning: The Agatston Score and Beyond. JACC Cardiovasc Imaging. 2016;9(12):1417-9.
184. Ramjattan NA, Lala V, Kousa O, Makaryus AN. Coronary CT Angiography. StatPearls. Treasure Island (FL): StatPearls Publishing

185. Gramer BM, Diez Martinez P, Chin AS, Sylvestre MP, Larrivée S, Stevens LM, et al. 256-slice CT angiographic evaluation of coronary artery bypass grafts: effect of heart rate, heart rate variability and Z-axis location on image quality. PLoS One. 2014;9(3):e91861.
186. Chartrand-Lefebvre C. Stepladder artifact in coronary computed tomography angiography. Catheter Cardiovasc Interv. 2007;69(6):922; author reply 3.
187. Li P, Xu L, Yang L, Wang R, Hsieh J, Sun Z, et al. Blooming Artifact Reduction in Coronary Artery Calcification by A New De-blooming Algorithm: Initial Study. Sci Rep. 2018;8(1):6945.

188. Tan S, Soulez G, Diez Martinez P, Larrivée S, Stevens LM, Goussard Y, et al. Coronary Stent Artifact Reduction with an Edge-Enhancing Reconstruction Kernel - A Prospective Cross-Sectional Study with 256-Slice CT. PLoS One. 2016;11(4):e0154292.
189. Nguyen PK, Lee WH, Li YF, Hong WX, Hu S, Chan C, et al. Assessment of the Radiation Effects of Cardiac CT Angiography Using Protein and Genetic Biomarkers. JACC Cardiovasc Imaging. 2015;8(8):873-84.
190. Sodickson A. Strategies for reducing radiation exposure from multidetector computed tomography in the acute care setting. Can Assoc Radiol J. 2013;64(2):119-29.
191. Nepveu S, Stevens LM, Chartrand-Lefebvre C. Iterative reconstruction in 256-MDCT of coronary artery bypass grafts: assessment of radiation dose reduction and image quality. AJR Am J Roentgenol. 2014;202(6):W599.
192. Shiina T, Nightingale KR, Palmeri ML, Hall TJ, Bamber JC, Barr RG, et al. WFUMB guidelines and recommendations for clinical use of ultrasound elastography: Part 1: basic principles and terminology. Ultrasound Med Biol. 2015;41(5):1126-47.
193. Sigrist RMS, Liau J, Kaffas AE, Chammas MC, Willmann JK. Ultrasound Elastography: Review of Techniques and Clinical Applications. Theranostics. 2017;7(5):1303-29.
194. Garra BS. Elastography: history, principles, and technique comparison. Abdom Imaging. 2015;40(4):680-97.
195. Itoh A, Ueno E, Tohno E, Kamma H, Takahashi H, Shiina T, et al. Breast disease: clinical application of US elastography for diagnosis. Radiology. 2006;239(2):341-50.
196. Lu Q, Wen JX, Huang BJ, Xue LY, Wang WP. Virtual Touch quantification using acoustic radiation force impulse (ARFI) technology for the evaluation of focal solid renal lesions: preliminary findings. Clin Radiol. 2015;70(12):1376-81.
197. Guibal A, Boularan C, Bruce M, Vallin M, Pilleul F, Walter T, et al. Evaluation of shearwave elastography for the characterisation of focal liver lesions on ultrasound. Eur Radiol. 2013;23(4):1138-49.
198. Samir AE, Dhyani M, Anvari A, Prescott J, Halpern EF, Faquin WC, et al. Shear-Wave Elastography for the Preoperative Risk Stratification of Follicular-patterned Lesions of the Thyroid: Diagnostic Accuracy and Optimal Measurement Plane. Radiology. 2015;277(2):565-73.
199. Samir AE, Dhyani M, Vij A, Bhan AK, Halpern EF, Méndez-Navarro J, et al. Shear-wave elastography for the estimation of liver fibrosis in chronic liver disease: determining accuracy and ideal site for measurement. Radiology. 2015;274(3):888-96.
200. Samir AE, Allegretti AS, Zhu Q, Dhyani M, Anvari A, Sullivan DA, et al. Shear wave elastography in chronic kidney disease: a pilot experience in native kidneys. BMC Nephrol. 2015;16:119.
201. Hong S, Woo OH, Shin HS, Hwang SY, Cho KR, Seo BK. Reproducibility and diagnostic performance of shear wave elastography in evaluating breast solid mass. Clin Imaging. 2017;44:42-5.
202. Park SY, Choi JS, Han BK, Ko EY, Ko ES. Shear wave elastography in the diagnosis of breast non-mass lesions: factors associated with false negative and false positive results. Eur Radiol. 2017;27(9):3788-98.
203. Boehm K, Salomon G, Beyer B, Schiffmann J, Simonis K, Graefen M, et al. Shear wave elastography for localization of prostate cancer lesions and assessment of elasticity thresholds: implications for targeted biopsies and active surveillance protocols. J Urol. 2015;193(3):794-800.
204. DeWall RJ, Slane LC, Lee KS, Thelen DG. Spatial variations in Achilles tendon shear wave speed. J Biomech. 2014;47(11):2685-92.
205. Mercure E, Cloutier G, Schmitt C, Maurice RL. Performance evaluation of different implementations of the Lagrangian speckle model estimator for non-invasive vascular ultrasound elastography. Med Phys. 2008;35(7):3116-26.

206. Roy Cardinal MH, Heusinkveld MHG, Qin Z, Lopata RGP, Naim C, Soulez G, et al. Carotid Artery Plaque Vulnerability Assessment Using Noninvasive Ultrasound Elastography: Validation With MRI. AJR Am J Roentgenol. 2017;209(1):142-51.
207. Ahmadi N, Nabavi V, Hajsadeghi F, Flores F, French WJ, Mao SS, et al. Mortality incidence of patients with non-obstructive coronary artery disease diagnosed by computed tomography angiography. Am J Cardiol. 2011;107(1):10-6.
208. Nerlekar N, Ha FJ, Cheshire C, Rashid H, Cameron JD, Wong DT, et al. Computed Tomographic Coronary Angiography-Derived Plaque Characteristics Predict Major Adverse Cardiovascular Events: A Systematic Review and Meta-Analysis. Circ Cardiovasc Imaging. 2018;11(1):e006973.
209. Roy Cardinal MH, Durand M, Chartrand-Lefebvre C, Fortin C, Baril JG, Trottier B, et al. Increased carotid artery wall stiffness and plaque prevalence in HIV infected patients measured with ultrasound elastography. Eur Radiol. 2020;30(6):3178-87.
210. El Jalbout R, Cloutier G, Roy-Cardinal MH, Henderson M, Levy E, Lapierre C, et al. The value of non-invasive vascular elastography (NIVE) in detecting early vascular changes in overweight and obese children. Eur Radiol. 2019;29(7):3854-61.
211. Durand M, Chartrand-Lefebvre C, Baril J-G, Trottier S, Trottier B, Harris M, et al. The Canadian HIV and aging cohort study-determinants of increased risk of cardio-vascular diseases in HIV-infected individuals: rationale and study protocol. BMC Infectious Diseases. 2017;17(1):611.
212. Bosomworth NJ. Practical use of the Framingham risk score in primary prevention: Canadian perspective. Can Fam Physician. 2011;57(4):417-23.
213. Durand M, Chartrand-Lefebvre C, Baril JG, Trottier S, Trottier B, Harris M, et al. The Canadian HIV and aging cohort study - determinants of increased risk of cardio-vascular diseases in HIV-infected individuals: rationale and study protocol. BMC Infect Dis. 2017;17(1):611.
214. Mishra P, Pandey CM, Singh U, Gupta A, Sahu C, Keshri A. Descriptive statistics and normality tests for statistical data. Ann Card Anaesth. 2019;22(1):67-72.
215. Alonso A, Barnes AE, Guest JL, Shah A, Shao IY, Marconi V. HIV Infection and Incidence of Cardiovascular Diseases: An Analysis of a Large Healthcare Database. J Am Heart Assoc. 2019;8(14):e012241.
216. Alsheikh MM, Alsheikh AM. Risk of Myocardial Infarction in HIV Patients: A Systematic Review. Cureus. 2022;14(11):e31825.
217. Tjan A, Widiana IGR, Martadiani ED, Ayusta IMD, Asih MW, Sitanggang FP. Carotid artery stiffness measured by strain elastography ultrasound is a stroke risk factor. Clinical Epidemiology and Global Health. 2021;12:100850.
218. Mattace-Raso FU, van der Cammen TJ, Hofman A, van Popele NM, Bos ML, Schalekamp MA, et al. Arterial stiffness and risk of coronary heart disease and stroke: the Rotterdam Study. Circulation. 2006;113(5):657-63.
219. Boesen ME, Singh D, Menon BK, Frayne R. A systematic literature review of the effect of carotid atherosclerosis on local vessel stiffness and elasticity. Atherosclerosis. 2015;243(1):211-22.
220. Den Ruijter HM, Peters SA, Anderson TJ, Britton AR, Dekker JM, Eijkemans MJ, et al. Common carotid intima-media thickness measurements in cardiovascular risk prediction: a meta-analysis. Jama. 2012;308(8):796-803.
221. van den Oord SC, Sijbrands EJ, ten Kate GL, van Klaveren D, van Domburg RT, van der Steen AF, et al. Carotid intima-media thickness for cardiovascular risk assessment: systematic review and meta-analysis. Atherosclerosis. 2013;228(1):1-11.
222. Cheng IT, Wong KT, Li EK, Wong PCH, Lai BT, Yim IC, et al. Comparison of carotid artery ultrasound and Framingham risk score for discriminating coronary artery disease in patients with psoriatic arthritis. RMD Open. 2020;6(3):e001364.

223. Finn AV, Kolodgie FD, Virmani R. Correlation between carotid intimal/medial thickness and atherosclerosis: a point of view from pathology. Arterioscler Thromb Vasc Biol. 2010;30(2):177-81.
224. Alsheikh-Ali AA, Kitsios GD, Balk EM, Lau J, Ip S. The vulnerable atherosclerotic plaque: scope of the literature. Ann Intern Med. 2010;153(6):387-95.
225. D'Agostino RB, Sr., Vasan RS, Pencina MJ, Wolf PA, Cobain M, Massaro JM, et al. General cardiovascular risk profile for use in primary care: the Framingham Heart Study. Circulation. 2008;117(6):743-53.
226. Raggi P, De Francesco D, Manicardi M, Zona S, Bellasi A, Stentarelli C, et al. Prediction of hard cardiovascular events in HIV patients. J Antimicrob Chemother. 2016;71(12):3515-8.
227. Feinstein MJ, Nance RM, Drozd DR, Ning H, Delaney JA, Heckbert SR, et al. Assessing and Refining Myocardial Infarction Risk Estimation Among Patients With Human Immunodeficiency Virus: A Study by the Centers for AIDS Research Network of Integrated Clinical Systems. JAMA Cardiol. 2017;2(2):155-62.
228. Friis-Møller N, Ryom L, Smith C, Weber R, Reiss P, Dabis F, et al. An updated prediction model of the global risk of cardiovascular disease in HIV-positive persons: The Data-collection on Adverse Effects of Anti-HIV Drugs (D:A:D) study. European journal of preventive cardiology. 2016;23(2):214-23.
229. Ambrose JA, Barua RS. The pathophysiology of cigarette smoking and cardiovascular disease: an update. J Am Coll Cardiol. 2004;43(10):1731-7.
230. Mayhan WG, Sharpe GM. Effect of cigarette smoke extract on arteriolar dilatation in vivo. J Appl Physiol (1985). 1996;81(5):1996-2003.
231. Ota Y, Kugiyama K, Sugiyama S, Ohgushi M, Matsumura T, Doi H, et al. Impairment of endothelium-dependent relaxation of rabbit aortas by cigarette smoke extract--role of free radicals and attenuation by captopril. Atherosclerosis. 1997;131(2):195-202.
232. Bermudez EA, Rifai N, Buring JE, Manson JE, Ridker PM. Relation between markers of systemic vascular inflammation and smoking in women. Am J Cardiol. 2002;89(9):1117-9.
233. Kalra VK, Ying Y, Deemer K, Natarajan R, Nadler JL, Coates TD. Mechanism of cigarette smoke condensate induced adhesion of human monocytes to cultured endothelial cells. J Cell Physiol. 1994;160(1):154-62.
234. Johnston PI, Wright SW, Orr M, Pearce FA, Stevens JW, Hubbard RB, et al. Worldwide relative smoking prevalence among people living with and without HIV. Aids. 2021;35(6):957-70.
235. Helleberg M, Afzal S, Kronborg G, Larsen CS, Pedersen G, Pedersen C, et al. Mortality attributable to smoking among HIV-1-infected individuals: a nationwide, population-based cohort study. Clinical infectious diseases : an official publication of the Infectious Diseases Society of America. 2013;56(5):727-34.
236. Marlatt KL, Kelly AS, Steinberger J, Dengel DR. The influence of gender on carotid artery compliance and distensibility in children and adults. J Clin Ultrasound. 2013;41(6):340-6.
237. Riley WA, Barnes RW, Evans GW, Burke GL. Ultrasonic measurement of the elastic modulus of the common carotid artery. The Atherosclerosis Risk in Communities (ARIC) Study. Stroke. 1992;23(7):952-6.

Chapter 8:

Appendices

Table 1. Association of Cardiovascular Risk Factors and ICA_IMT, ICA_CAT, N=154

Variables	**Multivariable model of Cardiovascular risk factors and ICA_IMT, ICA_CAT**	
	RR and 95 % CI	P value
Age (cof^[10])	1.10 (0.95-1.34)	0.19
Smoking Pack year (cof^[10])	1.09 (1.04 -1.10)	**<0.001**
Statin use	1.14 (0.89-1.45)	0.28
IMT-ICA	0.82 (0.13-4.97)	0.83
CAT-ICA	0.68 (0.14-3.37)	0.64

Table 2. Association of Cardiovascular Risk Factors and ICA_IMT, ICA_CLT, N=154

Variables	**Multivariable model of Cardiovascular risk factors and ICA_IMT, ICA_CLT**	
	RR and 95 % CI	**P value**
Age (cof^[10])	1.09 (0.94 -1.21)	0.23
Smoking Pack year (cof^[10])	1.09 (1.05 -1.10)	**<0.001**
Statin use	1.14 (0.89-1.46)	0.27
IMT_ICA	0.87 (0.14- 5.29)	0.88
CLT_ICA	0.68 (0.27-1.67)	0.40

Table 3. Association of Cardiovascular Risk Factors and ICA_IMT, ICA_CAS, N=154

Variables	**Multivariable model of Cardiovascular risk factors and ICA_IMT, ICA_CAS**

	RR and 95 % CI	P value
Age (cof^10)	1.11 (0.96 -1.34)	0.17
Smoking Pack year (cof^10)	1.09 (1.05 -1.10)	**<0.001**
Statin use	1.14 (0.90-1.46)	0.27
IMT_ICA	0.77 (0.13-4.57)	0.77
CAS_ICA	0.96 (0.86-1.08)	0.44

Table 4. Association of Cardiovascular Risk Factors and ICA_IMT, ICA_CShS, N=154

Variables	**Multivariable model of Cardiovascular risk factors and ICA_IMT, ICA_CShS**	
	RR and 95 % CI	P value
Age (cof^10)	1.06 (0.90 -1.21)	0.48
Smoking Pack year (cof^10)	1.11 (1.06 -1.21)	**<0.001**
Statin use	1.13 (0.89-1.44)	0.23
IMT_ICA	0.95 (0.15-5.97)	0.96
CShS_ICA	0.84 (0.70- 1.02)	0.073

Table 5. Association of Cardiovascular Risk Factors and CCA_IMT, CCA_CAT, N=154

Variables	**Multivariable model of Cardiovascular risk factors and CCA_IMT, CCA_CAT**	
	RR and 95 % CI	P value
Age (cof^10)	1.08 (0.92- 1.24)	0.29
Smoking Pack year (cof^10)	1.09 (1.04 -1.13)	**<0.001**
Statin use	1.12 (0.88-1.41)	0.34
IMT_CCA	2.95 (0.76-11.45)	0.11
CAT_CCA	0.73 (0.19-2.82)	0.65

Table 6. Association of Cardiovascular Risk Factors and CCA_IMT, CCA_CAS, N=154

Variables	**Multivariable model of Cardiovascular risk factors and CCA_IMT, CCA_CAS**	
	RR and 95 % CI	P value
Age (cof^^{10})	1.09 (0.93-1.24)	0.25
Smoking Pack year (cof^^{10})	1.09 (1.05- 1.14)	**<0.001**
Statin use	1.14 (0.90-1.44)	0.24
IMT_CCA	2.54 (0.68 -9.43)	0.16
CAS_CCA	0.94 (0.85-1.04)	0.28

Table 7. Association of Cardiovascular Risk Factors and CCA_IMT, CCA_CLT, N=154

Variables	**Multivariable model of Cardiovascular risk factors and CCA_IMT, CCA_CLT**	
	RR and 95 % CI	P value
Age (cof^^{10})	1.09 (0.93 -1.25)	0.26
Smoking Pack year (cof^^{10})	1.08 (1.04 -1.13)	**<0.001**
Statin use	1.13 (0.89-1.43)	0.29
IMT_CCA	2.76 (0.75-10.18)	0.12
CLT_CCA	1.10 (0.59-2.06)	0.75

Table 8. Association of Cardiovascular Risk Factors and CCA_IMT, CCA_CShS, N=154

Variables	**Multivariable model of Cardiovascular risk factors and CCA_IMT, CCA_CShS**	
Age (cof^^{10})	1.07 (0.92 -1.25)	0.37

Smoking Pack year (cof^^{10})	1.08 (1.04 -1.13)	**<0.001**
Statin use	1.12 (0.89-1.41)	0.32
IMT_CCA	2.76 (0.75-10.11)	0.12
CShS_CCA	1.07 (0.98-1.16)	0.10

Table 9. Association of Cardiovascular Risk Factors and CCA_CAT, Cardiovascular Risk Factors and ICA_CAT, N=154

Variables	**Multivariable model of Cardiovascular risk factors and CCA_CAT**		**Multivariable model of Cardiovascular risk factors and ICA_CAT**	
	RR and 95 % CI	**P value**	**RR and 95 % CI**	**P value**
Age (cof^^{10})	1.11 (0.96 -1.26)	0.16	1.10 (0.95-1.26)	0.18
Smoking Pack year (cof^^{10})	1.09 (1.05-1.13)	**<0.001**	1.09 (1.04 -1.13)	**<0.001**
Statin use	1.14 (0.89-1.45)	0.28	1.14 (0.89-1.45)	0.28
CAT_CCA	0.81 (0.21-3.08)	0.76		
CAT_ICA			0.68 (0.14-3.35)	0.46

Table 10. Association of Cardiovascular Risk Factors and CCA_CLT, Cardiovascular Risk Factors and ICA_CLT, N=154

Variables	**Multivariable model of Cardiovascular risk factors and CCA_CLT**		**Multivariable model of Cardiovascular risk factors and ICA_CLT**	
Age (cof^^{10})	1.11 (0.96-1.26)	0.15	1.09 (0.94-1.21)	0.23
Smoking Pack year (cof^^{10})	1.09 (1.05-1.13)	**<0.001**	1.09 (1.05-1.21)	**<0.001**
Statin use	1.14 (0.89-1.45)	0.26	1.14 (0.89-1.46)	0.28
CLT_CCA	0.81 (0.21-3.08)	0.75		
CLT_ICA			0.67 (0.27-1.66)	0.39

Table 11. Association of Cardiovascular Risk Factors and CCA_CAS, Cardiovascular Risk Factors and ICA_CAS, N=154

Variables	**Multivariable model of Cardiovascular risk factors and CCA_CAS**		**Multivariable model of Cardiovascular risk factors and ICA_CAS**	
	RR and 95 % CI	**P value**	**RR and 95 % CI**	**P value**
Age (cof^[10])	1.11 (0.96-1.26)	0.15	1.11 (0.96-1.26)	0.16
Smoking Pack year (cof^[10])	1.09 (1.05-1.14)	**<0.001**	1.09 (1.05-1.14)	**<0.001**
Statin use	1.16 (0.91-1.47)	0.21	1.14 (0.89-1.45)	0.28
CAS_CCA	0.94 (0.84- 1.04)	0.24		
CAS_ICA			0.96 (0.86-1.07)	0.50

Table 12. Association of Cardiovascular Risk Factors and CCA_CShS, Cardiovascular Risk Factors and ICA_CShS, N=154

Variables	**Multivariable model of Cardiovascular risk factors and CCA_CShS**		**Multivariable model of Cardiovascular risk factors and ICA_CShS**	
	RR and 95 % CI	P value	RR and 95 % CI	P value
Age (cof^[10])	1.09 (0.94 -1.25)	0.22	1.06 (0.90 -1.21)	0.48
Smoking Pack year (cof^[10])	1.09 (1.04 -1.13)	**<0.001**	1.11 (1.06 -1.21)	**<0.001**
Statin use	1.13 (0.89-1.44)	0.29	1.13 (0.89-1.44)	0.30
CShS_CCA	1.07 (0.98-1.16)	0.10		
CShS_ICA			0.84 (0.70-1.01)	0.071